

TENSOR DIAGRAMS AND CLUSTER ALGEBRAS

SERGEY FOMIN AND PAVLO PYLYAVSKYY

To the memory of Andrei Zelevinsky

ABSTRACT. The rings of $\mathrm{SL}(V)$ invariants of configurations of vectors and linear forms in a finite-dimensional complex vector space V were explicitly described by Hermann Weyl in the 1930s. We show that when V is 3-dimensional, each of these rings carries a natural cluster algebra structure (typically, many of them) whose cluster variables include Weyl's generators. We describe and explore these cluster structures using the combinatorial machinery of tensor diagrams. A key role is played by the web bases introduced by G. Kuperberg.

CONTENTS

Introduction	2
Preliminaries	6
1. Tensors	6
2. $\mathrm{SL}(V)$ invariants	8
3. Cluster algebras	10
4. Tensor diagrams	14
5. Webs	21
6. Special invariants	23
7. Seeds associated to triangulations	29
Results and conjectures	34
8. Main results	34
9. Main conjectures	39
10. Arborization	42
11. Web gallery	45
Proofs	49
12. Properties of special invariants	49
13. Properties of special seeds	54
14. Building a quiver	56
15. Proof of the main theorem	58
16. Other proofs	60
Appendices	68
17. Special choice of an initial seed	68
18. Additional examples of seeds	70
References	71

Date: May 7, 2015 .

1991 *Mathematics Subject Classification.* Primary 13F60, Secondary 05E99, 13A50, 15A72.

Key words and phrases. Cluster algebra, invariant theory, web basis, tensor diagram.

Partially supported by NSF grants DMS-1101152 (S. F.) and DMS-1068169 (P. P.).

Introduction

Homogeneous coordinate rings of Grassmannians are among the most important examples of cluster algebras. Cluster structures in these rings [24, 52] play a prominent role in applications of cluster theory arising in connection with integrable systems, algebraic Lie theory, Poisson geometry, Teichmüller theory, total positivity, and beyond; see, e.g., [22, 25, 26, 30, 33] and references therein. Within cluster algebra theory proper, Grassmannians provide the most concrete and accessible examples of naturally defined cluster algebras of infinite mutation type.

Despite their importance, cluster structures on Grassmannians are not well understood at all, apart from a few special cases. Just a tiny subset of their cluster variables have been explicitly described; we do not know which quivers appear in their seeds; we do not understand the structure of their underlying cluster complexes; and so on.

Let $\text{Gr}_{k,N}$ denote the Grassmann manifold of k -subspaces in an N -dimensional complex vector space. The corresponding cluster algebra has finite type (i.e., has finitely many seeds) if and only if $(k-2)(N-k-2) \leq 3$. All of the problems mentioned above are open for any Grassmannian of infinite cluster type, so in particular for $k=3$, $N \geq 9$. (The case $k=2$ has been well understood since the early days of cluster algebras, see [17, Section 12.2].)

We advocate the point of view that many aspects of cluster structures on Grassmannians are best understood within a broader range of examples coming from classical invariant theory. Recall that the homogeneous coordinate ring of $\text{Gr}_{k,N}$ (with respect to a Plücker embedding) is isomorphic to the ring of $\text{SL}(V)$ invariants of N -tuples of vectors in a k -dimensional complex vector space V . More general rings of $\text{SL}(V)$ invariants of collections of vectors and linear forms have been thoroughly studied by classical invariant theory. We conjecture that *every such ring carries a natural cluster algebra structure*. In fact, there are typically many such structures, depending on a choice of a cyclic ordering of the tuples of vectors and covectors.

In this paper, we prove this claim in the special case when V is 3-dimensional. Our main result (Theorem 8.1) describes a family of cluster structures in the rings of SL_3 -invariants of collections of vectors and covectors in $V \cong \mathbb{C}^3$. The cluster structure (and moreover the mutation type of the corresponding quiver) depends on the choice of a *cyclic signature*, a binary word describing the order in which vectors and covectors are arranged around a circle. An accurate formulation of this result requires a description of (some of) the seeds defining the cluster structure in question; this in turn relies on the development of fairly technical combinatorial vocabulary, not to mention the requisite background on cluster algebras, tensor calculus, and basic invariant theory. This makes it impractical to include the precise statement of our main result in this introduction.

What makes the case $k=3$ special, and amenable to combinatorial approaches that cannot be straightforwardly generalized to higher dimensions? From our perspective, the distinguishing characteristic of the 3-dimensional case is the existence of a beautiful *web basis* discovered by Greg Kuperberg [35]. Our investigations were largely motivated by the desire to understand the cluster-theoretic significance of Kuperberg's basis. The main new feature of our approach is an emphasis on the

multiplicative properties of the web basis, which along with its compatibility with tensor contraction play a central role in the study of cluster algebra structures in these rings of invariants.

While all of our results hold for arbitrary rings of SL_3 -invariants, with an (almost) arbitrary cyclic ordering of vectors and covectors, many of our theorems are new already in the case of Grassmannians $Gr_{3,N}$. The list of such results includes:

- a large family of new “non-Plücker” cluster variables;
- compatibility of cluster structures across different values of N ;
- examples of “imaginary” elements in the web basis;
- examples of negative structure constants;
- a description of clusters associated with arbitrary triangulations of an N -gon.

The latter description extends a construction given by J. Scott [52], and suggests an extension to other Riemann surfaces, which we plan to pursue in a separate paper.

We describe conjectural ways in which each cluster structure in a classical ring of SL_3 -invariants is intrinsically determined by the corresponding web basis. We believe that this type of relationship extends to many other settings in which multiplicative properties of some distinguished additive basis in a given commutative ring dictate a “canonical” choice of a cluster structure in the ring. We also believe that, conversely, each cluster algebra of geometric type has an additive basis with certain remarkable properties; see Conjecture 9.5.

Perhaps most significantly, we formulate a conjectural combinatorial description (see Conjecture 10.1) of *all* cluster variables in each of our cluster algebras. To the best of our knowledge, this is the first class of cluster algebras of infinite mutation type for which such a description has been proposed.

We next outline the general plan of the paper, and review the contents of each section.

Sections 1–5 cover the requisite background, some of which may be familiar to the reader. Section 1 is a reminder on the basic notions of tensor calculus. Section 2 introduces our main object of study, the ring $R_{a,b}(V)$ of $SL(V)$ invariants of collections of b vectors and a covectors (i.e., linear forms) in a complex vector space V . Fundamentals of cluster algebras are reviewed in Section 3. We limit ourselves to the case of cluster algebras defined by quivers, as this is all the generality we need. At the end of the section, we state sufficient conditions that ensure that a particular seed, i.e., a quiver whose vertices are labeled by elements of a given ring R , defines a cluster algebra structure in R ; see Proposition 3.6 and Corollary 3.7.

Starting with Section 4, we assume that the space V is 3-dimensional. Section 4 is a primer on *tensor diagrams*, a particular kind of combinatorial gadgets that can be used to define $SL(V)$ invariants. This diagrammatic calculus, popular among physicists, has the advantage of reducing cumbersome calculations with tensors and invariants to repeated applications of certain (purely combinatorial) local transformation rules called skein relations.

Section 5 presents the crown jewel of the theory of tensor diagrams: Kuperberg’s construction of the web basis in $R_{a,b}(V)$. This basis, which depends on a choice of a

cyclic signature, consists of *web invariants*, the $\mathrm{SL}(V)$ invariants defined by planar tensor diagrams without short internal cycles.

Sections 6 and 7 introduce the key combinatorial construction of the paper: a family of “special” seeds designed to define a cluster structure in $R_{a,b}(V)$. In Section 6, we describe the “special” invariants that appear in those seeds, and state their basic properties. We then explain in Section 7 how each triangulation of a convex $(a+b)$ -gon gives rise to an extended cluster consisting of $\dim(R_{a,b}(V)) = 3(a+b) - 8$ special invariants, and to a quiver whose vertices are labeled by them. An impatient reader unwilling to labor through the rather intricate technicalities of this construction may decide to skip the details, and go directly to Section 8.

Sections 8–11 present the main results and conjectures of the paper. (The proofs are deferred until later.) The main theorem (Theorem 8.1) asserts that each of the special seeds described in Section 7 defines a cluster algebra structure in the ring of invariants $R_{a,b}(V)$. This cluster structure is independent of the choice of such a seed; in other words, all special seeds are mutation equivalent. The cluster structure does however depend on the choice of a signature. In fact, this choice affects the (cluster) type of the resulting cluster algebra, and whether it is of finite or infinite type (resp., finite or infinite mutation type). This can be seen in Figure 20 that lists the cluster types of $R_{a,b}(V)$ for all signatures with $a+b \leq 8$.

Our main construction has nice functoriality properties: it is preserved by the duality between vectors and covectors, and respected by the natural embeddings of smaller invariant rings into larger ones, induced by the forgetful maps (dropping a (co)vector from a collection) or the maps defined by taking a cross product of two consecutive (co)vectors. As a corollary, we establish that if a tensor diagram is a planar tree, then the corresponding web invariant is a cluster or coefficient variable.

In Section 9, we discuss many conjectural connections between our main construction and Kuperberg’s web basis. In particular, we expect this basis to contain all cluster monomials. Furthermore, we expect two cluster variables to be compatible if and only if their product is a web invariant. We formulate criteria that should distinguish cluster variables/monomials among more general web invariants.

While the web basis has many wonderful properties, it *may* have negative structure constants (cf. Conjecture 9.10 and Proposition 9.11). This is perhaps not so surprising in light of the discovery, made by M. Khovanov and G. Kuperberg [31], that the web basis is generally different from the *dual canonical basis*, i.e., the basis dual to G. Lusztig’s canonical basis [43]. Putting things into a cluster-theoretic context allows us to “explain” the Khovanov-Kuperberg smallest counterexample: it corresponds to the square of the simplest web invariant which is not a cluster variable. As established by B. Leclerc [38] and P. Lampe [36], for the cluster type at hand the appropriate element of the dual canonical basis is given by the quadratic Chebyshev polynomial of the second kind. Using the Chebyshev polynomial of the first kind recovers the corresponding element of the “atomic” basis of P. Sherman and A. Zelevinsky [54], while the square lies in the *dual semicanonical basis*, see [20, 44]. It is then natural to ask: Does the web basis always coincide with the appropriate dual semicanonical (or “generic”) basis, in the sense of [20, 23]?

Section 10 begins by our favorite conjecture of the paper (Conjecture 10.1) that describes, in simple combinatorial terms, the entire set of cluster monomials in $R_{a,b}(V)$. According to this conjecture, a cluster monomial is an $\mathrm{SL}(V)$ invariant that possesses two alternative presentations by a single tensor diagram: first, by a (planar, non-elliptic) web; second, by a (possibly non-planar) forest. If, in addition, this invariant does not factor (so that this forest is actually a tree), then the invariant is a cluster or coefficient variable. We then present an explicit *arborization* algorithm that conjecturally detects whether a given web defines a cluster monomial (resp., a cluster or coefficient variable) by applying a sequence of skein relations that either transform the web into a forest (resp., tree), or else determine that this is impossible.

Section 11 presents a gallery of fairly complicated examples of webs illustrating various phenomena that we discovered. These include: non-arborizable webs, both “real” and “imaginary” (in the sense of B. Leclerc [37]); “fake” exchange relations involving web invariants; and the aforementioned negative structure constants.

Sections 12–16 contain the proofs of the results stated in Sections 6–8 and 10. Specifically, the properties of special invariants and special seeds formulated in Sections 6–7 are proved in Sections 12–13. The construction of the quiver associated with a special seed defined by an arbitrary triangulation is outlined in Section 14. The main Theorem 8.1 is proved in Section 15. Other results stated in Sections 8 and 10 are proved in Section 16.

The last two sections play the role of appendices. Section 17 describes, in precise combinatorial terms, the construction of a special seed associated with a particular choice of a triangulation. This is in principle sufficient to identify a cluster structure in the ring $R_{a,b}(V)$ once the main theorem has been proved. Section 18 shows a couple of additional examples of special seeds, illustrating the main construction.

The paper contains a large number of pictures, which are best viewed in **color**.

The first version of this paper [13] was circulated in October 2012. While the text subsequently underwent extensive editorial revisions of expository nature, the main results of the paper, and the arguments used in their proofs, remained essentially unchanged. We also refrained from describing the developments that took place in this research subfield after the first **arXiv** posting.

Acknowledgments. We were influenced in our work by the research of many friends and colleagues on the subject of cluster algebras. We are grateful to Arkady Berenstein, Thomas Lam, Bernard Leclerc, Jan Schröer, David Speyer, and Andrei Zelevinsky for helpful advice and stimulating discussions, and to Igor Dolgachev, Rob Lazarsfeld, Ivan Losev, Ezra Miller, and Mircea Mustața for answering our questions on invariant theory. We thank Bernard Leclerc, Gregg Musiker, and the anonymous referees whose multiple comments on the earlier versions of the paper were critical in improving the quality of exposition.

Our main sources of inspiration outside cluster theory included the timeless texts by H. Weyl [57] and V. Popov–E. Vinberg [48] on the foundations of classical invariant theory; the pioneering work by G. Kuperberg [35] on the web bases; and the groundbreaking paper by V. Fock and A. Goncharov [12] on PGL_3 -Teichmüller spaces.

Our work on this paper began and ended at the Mathematical Sciences Research Institute in Berkeley, CA. It started in 2008 during MSRI's Combinatorial Representation Theory program, and was completed in 2012 during the Cluster Algebras program. We are grateful to MSRI for an excellent work environment.

The main results of this paper were first reported at the Hausdorff Institute (Bonn) and the Abel Symposium (Balestrand) in April and June 2011, respectively. The first author thanks the organizers of these events for their hospitality and support.

This paper is dedicated to the memory of Andrei Zelevinsky, a dear friend, collaborator, and mentor. His beautiful theorems, his penetrating insights, and his unique approach to combinatorial and representation-theoretic problems made him one of the leaders of his generation of researchers. His deep and original ideas influenced, and will continue to inspire, a great many mathematicians, ourselves included.

Preliminaries

1. TENSORS

Let V be a k -dimensional complex vector space. The word *vector* will always refer to an element of V . The elements of the dual space V^* (the linear forms on V) are called *covectors*. A *tensor* T of *type* (a, b) is an element of the tensor product

$$\underbrace{V \otimes \cdots \otimes V}_a \otimes \underbrace{V^* \otimes \cdots \otimes V^*}_b,$$

or alternatively a multilinear map

$$(1.1) \quad T : \underbrace{V^* \times \cdots \times V^*}_a \times \underbrace{V \times \cdots \times V}_b \longrightarrow \mathbb{C}.$$

In this paper, we consistently use the latter viewpoint. We will also need a slight notational variation that allows an arbitrary ordering of the *contravariant* arguments of T (vectors in V) and its *covariant* arguments (covectors in V^*).

The simplest examples of tensors are vectors (linear forms on V^*) and covectors (linear forms on V); they have types $(1, 0)$ and $(0, 1)$, respectively. Tensors of type $(1, 1)$ are cryptomorphic to linear operators in $\text{End}(V)$. Indeed, a tensor $T : V^* \times V \rightarrow \mathbb{C}$ corresponds to a linear map $V \rightarrow (V^*)^* \cong V$ that sends $v \in V$ to the linear form on V^* given by $u^* \mapsto T(u^*, v)$. The *identity tensor* I is the type $(1, 1)$ tensor that corresponds to the identity operator on V .

One can accordingly define the *trace* of a type $(1, 1)$ tensor, denoted by $\text{Tr}(T)$. For example, $\text{Tr}(I) = \dim(V) = k$.

The k th exterior power of V^* is one-dimensional. Let us fix an element in $\wedge^k V^*$, a *volume form* on V . The corresponding *volume tensor* $\text{vol} : V^k \rightarrow \mathbb{C}$ has type $(0, k)$. Its evaluation $\text{vol}(v_1, \dots, v_k)$ is the oriented volume of the parallelotope with sides v_1, \dots, v_k . The *dual volume tensor* vol^* of type $(k, 0)$ is defined by the identity

$$(1.2) \quad \text{vol}(v_1, \dots, v_k) \text{vol}^*(u_1^*, \dots, u_k^*) = \det(u_j^*(v_i))_{\substack{1 \leq i \leq k \\ 1 \leq j \leq k}}.$$

Let T and U be tensors of types (a, b) and (c, d) , respectively. The *tensor product* $T \otimes U$ is a tensor of type $(a + c, b + d)$ defined by

$$\begin{aligned} (T \otimes U)(u_1^*, \dots, u_{a+c}^*; v_1, \dots, v_{b+d}) \\ = T(u_1^*, \dots, u_a^*; v_1, \dots, v_b) \cdot U(u_{a+1}^*, \dots, u_{a+c}^*; v_{b+1}, \dots, v_{b+d}). \end{aligned}$$

In some instances, the arguments of T and U are re-shuffled in the process, resulting in different variants of the notion of a tensor product.

We will also need the concept of a *contraction* of a tensor with respect to a pair of arguments of opposite variance, i.e., a vector argument and a covector argument. For a tensor T of type (a, b) given by (1.1), its contraction with respect to, say, the first covariant and the first contravariant arguments is the type $(a - 1, b - 1)$ tensor T' obtained by viewing T as the function of those two arguments (temporarily fixing all the rest) and evaluating the trace of the resulting tensor:

$$T'(v_2^*, \dots, v_a^*; u_2, \dots, u_b) = \text{Tr}(T(\bullet, v_2^*, \dots, v_a^*; \bullet, u_2, \dots, u_b)).$$

One can also define a contraction of two tensors with respect to a contravariant argument of one of them and a covariant argument of another. The result is obtained by first computing the tensor product of the two tensors, then contracting as above.

Example 1.1.

1. Contracting a vector v and a covector u^* produces a scalar $u^*(v)$. More generally, an $(a + b)$ -fold contraction of a type (a, b) tensor T against an ordered collection of a covectors and b vectors returns the evaluation of T at this collection.
2. Contracting the two arguments of a type $(1, 1)$ tensor against each other yields the trace of the corresponding linear operator.
3. Given two tensors of type $(1, 1)$, contracting a contravariant argument of one tensor against the covariant argument of the other tensor corresponds to composition of respective linear operators.
4. Two-fold contraction of two such tensors (matching each contravariant argument to the covariant argument of the other tensor) yields the trace of the product of the corresponding linear operators.
5. A k -fold contraction of the volume tensor against its dual yields the scalar $k!$.

All of the above can be recast in the basis-dependent language of coordinates and matrices, once we designate a “standard” basis $(\mathbf{e}_1, \dots, \mathbf{e}_k)$ in V satisfying

$$\text{vol}(\mathbf{e}_1, \dots, \mathbf{e}_k) = 1.$$

(Note that in view of (1.2), the dual basis $(\mathbf{e}_1^*, \dots, \mathbf{e}_k^*)$ in V^* has the similar property:

$$\text{vol}^*(\mathbf{e}_1^*, \dots, \mathbf{e}_k^*) = 1.)$$

After a standard basis has been chosen, tensors of type (a, b) become $(a + b)$ -dimensional arrays of complex scalars (the *components* of a tensor) indexed by tuples of a “row indices” and b “column indices;” each index takes values from 1 to k . In particular, vectors become column vectors (with k components), covectors become row vectors, tensors of type $(1, 1)$ become $k \times k$ matrices, and so on. The trace becomes the usual trace of a matrix. The evaluation of a volume tensor at a k -tuple

of column vectors is given by the determinant of a square matrix formed by placing them side-by-side in the given order. The contraction of a tensor with respect to a row index and a column index is obtained by summing over all assignments of matching values to these two indices.

In coordinate notation described above, the identity tensor is given by the identity matrix (δ_{ij}) , also known as the *Kronecker symbol*. In *Einstein notation*, commonly used in physics, the row indices are placed as superscripts while column indices appear as subscripts; one then writes the Kronecker symbol as δ_j^i .

The volume tensor on V is given in the coordinates associated with the standard basis as the *Levi-Civita symbol* $(\varepsilon_{i_1, \dots, i_k})$ defined by

$$\varepsilon_{i_1, \dots, i_k} = \begin{cases} \text{the sign of the permutation } (i_1, \dots, i_k) & \text{if } i_1, \dots, i_k \text{ are all distinct;} \\ 0 & \text{otherwise.} \end{cases}$$

The dual volume tensor on V^* is given by the same symbol (denoted $(\varepsilon^{i_1, \dots, i_k})$ in Einstein notation).

2. $\mathrm{SL}(V)$ INVARIANTS

The special linear group $\mathrm{SL}(V)$ naturally acts on both V and V^* ; to make the latter a left action, one sets $(gu^*)(v) = u^*(g^{-1}(v))$, for $v \in V$, $u^* \in V^*$, and $g \in \mathrm{SL}(V)$. The group $\mathrm{SL}(V)$ consequently acts on the vector space

$$(2.1) \quad (V^*)^a \times V^b = \underbrace{V^* \times \cdots \times V^*}_{a \text{ copies}} \times \underbrace{V \times \cdots \times V}_{b \text{ copies}},$$

and therefore on its coordinate (polynomial) ring.

In this paper, we focus our attention on the ring

$$R_{a,b}(V) = \mathbb{C}[(V^*)^a \times V^b]^{\mathrm{SL}(V)}$$

of $\mathrm{SL}(V)$ -invariant polynomials on $(V^*)^a \times V^b$. In coordinate notation, this ring is described as follows. Consider two matrices filled with indeterminates: the matrix $y = (y_{ij})$ of size $a \times k$ and the matrix $x = (x_{ij})$ of size $k \times b$. The ring $R_{a,b}(V)$ consists of polynomials in these $(a+b)k$ variables which are invariant under the transformation that simultaneously replaces x by gx , and y by yg^{-1} , for any matrix $g \in \mathrm{SL}_k(\mathbb{C})$. One example of such a polynomial is a *Plücker coordinate* P_J where J is a k -element subset of columns in x ; by definition, P_J is the $k \times k$ minor of x obtained by selecting the columns in J . (In coordinate-free terms, we evaluate the volume tensor on the k -element subset, labeled by J , of the last b factors in (2.1).) One similarly defines the “dual” Plücker coordinate P_I^* , for I a k -element subset of rows, as the corresponding maximal minor of y . Another example of an $\mathrm{SL}(V)$ invariant is a bilinear form $Q_{ij} = \sum_{\ell} y_{i\ell} x_{\ell j}$ where i is a row index for y , and j a column index for x ; thus, this invariant is obtained by pairing a particular V^* factor in (2.1) with a V factor.

The ring $R_{a,b}(V)$ is one of the archetypal objects of classical invariant theory; see, e.g., [10, Chapter 2], [34, 42, 47], [48, §9], [50, Section 11], [56, 57]. It was explicitly described by Hermann Weyl [57] in the 1930s in terms of generators and relations.

The First Fundamental Theorem of invariant theory states that the ring $R_{a,b}(V)$ is generated by the following multilinear polynomials (tensors):

- the $\binom{a}{k}$ (“dual”) Plücker coordinates P_I^* ,
- the $\binom{b}{k}$ Plücker coordinates P_J , and
- the ab pairings Q_{ij} .

Thus, in a sense, all $SL(V)$ invariants are obtained from three fundamental ones: the volume tensors on V and V^* , and the identity tensor.

Weyl also described the ideal of relations among the generators P_I^* , P_J , and Q_{ij} . His Second Fundamental Theorem, which we will not rely upon, states that this ideal is generated by the quadratic *Grassmann-Plücker relations* for the P_I^* 's, the similar relations for the P_J 's, and the non-homogeneous (for $k \neq 2$) relations $P_I^*P_J = \det(Q_{ij})_{i \in I, j \in J}$ (cf. (1.2)).

The First Fundamental Theorem implies that for $b \geq k$ the ring $R_{0,b}(V)$ is isomorphic to the homogeneous coordinate ring $\mathbb{C}[\text{Gr}_{k,b}]$ of the Grassmann manifold $\text{Gr}_{k,b}$ of k -dimensional subspaces in \mathbb{C}^b with respect to its Plücker embedding (see, e.g., [10, Corollary 2.3]). It is not hard to show that $R_{1,b}(V)$ is isomorphic to the homogeneous coordinate ring of the two-step partial flag manifold

$$\{(V_1, V_k) : V_1 \in \text{Gr}_{1,b}, V_k \in \text{Gr}_{k,b}\}.$$

We do not know a similar interpretation of $R_{a,b}(V)$ for general values of a and b .

In our discussions of the spaces $R_{a,b}(V)$, it will be important to distinguish between their incarnations that involve different orderings of the contravariant and covariant arguments. To this end, we will use the notion of a *signature*, a word in the alphabet $\{\bullet, \circ\}$ that reflects the order of the $a + b$ arguments of an invariant f . Specifically, each of the a factors V^* will be represented by the symbol \circ , and each of the b factors V by the symbol \bullet . Thus for example an $SL(V)$ -invariant polynomial

$$f : V^* \times V \times V \times V^* \rightarrow \mathbb{C}$$

is an invariant of signature $\sigma = [\circ \bullet \bullet \circ]$. We denote by $R_\sigma(V)$ the ring of $SL(V)$ invariants of signature σ . If σ consists of a copies of \circ and b copies of \bullet , we say that it has *type* (a, b) . Thus for σ of type (a, b) , we have $R_\sigma(V) \cong R_{a,b}(V)$.

The natural action of the $(a + b)$ -dimensional torus defines a multi-grading of the ring $R_\sigma(V) \cong R_{a,b}(V)$. If an invariant $f \in R_\sigma(V)$ is multi-homogeneous of degrees d_1, \dots, d_{a+b} in its $a + b$ arguments, we then call the tuple

$$(2.2) \quad \text{multideg}(f) = (d_1, \dots, d_{a+b})$$

the *multidegree* of f . For example, the Plücker coordinate $P_{\{1, \dots, k\}} \in R_{0,b}(V)$ has multidegree $(1, \dots, 1, 0, \dots, 0)$ (the first k entries are 1's).

There are known combinatorial formulas for the dimensions of multigraded components of the ring $R_{a,b}(V)$ in terms of the iterated Littlewood-Richardson Rule. In some cases, more explicit formulas can be given. For example, the multilinear component of $R_{0,b}(V)$ (i.e., the space of SL_k -invariant b -covariant tensors in \mathbb{C}^k) is only nontrivial when k divides b ; if it does, then the dimension of this space is equal to the number of standard Young tableaux of rectangular shape $k \times \frac{b}{k}$. As such, this dimension is given by the hooklength formula.

Being a subring of a polynomial ring, $R_{a,b}(V)$ is a domain. By (the modern version of) Hilbert’s theorem, it is finitely generated; as mentioned above, H. Weyl [57] described the generators explicitly. Finally, the ring $R_{a,b}(V)$ is factorial:

Lemma 2.1 (see [48], Theorem 3.17). *The algebra of invariants $R_{a,b}(V)$ is a finitely generated unique factorization domain.*

3. CLUSTER ALGEBRAS

This section offers a quick introduction to cluster algebras, limited in scope to our immediate needs. Further details can be found in [15, 17, 18]. The only non-standard material in this section is Proposition 3.6 (and its Corollary 3.7) which provides a test for verifying that a given set of algebraic/combinatorial data inside a commutative ring makes the latter into a cluster algebra.

Cluster algebras are a class of commutative rings endowed with a combinatorial structure of a particular kind. The concept can be defined in varying degrees of generality. In this paper, we will only need the notion of a cluster algebra which (i) is of *geometric type*, (ii) has \mathbb{C} as its field of scalars, and (iii) has *skew-symmetric exchange matrices*. To simplify terminology, we call such gadgets “cluster algebras” without further qualifications.

The combinatorial data defining a cluster algebra are encoded in a *quiver* Q , a finite oriented loopless graph with no oriented 2-cycles. Some vertices of Q are designated as *mutable*; the remaining ones are called *frozen*.

Definition 3.1. Let z be a mutable vertex in a quiver Q . The *quiver mutation* μ_z transforms Q into the new quiver $Q' = \mu_z(Q)$ via a sequence of three steps. At the first step, for each pair of directed edges $x \rightarrow z \rightarrow y$ passing through z , introduce a new edge $x \rightarrow y$ (unless both x and y are frozen, in which case do nothing). At the second step, reverse the direction of all edges incident to z . At the third step, repeatedly remove oriented 2-cycles until unable to do so. See Figure 1.

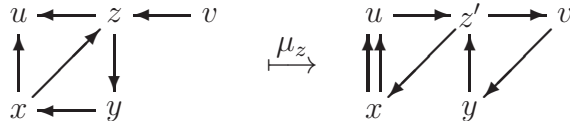


Figure 1: A quiver mutation. Vertices u and v are frozen.

Quiver mutations can be iterated *ad infinitum*, using an arbitrary sequence of mutable vertices of an evolving quiver. This combinatorial dynamics drives the algebraic dynamics of *seed mutations* that we describe next.

Definition 3.2. Let \mathcal{F} be a field containing \mathbb{C} . A *seed* in \mathcal{F} is a pair (Q, \mathbf{z}) consisting of a quiver Q as above together with a collection \mathbf{z} , called an *extended cluster*, consisting of algebraically independent (over \mathbb{C}) elements of \mathcal{F} , one for each vertex of Q . The elements of \mathbf{z} associated with the mutable vertices are called *cluster variables*; they form a *cluster*. The elements associated with the frozen vertices are called *frozen variables*, or *coefficient variables*.

A *seed mutation* μ_z at a mutable vertex associated with a cluster variable z transforms (Q, \mathbf{z}) into the seed $(Q', \mathbf{z}') = \mu_z(Q, \mathbf{z})$ defined as follows. The new quiver is $Q' = \mu_z(Q)$. The new extended cluster is $\mathbf{z}' = \mathbf{z} \cup \{z'\} \setminus \{z\}$ where the new cluster variable z' replacing z is determined by the *exchange relation*

$$(3.1) \quad z z' = \prod_{z \leftarrow y} y + \prod_{z \rightarrow y} y.$$

(The two products are over the edges directed at and from z , respectively.)

To illustrate, the exchange relation associated with the quiver mutation μ_z shown in Figure 1 is $z z' = vx + uy$, while applying μ_x to the quiver on the right would invoke the exchange relation $xx' = z' + u^2$.

We note that the mutated seed (Q', \mathbf{z}') contains the same coefficient variables as the original seed (Q, \mathbf{z}) .

It is easy to check that one can recover (Q, \mathbf{z}) from (Q', \mathbf{z}') by performing a seed mutation at z' .

Definition 3.2 deviates from the usual convention of using the field of rational functions $\mathbb{C}(\mathbf{z})$ as the ambient field \mathcal{F} . This distinction is inconsequential since, as we shall see, all the action is taking place inside $\mathbb{C}(\mathbf{z})$.

Definition 3.3 (*Cluster algebra*). Two seeds that can be obtained from each other by a sequence of mutations are called *mutation equivalent*. The *cluster algebra* $\mathcal{A}(Q, \mathbf{z})$ associated to a seed (Q, \mathbf{z}) is defined as the subring of \mathcal{F} generated by all elements of all extended clusters of the seeds mutation equivalent to (Q, \mathbf{z}) .

Thus, to construct a cluster algebra, one begins with an arbitrary *initial seed* (Q, \mathbf{z}) in \mathcal{F} , repeatedly applies seed mutations in all possible directions, and takes the \mathbb{C} -subalgebra generated by all elements of \mathcal{F} appearing in all seeds produced by this recursive process.

Note that the above construction of $\mathcal{A}(Q, \mathbf{z})$ does not depend, up to a natural isomorphism, on the choice of the extended cluster \mathbf{z} : everything, save for the embedding of the resulting cluster algebra into \mathcal{F} , is determined by the initial quiver Q , and indeed by its mutation equivalence class.

The *rank* of a cluster algebra $\mathcal{A}(Q, \mathbf{z})$ is the number of cluster variables in each of its seeds, or equivalently the number of mutable vertices in each of its quivers.

When a quiver Q undergoes a mutation, its mutable part (that is, the induced subquiver on the set of mutable vertices) does so, too. Thus the mutable parts of the quivers at different seeds of a given cluster algebra \mathcal{A} are all mutation equivalent. This mutation equivalence class determines the (cluster) *type* of \mathcal{A} .

The same ring can be endowed with cluster structures of different type; see, e.g., [17, Example 12.10]. Many more examples of this kind appear later in this paper.

A cluster algebra is said to be of *finite type* if it has finitely many distinct seeds. One of the basic structural results of cluster theory is the *finite type classification*:

Theorem 3.4 ([17]). *A cluster algebra is of finite type if and only if it has a quiver whose mutable part is an orientation of a disjoint union of Dynkin diagrams.*

Thus the terminology is consistent: the property of being of finite type depends only on the cluster type of a cluster algebra.

If a cluster algebra \mathcal{A} (say of rank n) has a quiver whose mutable part is an orientation of a Dynkin diagram X_n , then we say that \mathcal{A} is “of type X_n .” This convention applies as well to the extended Dynkin diagrams of affine and elliptic (or extended affine) types; see, e.g., [14, Section 12] for further details. It is worth noting that all orientations of any such diagram X_n are mutation equivalent whenever X_n is a tree (thus in particular in finite type). Furthermore, orientations of non-isomorphic diagrams are mutation inequivalent.

Another basic property of cluster algebras is the *Laurent Phenomenon*:

Theorem 3.5 ([15, 17]). *Any element of a cluster algebra $\mathcal{A}(Q, \mathbf{z})$ is expressed in terms of the extended cluster \mathbf{z} as a Laurent polynomial. Furthermore, none of the coefficient variables appears in the denominator of this Laurent expression (reduced to lowest terms).*

Since $\mathcal{A}(Q, \mathbf{z})$ is generated by cluster variables from the seeds mutation equivalent to (Q, \mathbf{z}) , Theorem 3.5 can be restated as saying that each of those cluster variables is given by a Laurent expression of the aforementioned kind.

The Laurentness part of Theorem 3.5 is a special case of [15, Theorem 3.1]. The last statement of Theorem 3.5 was established in [17, Proposition 11.2], modulo a technical condition [17, (11.3)] which is in fact satisfied in all applications appearing in this paper. This condition can be removed using [18, Theorem 3.7] in combination with [18, Conjecture 5.4]; the latter was proved (in the generality considered in the current paper) in [9, Theorem 1.7].

Many important rings arising in Lie theory possess a natural structure of a cluster algebra. The list includes homogeneous coordinate rings of partial flag manifolds, Schubert varieties, and double Bruhat cells in semisimple Lie groups; see, e.g., [3, 16, 19, 29, 39].

Of particular importance to us is the example of a Grassmannian $\text{Gr}_{k,b}$. As mentioned earlier, its homogeneous coordinate ring (with respect to the Plücker embedding) is canonically isomorphic to the ring $R_{0,b}(\mathbb{C}^k)$ of SL_k -invariants of configurations of b vectors in a k -dimensional vector space. This ring has a natural cluster algebra structure, first defined in J. Scott’s Ph.D. thesis [52] (cf. also [24, 25]). It is important to note that this cluster structure on $R_{0,b}(V)$ depends on the choice of a cyclic ordering of the b vectors; choosing a different ordering results in a different (albeit isomorphic) cluster structure.

Any cluster algebra, being a subring of a field, is an integral domain (and under our conventions, a \mathbb{C} -algebra). Conversely, given such a domain R , one may be interested in identifying R as a cluster algebra. As an ambient field \mathcal{F} , we can always use the quotient field $\text{QF}(R)$. The challenge is to find a seed (Q, \mathbf{z}) in $\text{QF}(R)$ such that $\mathcal{A}(Q, \mathbf{z}) = R$. We next present a set of conditions that are sufficient to ensure that a particular choice of a seed solves this problem.

Recall that an integral domain R is called *normal* if it is integrally closed in $\text{QF}(R)$.

Proposition 3.6. *Let R be a finitely generated \mathbb{C} -algebra and a normal domain. Let (Q, \mathbf{z}) be a seed in $\text{QF}(R)$ satisfying the following conditions:*

- *all elements of \mathbf{z} belong to R ;*
- *the cluster variables in \mathbf{z} are pairwise coprime (in R);*
- *for each cluster variable $z \in \mathbf{z}$, the seed mutation μ_z replaces z with an element z' (cf. (3.1)) that lies in R and is coprime to z .*

(Here we call two elements of R coprime if the locus of their common zeros has codimension ≥ 2 in $\text{Spec}(R)$.) Then $R \supset \mathcal{A}(Q, \mathbf{z})$.

If, in addition, R has a set of generators each of which appears in the seeds mutation equivalent to (Q, \mathbf{z}) , then $R = \mathcal{A}(Q, \mathbf{z})$.

Proposition 3.6 (and its proof given below) extends some of the ideas used in [3, Proof of Theorem 2.10], and subsequently in [52, Proof of Proposition 7].

The argument given below actually establishes a stronger statement: under the conditions of Proposition 3.6, the ring R contains the *upper cluster algebra* $\overline{\mathcal{A}}(Q, \mathbf{z})$ (see [3]), or more precisely the subalgebra of $\text{QF}(R)$ consisting of the elements which, when expressed in terms of any extended cluster, are Laurent polynomials in the cluster variables and ordinary polynomials in the coefficient variables. In particular, the conditions of Proposition 3.6 imply that in this case, the upper cluster algebra coincides with the ordinary cluster algebra (localized at coefficient variables).

Proof. The last implication is clear since its premise ensures that $R \subset \mathcal{A}(Q, \mathbf{z})$.

To prove that $R \supset \mathcal{A}(Q, \mathbf{z})$, we need to show that each cluster variable \bar{z} from any seed $(\bar{Q}, \bar{\mathbf{z}})$ mutation equivalent to (Q, \mathbf{z}) belongs to R . This is done using some basic algebraic geometry. Our assumptions on the ring R mean that it can be identified with the coordinate ring of an (irreducible) normal affine complex algebraic variety $X = \text{Spec}(R)$. Then $\text{QF}(R) = \mathbb{C}(X)$, the field of rational functions on X . Our goal is to show that each “distant” cluster variable \bar{z} as above is not just a rational function in $\mathbb{C}(X)$ but a regular function in $\mathbb{C}[X] = R$. The key property that we need is the algebraic version of Hartogs’ continuation principle for normal varieties (see, e.g., [8, Chapter 2, 7.1]) which asserts that a function on X that is regular outside a closed algebraic subset of codimension ≥ 2 is in fact regular everywhere on X .

Let $Y \subset X$ be the locus where at least two of the cluster variables in \mathbf{z} vanish, or else one of them, say z , vanishes together with the element z' defined by (3.1). By the coprimeness conditions imposed on the seed (Q, \mathbf{z}) , the codimension of Y in X is 2. The complement $X \setminus Y$ consists of the points $x \in X$ such that

- at most one of the cluster variables in \mathbf{z} vanishes at x , and
- for each pair (z, z') as above, either z or z' does not vanish at x .

This means that there is a seed (Q', \mathbf{z}') (either the original seed (Q, \mathbf{z}) or one of the adjacent seeds $\mu_z(Q, \mathbf{z})$) none of whose cluster variables vanishes at x ; moreover $\mathbf{z}' \subset \mathbb{C}[X]$. Then the Laurent Phenomenon (Theorem 3.5) implies that our distant cluster variable \bar{z} is regular at x . By the algebraic Hartogs’ principle mentioned above, it follows that \bar{z} is regular on X , and we are done. \square

Corollary 3.7. *Let R be a finitely generated unique factorization domain over \mathbb{C} . Let (Q, \mathbf{z}) be a seed in the quotient field of R such that all elements of \mathbf{z} and all elements of clusters adjacent to \mathbf{z} are irreducible elements of R . Then $R \supset \mathcal{A}(Q, \mathbf{z})$.*

If, in addition, the union of extended clusters in $\mathcal{A}(Q, \mathbf{z})$ contains a generating set for R , then $R = \mathcal{A}(Q, \mathbf{z})$.

Proof. Let us check the conditions of Proposition 3.6. Any UFD is a normal domain. To verify the coprimality conditions, we first note that two elements of \mathbf{z} cannot differ by a scalar factor since they are algebraically independent. Similarly, the elements of an exchange pair (z, z') cannot differ by a scalar factor, or else the exchange relation would give an algebraic dependence in \mathbf{z} . Now, an irreducible element in a UFD generates a prime ideal, so the vanishing locus in $\text{Spec}(R)$ for each of our irreducible elements is an (irreducible) subvariety. These subvarieties are pairwise distinct (cf. above), so their pairwise intersections have codimensions ≥ 2 . \square

In view of Lemma 2.1, in order to identify a cluster algebra structure in the ring of invariants $R_{a,b}(V)$, all we need to do is find a seed (Q, \mathbf{z}) satisfying the conditions in Corollary 3.7. This is a lot easier said than done.

4. TENSOR DIAGRAMS

From now on, we assume that $k = 3$, so that $V \cong \mathbb{C}^3$.

Our description of cluster structures in the classical rings of invariants $R_{a,b}(V)$ will be based on the calculus of tensor diagrams [2, 7, 51, 55], particularly in its version of the “ A_2 spider” developed by G. Kuperberg [35]. This calculus, in turn, is based on two simple observations. The first one was already mentioned in connection with the First Fundamental Theorem:

- (i) the identity tensor and the volume tensors on V and V^* are $\text{SL}(V)$ -invariant.

The second observation is that

- (ii) the operations of tensor product and contraction preserve $\text{SL}(V)$ invariance.

By combining the ingredients derived from (i) using the operations in (ii), one can build a surprisingly rich supply of $\text{SL}(V)$ -invariant tensors—and from them, a large class of polynomial invariants. We next explain how, without claiming any originality: the machinery described below is a variation of diagrammatic calculus whose various versions were (re)discovered multiple times, under different guises and names, see in particular [2, 7, 35] and especially [1, Section 8].

Tensor diagrams are built using three types of building blocks shown in Figure 2. These blocks correspond, left to right, to the three basic $\text{SL}(V)$ -invariant tensors: the volume tensor, the dual volume tensor, and the identity tensor. The endpoints of a block correspond to the tensor’s arguments: a sink to a vector, a source to a covector. In order for either of the volume tensors to be well defined, a cyclic ordering of the three arguments must be specified.

We then combine these building blocks by plugging arrowheads into arrowtails. Interpreting this operation as contraction of the corresponding tensors, we obtain a well defined notion of a tensor associated with the resulting combinatorial gadget.



Figure 2: Basic building blocks for tensor diagrams. The arrows are to be thought of as flexible strings which can be bent and/or stretched.

Note that plugging one end of a two-pronged block (corresponding to the identity tensor) into an end of opposite valence in some tensor diagram does not change the tensor that the latter represents. Consequently, for any diagram assembled using the above procedure from the three basic types of blocks, the associated tensor does not depend on the locations (or number) of plug-in joints along unbranched stretches. Erasing those joints produces a directed graph with trivalent and univalent vertices in which every trivalent vertex is a source or a sink. Any such graph, together with the additional data specifying cyclic ordering of edges incident to trivalent vertices, represents a well defined tensor.

We are going to draw all our diagrams in an oriented disk, obeying the following conventions. We will usually erase the arrows, introducing instead a bi-coloring of the vertices: the sinks will be colored black, and the sources white. We place the boundary vertices on the boundary of the disk, in the order mirroring the one used to define the direct product of the $a + b$ spaces V and V^* whose $SL(V)$ invariants we study. We place the interior vertices inside the disk, and draw the edges as simple curves that are allowed to intersect transversally. Last but not least, we make sure that the cyclic ordering specified at each interior vertex of the diagram matches the clockwise ordering of the three curves meeting at the corresponding point in the disk.

The last step in the construction of a general tensor diagram involves gluing together some of the univalent vertices of a directed graph as above. We interpret this step as substituting the same (co)vector into the arguments of the associated tensor which correspond to the glued endpoints. At this point, the $SL(V)$ invariant represented by the graph ceases to be multilinear. This last operation is sometimes called (partial) *restitution*, and is inverse to *polarization*.

An example illustrating different stages of the construction outlined above is shown in Figure 3.

Definition 4.1. A *tensor diagram* is a finite bipartite graph D with a fixed *proper* coloring of its vertices into two colors, black and white, and with a fixed partition of its vertex set into the set $\text{bd}(D)$ of *boundary* vertices and the set $\text{int}(D)$ of *internal* vertices, satisfying the following conditions:

- each internal vertex is trivalent;
- for each internal vertex, a cyclic order on the edges incident to it is fixed.

The last condition ensures that each of the six permutations of the three edges incident to an internal vertex has a well-defined sign.

If $\text{bd}(D)$ consists of a white vertices and b black ones, then we say that D is of *type* (a, b) .

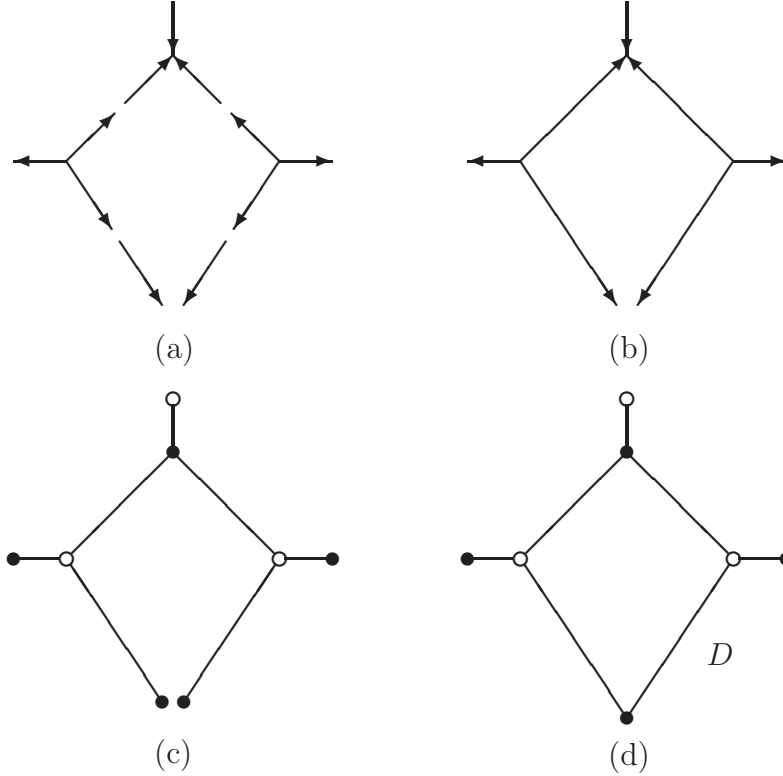


Figure 3: Assembling a tensor diagram. In this example, we use five building blocks. They correspond to two copies of the volume tensor, one copy of the dual volume tensor, and two copies of the identity tensor. The resulting tensor diagram D of type $(1, 3)$ represents an invariant of multidegree $(1, 2, 1, 1)$ in $R_{1,3}(V)$. The disk containing D is not shown.

We regard each edge of a tensor diagram as being oriented so that it points away from its white endpoint and towards the black one. While drawing tensor diagrams, this orientation is routinely omitted.

A tensor diagram D of type (a, b) defines an $\mathrm{SL}(V)$ invariant $[D] \in R_{a,b}(V)$ obtained by repeated contraction of elementary $\mathrm{SL}(V)$ -invariant tensors (followed by bundling up some of the arguments), as explained above. To compensate for the informality of that explanation, we next provide a precise definition of the invariant $[D]$ in the language of coordinates.

Let us identify $R_{a,b}(V)$ with the ring of SL_3 invariants of collections of a covectors

$$y(v) = [y_1(v) \quad y_2(v) \quad y_3(v)]$$

and b vectors

$$x(v) = \begin{bmatrix} x_1(v) \\ x_2(v) \\ x_3(v) \end{bmatrix}$$

labeled by a fixed collection of a white and b black vertices on the boundary of a disk. The invariant $[D]$ associated with a tensor diagram D with those boundary

vertices is then given by

$$(4.1) \quad [D] = \sum_{\ell} \left(\prod_{v \in \text{int}(D)} \text{sign}(\ell(v)) \right) \left(\prod_{\substack{v \in \text{bd}(D) \\ v \text{ black}}} x(v)^{\ell(v)} \right) \left(\prod_{\substack{v \in \text{bd}(D) \\ v \text{ white}}} y(v)^{\ell(v)} \right),$$

where

- ℓ runs over all proper labelings of the edges in D by the numbers 1, 2, 3; to wit, we require that for each internal vertex v , the labels associated with the three edges incident to v are all distinct;
- $\text{sign}(\ell(v))$ denotes the sign of the (cyclic) permutation of those three labels determined by the cyclic ordering of the edges incident to v ;
- $x(v)^{\ell(v)}$ denotes the monomial $\prod_e x_{\ell(e)}(v)$, product over all edges e incident to v , and similarly for $y(v)^{\ell(v)}$.

Example 4.2 below illustrates formula (4.1). Many more examples of tensor diagrams are scattered throughout the paper.

Example 4.2. Consider the tensor diagram D shown in Figure 3(d). We label the black boundary vertices 1, 2, and 3, in clockwise order, and label the white vertex 4. We denote the corresponding three column vectors and one row covector by

$$\begin{bmatrix} x_{11} \\ x_{21} \\ x_{31} \end{bmatrix}, \quad \begin{bmatrix} x_{12} \\ x_{22} \\ x_{32} \end{bmatrix}, \quad \begin{bmatrix} x_{13} \\ x_{23} \\ x_{33} \end{bmatrix}, \quad \text{and} \quad [y_1 \ y_2 \ y_3],$$

respectively. There are 24 proper labelings of the edges of D . They can be broken into four six-tuples as shown in Figure 4. The corresponding monomial weights are

$$\varepsilon x_{\gamma 1} x_{\alpha 2}^2 x_{\beta 3} y_{\alpha}, \quad \varepsilon x_{\gamma 1} x_{\alpha 2} x_{\beta 2} x_{\beta 3} y_{\beta}, \quad \varepsilon x_{\gamma 1} x_{\alpha 2} x_{\gamma 2} x_{\beta 3} y_{\gamma}, \quad -\varepsilon x_{\beta 1} x_{\alpha 2} x_{\gamma 2} x_{\beta 3} y_{\beta},$$

where ε denotes the sign of the permutation (α, β, γ) in the symmetric group \mathcal{S}_3 . The weights of the labelings in the fourth group cancel each other out under the sign-reversing involution that switches α and γ . Consequently, (4.1) becomes

$$(4.2) \quad \begin{aligned} [D] &= \sum_{(\alpha, \beta, \gamma) \in \mathcal{S}_3} \text{sgn}(\alpha, \beta, \gamma) x_{\gamma 1} x_{\alpha 2} x_{\beta 3} (x_{\alpha 2} y_{\alpha} + x_{\beta 2} y_{\beta} + x_{\gamma 2} y_{\gamma}) \\ &= \det(x_{ij})_{i,j \in (1,2,3)} (x_{12} y_1 + x_{22} y_2 + x_{32} y_3), \end{aligned}$$

coinciding with the invariant given by the tensor diagram shown in Figure 5.

The $\text{SL}(V)$ invariant $[D]$ defined by a tensor diagram D is homogeneous in each of its arguments $x(v)$, for v a boundary vertex. The degree of $[D]$ with respect to $x(v)$ is equal to the degree d_v of v (in the graph theory sense). The *multidegree* of D is, by definition, the multidegree of $[D]$ (cf. (2.2)):

$$(4.3) \quad \text{multideg}(D) = \text{multideg}([D]) = (d_v)_{v \in \text{bd}(D)}.$$

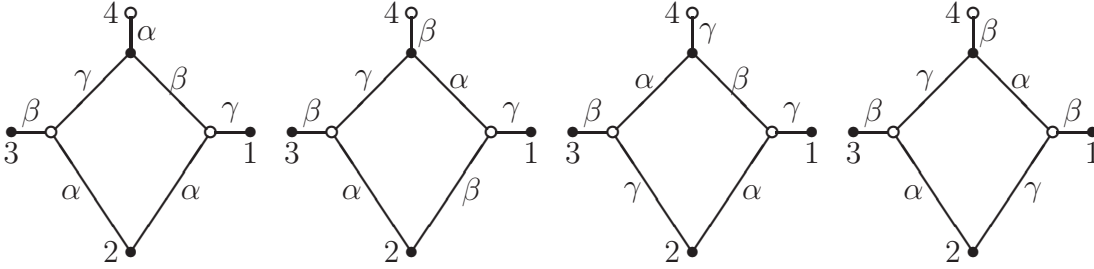


Figure 4: The proper labelings of the edges of a tensor diagram. Here (α, β, γ) runs over all permutations of 1, 2, 3.

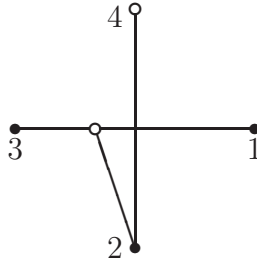


Figure 5: A tensor diagram defining the same invariant as the one in Figure 4.

Remark 4.3. An SL_3 invariant $[D]$ associated with a tensor diagram D without multiple edges can be alternatively defined by a determinantal formula, as explained below. Although we do not rely on such formulas in this paper, they may be useful in some calculations.

As before, suppose that D has type (a, b) . Assume that no two boundary vertices are directly connected by an edge. (Otherwise, factor out the corresponding scalar product, and remove the edge.) Assume that D has $c + d$ interior vertices, c of them white and d black. Clearly $a + 3c = b + 3d$, the number of edges in D . We now build a square $(a + 3c) \times (b + 3d)$ matrix $M(D)$ as follows:

- the rows of $M(D)$ come from the white vertices in $\text{int}(D)$ (each such vertex contributes three rows) as well as from the edges incident to the white vertices in $\text{bd}(D)$ (each such edge contributes one row);
- similarly, the columns of $M(D)$ come from the black interior vertices (each contributes three) and from the edges incident to the black boundary vertices (each contributes one).

The matrix $M(D)$ is then built out of rectangular blocks $M(i, j)$ of sizes 3×3 , 3×1 , 1×3 , and 1×1 , defined as follows:

- if i is a white interior vertex and j is a black interior vertex incident to i , then $M(i, j)$ is a 3×3 identity matrix;
- if i is a white interior vertex and j is an edge incident to i and a black boundary vertex v , then $M(i, j)$ is the column vector $x(v)$;
- if j is a black interior vertex and i is an edge incident to j and a white boundary vertex v , then $M(i, j)$ is the row (co)vector $y(v)$;
- otherwise, $M(i, j)$ consists entirely of zeroes.

It is straightforward to check that $\det(M(D)) = \pm[D]$. (The sign depends on the ordering of the rows and columns in $M(D)$.) It is also easy to see directly that $\det(M(D))$ is an SL_3 invariant.

We illustrate this construction for the tensor diagram shown in Figure 3(d), using the notation introduced in Example 4.2. The recipe described above gives

$$M(D) = \left[\begin{array}{ccc|ccc|cc} 1 & 0 & 0 & x_{11} & x_{12} & 0 & 0 \\ 0 & 1 & 0 & x_{21} & x_{22} & 0 & 0 \\ 0 & 0 & 1 & x_{31} & x_{32} & 0 & 0 \\ \hline 1 & 0 & 0 & 0 & 0 & x_{12} & x_{13} \\ 0 & 1 & 0 & 0 & 0 & x_{22} & x_{23} \\ 0 & 0 & 1 & 0 & 0 & x_{32} & x_{33} \\ \hline y_1 & y_2 & y_3 & 0 & 0 & 0 & 0 \end{array} \right].$$

It is then easy to see that

$$-\det(M(D)) = \det \begin{bmatrix} x_{11} & x_{12} & x_{13} \\ x_{21} & x_{22} & x_{23} \\ x_{31} & x_{32} & x_{33} \end{bmatrix} (x_{12}y_1 + x_{22}y_2 + x_{32}y_3),$$

matching (4.2).

The calculus of tensor diagrams includes natural counterparts for both the additive and the multiplicative structures in the ring of invariants. For the former, allow formal linear combinations of tensor diagrams, and extend the definition of $[D]$ by linearity. For the latter, use superposition of diagrams: if D is a union of subdiagrams D_1, D_2, \dots connected only at boundary vertices, then $[D] = [D_1][D_2] \cdots$; cf. Figure 5.

The Weyl generators of the ring $R_{a,b}(V)$ are encoded by the simplest possible tensor diagrams: two types of *tripods* (corresponding to two kinds of Plücker coordinates) and simple edges. To rephrase, one takes each of the three types of building blocks shown in Figure 2 and attaches it directly to the boundary vertices. The First Fundamental Theorem implies that any $SL(V)$ invariant can be represented (non-uniquely) as a linear combination of invariants associated with tensor diagrams obtained by superposition of tripods and edges.

An important class of relations among invariants associated with tensor diagrams on an oriented plane is obtained from *local transformation rules*. Such a rule transforms a small fragment F of a tensor diagram D into a linear combination $\sum_i c_i F_i$ of other such pieces (corresponding to tensors of the same type) while keeping the rest of the diagram intact. The intrinsic definition of the invariants $[D]$ implies that if $[F] = \sum_i c_i [F_i]$ (i.e., the tensor does not change locally), then $[D] = \sum_i c_i [D_i]$, where D_i denotes the tensor diagram obtained from D by replacing F by F_i .

Figure 6 shows several fundamental relations of this kind. Checking their validity is straightforward.

Several basic relations involving boundary vertices are shown in Figure 7.

Figure 8 shows a few additional relations which are immediate from the definition of the invariants associated with tensor diagrams. These relations can also be deduced from those in Figure 6.

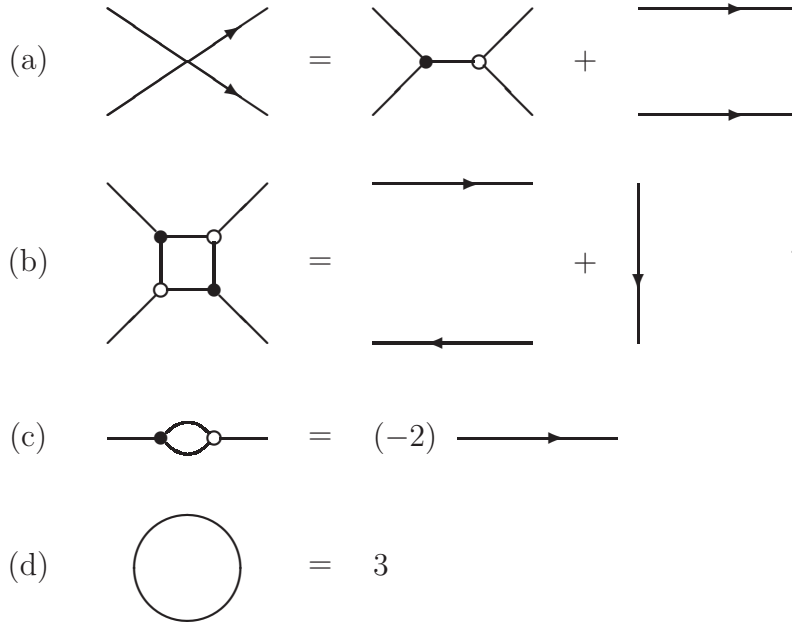


Figure 6: Skein relations for tensor diagrams. All edges are oriented towards their black endpoints. The cycle in relation (d) can be oriented either way. Kuperberg [35] gives q -versions of relations (a), (c) and (d).

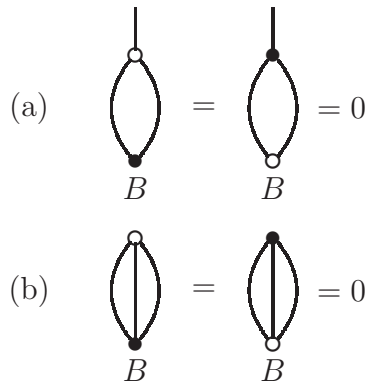


Figure 7: Local relations involving a vertex B lying on the boundary.

It is possible to develop a diagrammatic calculus based on the local relations listed above without making any mention of tensors or the special linear group SL_3 ; see in particular [35] and references therein. Such diagrammatic calculus, and its q -analogues, can in particular be used to construct invariants of knots and links. We do not discuss these connections in this paper.

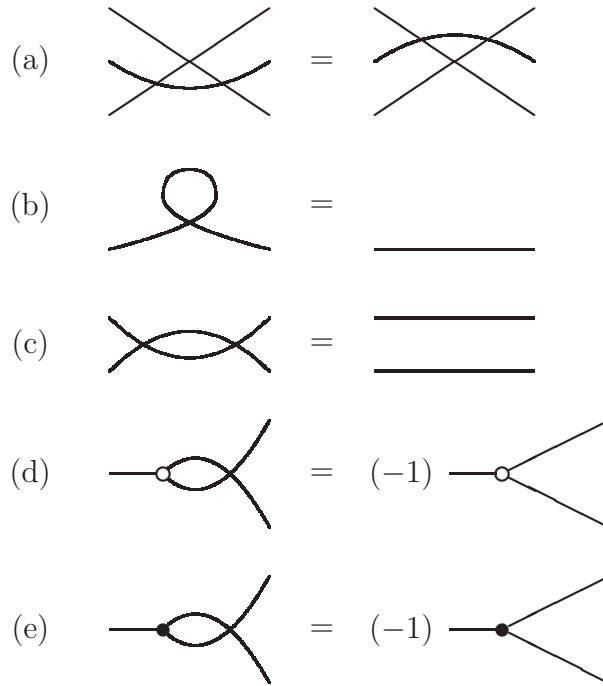


Figure 8: Yang-Baxter-type relations for tensor diagrams. In relations (a)–(c), edge orientations on the left-hand sides can be arbitrary; the orientations on each right-hand side should match those on the left.

5. WEBS

Informally speaking, webs are *planar* tensor diagrams. The systematic study of webs was pioneered by G. Kuperberg [35] whose foundational results are reviewed below, in slightly different terminology.

Definition 5.1 (Webs). A (planar) *web* is a tensor diagram D embedded in an oriented disk as described above in Section 4, so that its edges do not cross or touch each other, except at endpoints. Each web is considered up to an isotopy of the disk that fixes its boundary—so it is in essence a combinatorial object.

Recall that the boundary (respectively internal) vertices of D must lie on the boundary (respectively in the interior) of the disk, and the three edges meeting at each internal vertex are viewed as cyclically ordered clockwise.

A web is called *non-elliptic* if it has no multiple edges, and no 4-cycles whose all four vertices are internal.

An invariant $[D]$ associated with a non-elliptic web D is called a *web invariant*.

A web D of type (a, b) has a white boundary vertices and b black ones. The cyclic pattern of colors of the boundary vertices is encoded by the (cyclic) *signature* of D (cf. a similar notion introduced in Section 2), a cyclically ordered binary string, or more precisely a word in the alphabet $\{\bullet, \circ\}$ considered up to a cyclic permutation. For example, the webs in Figures 4–5 have signature

$$[\bullet \bullet \bullet \circ] = [\bullet \bullet \circ \bullet] = [\bullet \circ \bullet \bullet] = [\circ \bullet \bullet \bullet]$$

The following highly nontrivial result is the cornerstone of the theory of webs.

Theorem 5.2 (G. Kuperberg [35]). *Web invariants with a fixed signature σ of type (a, b) form a linear basis in the ring of invariants $R_\sigma(V) \cong R_{a,b}(V)$.*

Being a special kind of tensor diagrams, webs have *multidegrees*, cf. (4.3); the invariants they define are multi-homogeneous. Kuperberg’s theorem can be restated as saying that web invariants with a fixed signature σ and a fixed multidegree make up a linear basis in the corresponding multi-homogeneous component of $R_\sigma(V)$.

Example 5.3. For the ring of invariants $R_{4,2}(V)$, choose the signature

$$\sigma = [\bullet \circ \bullet \circ \circ \circ]$$

and the multidegree $(1, 1, 1, 1, 2, 1)$. There are 5 non-elliptic webs of such signature and multidegree, shown in Figure 9 at the top. Thus the corresponding multi-homogeneous component of $R_\sigma(V) \cong R_{4,2}(V)$ is 5-dimensional.

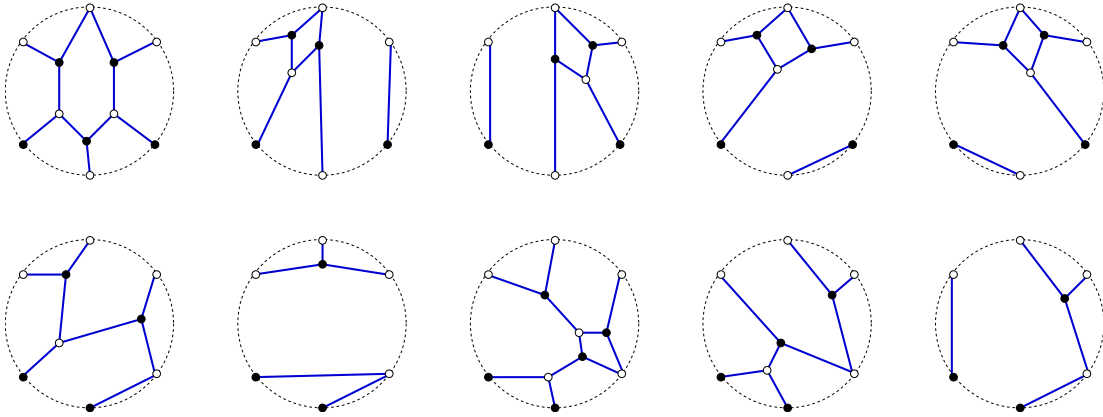


Figure 9: Two web bases in a multi-homogeneous component of $R_{4,2}(V)$.

Remark 5.4. Theorem 5.2 implies that the number of non-elliptic webs of given multidegree does not depend on the choice of a signature of given type (a, b) . To illustrate, continue with Example 5.3. Taking instead the signature $[\bullet \bullet \circ \circ \circ \circ]$ of the same type $(4, 2)$, and choosing the multidegree $(1, 1, 1, 1, 1, 2)$ —so that, as before, the invariants in question are multilinear in all arguments except for a single covector—we get the 5 webs (same number!) shown in Figure 9 at the bottom.

Remark 5.5. Any linear combination of tensor diagrams can be transformed into a linear combination of non-elliptic webs by repeated application of local relations shown in Figures 6–7. (Just apply them left-to-right.) It follows that $R_\sigma(V)$ is spanned by the web invariants. The content of Theorem 5.2 is that web invariants are linearly independent, so the reduction process described above is *confluent*.

Theorem 5.2 implies that two linear combinations of tensor diagrams define the same invariant if and only if they can be transformed into each other using the relations in Figures 6–7.

Remark 5.6. It is tempting to hypothesize, as M. Khovanov and G. Kuperberg originally did [31], that the web basis in a space of multilinear invariants (of some fixed signature) coincides with the corresponding instance of G. Lusztig’s *dual canonical basis* (see [31] for definitions and references). Their investigation however established that web bases for SL_3 are generally *not* dual canonical. The first discrepancy occurs in degree 12, for the signature $\bullet\bullet\circ\circ\bullet\circ\circ\bullet\bullet\circ\circ$. See Section 11.2 for a cluster-theoretic interpretation of this counterexample.

A *closed* tensor diagram (without boundary vertices) represents a tensor of type $(0, 0)$, *i.e.* a scalar. This scalar has the following direct description.

Proposition 5.7. *Let D be a closed web with m white and m black vertices. Then $[D]$ is equal to $(-1)^m$ times the number of proper colorings of the edges of D into three colors. (That is, we require the colors of the three edges incident to each vertex of D to be distinct.)*

The simplest illustration of Proposition 5.7 is provided by formula (d) in Figure 6 (with $m = 0$). A more interesting example: let D be the 1-skeleton of the (three-dimensional) cube; then $[D] = 24$.

The proof of Proposition 5.7 is omitted; we do not rely on it elsewhere in the paper.

6. SPECIAL INVARIANTS

Fix a (cyclic) signature σ of type (a, b) with $a + b \geq 5$. We assume that σ is *non-alternating*, *i.e.*, it has two adjacent vertices of the same color. In this section, we construct a family of “special” elements in the ring of invariants $R_\sigma(V) \cong R_{a,b}(V)$. These special invariants will play a key role in our main construction.

The proofs of the propositions stated in Sections 6–7 are given in Section 12.

As before, we work in a disk with $a + b$ marked points (vertices) on the boundary, a of them white and b of them black, arranged in accordance with the signature σ . We label these vertices $1, \dots, a + b$, going clockwise, and work with them modulo $a + b$.

For each boundary vertex p , we next define two trees Λ_p and Λ^p embedded into our disk. These trees will then serve as building blocks for certain tensor diagrams.

If the vertex p is black, then Λ_p has one vertex, namely p , and no edges. If p is white, then place a new black vertex (which we call the *proxy* of p) inside the disk and connect it to p . We then examine $p + 1$. If $p + 1$ is white, then we connect it to the proxy vertex, and stop; see Figure 10(a). If p is white and $p + 1$ is black, then we look at $p + 2$. If $p + 2$ is black, then put a white vertex inside the disk, connect it to both $p + 1$ and $p + 2$, and to the proxy vertex; see Figure 10(b). If p is white, $p + 1$ is black, and $p + 2$ is white, then examine $p + 3$, and so on, *cf.* Figure 10(c). In general, we proceed clockwise from p until we find two consecutive vertices of the same color (here we need the condition that σ is non-alternating), then build a caterpillar-like bi-colored tree whose all interior vertices have degree 3 except for the proxy vertex which has degree 2.

The graph Λ^p is defined in the same way, with the colors swapped. The proxy vertex is defined analogously (if p is white).

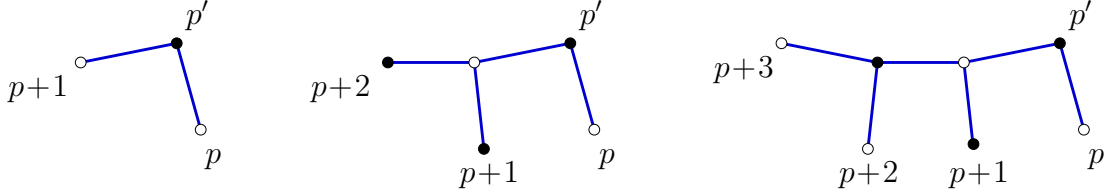


Figure 10: Trees Λ_p . The proxy vertex is denoted by p' .

At the next stage, we stitch together several caterpillar trees to build tensor diagrams. In anticipation of this stage, we draw each of these trees without self-intersections, and sufficiently close to the boundary of the disk, so as to avoid ambiguities later on related to the choice of cyclic ordering at each vertex of the tensor diagram.

Definition 6.1 (*Special invariants*). Let p and q be boundary vertices, $p \neq q$. The special invariant J_p^q is defined by the tensor diagram obtained by connecting the trees Λ_p and Λ^q by a single edge. One of its endpoints is p if the latter is black, or else take the proxy of p . The other endpoint is q if the latter is white, or else take the proxy of q . Make sure the connector edge approaches every proxy vertex from the same side where the disk's center lies. See Figure 11 for a couple of examples.

Now, let p, q, r be distinct boundary vertices, ordered clockwise. The special invariants J_{pqr} and J^{pqr} are defined by tensor diagrams constructed in a similar fashion to those used for J_p^q . For J_{pqr} , place a white vertex in the middle, and draw edges from it to each of $\Lambda_p, \Lambda_q, \Lambda_r$. As the other endpoints of these three edges, use the vertices p, q, r whenever they are black, or else take their respective proxies. For J^{pqr} , reverse the roles of the colors. See Figure 11.

Finally, let p, q, r, s be four boundary vertices, ordered clockwise. The invariant J_{pq}^{rs} is defined by the tensor diagram obtained as follows. Place a white vertex W and a black vertex B near the center of the disk. Connect them by an edge. Connect W to Λ_p and Λ_q using p and q if these two are black, or else using their proxies as needed. Similarly, connect B to the appropriate white vertices in Λ^r and Λ^s . Make sure that the five edges incident to B and W do not cross each other.

Some special invariants are identically equal to zero. The vanishing invariants of the form J_p^q are identified in the following proposition, whose straightforward proof we omit.

Proposition 6.2. *If the vertices p and q are not adjacent, then J_p^q is a nontrivial invariant. If p and q are adjacent, then exactly one of the two invariants J_p^q and J_q^p vanishes. Specifically, if p is white, then $J_p^{p+1} = 0$; if p is black, then $J_{p+1}^p = 0$.*

For example, for the signature in Figure 11 we have $J_1^2 = J_2^3 = J_3^4 = J_4^5 = J_5^6 = J_6^7 = J_7^8 = J_8^1 = 0$.

Some nonzero special invariants are equal to each other. We do not catalogue all such instances (although we could). Cf. the caption to Figure 11.

Proposition 6.3. *Each nonzero special invariant is a web invariant.*

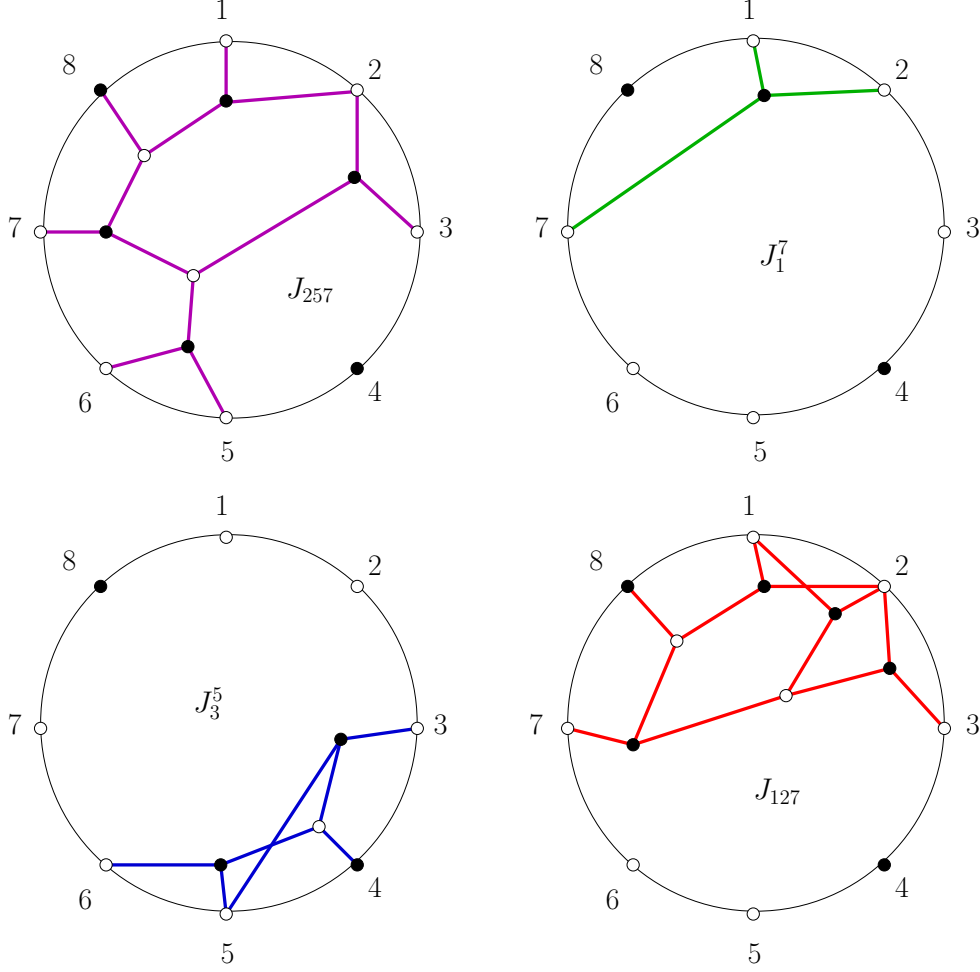


Figure 11: Examples of special invariants for $\sigma = [\circ\circ\circ\bullet\circ\circ\circ\bullet]$. Note that $J_{257} = J_{25}^{78}$, $J_1^7 = J^{127}$, $J_3^5 = J^{345}$.

To illustrate, refer to Figure 11. While the two tensor diagrams in the top row are non-elliptic webs, the ones in the bottom row are not. They can however be transformed using skein relations into the non-elliptic webs shown in Figure 12.

The following proposition is straightforwardly verified.

Proposition 6.4. *Special invariants satisfy the following factorization identities:*

- (1) if p is white and $p+1$ is black, then $J_p^{p+2} = J_{p+2}^p J_{p+1}^{p+2}$;
- (2) if p is white, $p+1$ is black, and $p+2$ is white, then $J_p^{p+3} = J_{p+1}^{p+3} J_{p+2}^p$;
- (3) if p is white, then $J_{p,p+1,q} = J_{p+1}^p J_q^{p+1}$;
- (4) if p is white and $p+1$ is black, then $J_{p,p+2,q} = J_{p+2}^p J_q^{p+1}$;
- (5) if p is white, then $J_{p,p+1}^{q,r} = J_{p+1}^p J_{p+1,q,r}^{p+1}$;
- (6) if p is white, then $J_{rp}^{p+1,q} = J_r^{p+1} J_p^q$;
- (7) if p is white and $p+1$ is black, then $J_{p,p+2}^{qr} = J_{p+2}^p J_{p+1,q,r}^{p+1}$;

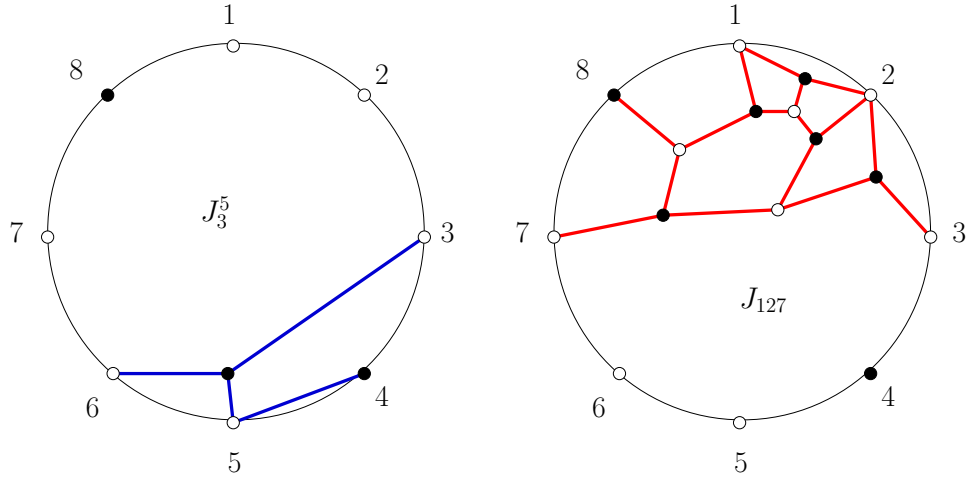


Figure 12: J_3^5 and J_{127} are web invariants.

(8) if the colors are reversed (i.e., p is black, etc.), then switch the colors and swap subscripts with superscripts in rules (1)–(7) above.

We next show that “almost all” special invariants are *irreducible* elements of $R_\sigma(V)$. Incidentally, [48, Theorem 3.17] asserts that $f \in R_\sigma(V)$ is irreducible (as an element of $R_\sigma(V)$) if and only if f is an irreducible polynomial. In other words, if an $SL(V)$ -invariant polynomial f factors nontrivially in the polynomial ring $\mathbb{C}[(V^*)^a \times V^b]$, then the factors must be $SL(V)$ -invariant. We will not rely on this result.

Proposition 6.5. *A nonzero special invariant is irreducible unless it fits one of the descriptions listed in Proposition 6.4.*

In our running example of signature $\sigma = [\circ \circ \circ \bullet \circ \circ \circ \bullet]$, the invariants J_{257} and J_1^7 are irreducible whereas J_3^5 and J_{127} are not: $J_3^5 = J_5^3 J_4^5$ and $J_{127} = J_8^2 J_2^1 J_1^7$.

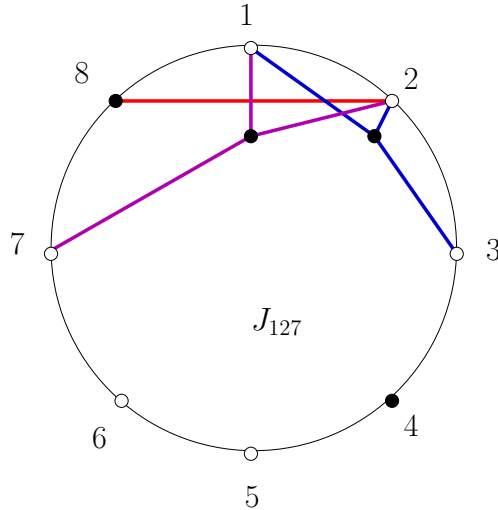


Figure 13: Factorization of J_{127} into irreducible special invariants

Proposition 6.6. *Each nonzero special invariant is represented uniquely as a product of irreducible special invariants.*

Such a factorization can be found by iterating the formulas (1)–(8); see Section 12.

Irreducible special invariants will eventually play the role of (a subset of) generators for the cluster structure in $R_\sigma(V)$.

We call two special invariants *compatible* if their product is a single web invariant. This terminology will prove consistent with the notion of compatibility of cluster variables; cf. Conjecture 9.2. The reader is welcome to check (this may take some time) that the four special invariants in Figure 11 are pairwise compatible.

Proposition 6.7. *Let σ be a signature of type (a, b) , with $a + b \geq 5$, $a \leq b$, and $\sigma \neq [\bullet \circ \bullet \circ \bullet]$. Then there are $a + b$ special invariants compatible with all special invariants. These $a + b$ invariants are the (irreducible) nonzero invariants of the form $J_p^{p \pm 1}$. Moreover the product of any of them and any web invariant is a web invariant.*

Anticipating their future role, we call these special invariants *coefficient invariants*. We denote the $(a + b)$ -element set of these invariants by \mathbf{c}_σ . See Figure 14.

Remark 6.8. For $\sigma = [\bullet \circ \bullet \circ \bullet]$, the special invariant J_5^1 factors: $J_5^1 = J_3^5 J_4^2$. As a result, there are 6 coefficient invariants in this case, namely $J_1^2, J_3^2, J_3^4, J_4^4, J_5^5, J_4^2$.

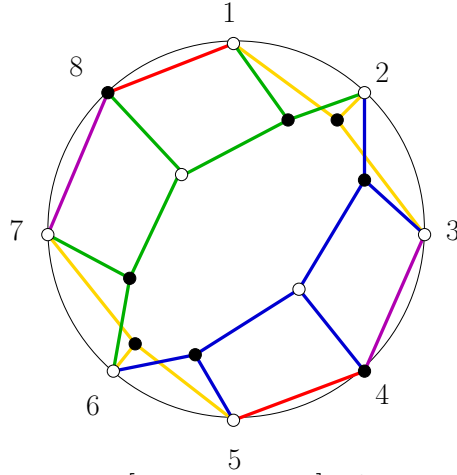


Figure 14: For the signature $\sigma = [\circ \circ \circ \bullet \circ \circ \circ \bullet]$, the set of coefficient invariants is $\mathbf{c}_\sigma = \{J_2^1, J_3^2, J_4^3, J_4^5, J_6^5, J_7^6, J_8^7, J_8^1\}$.

In order to write exchange relations for the cluster algebra $R_\sigma(V)$, we will need certain 3-term *skein relations* for special invariants.

Proposition 6.9. *Let p, q, r (respectively p, q, r, s) be distinct boundary vertices, listed in clockwise order. Then*

$$(6.1) \quad J_{pqr} J^{pqr} = J_r^p J_q^r J_p^q + J_r^q J_p^r J_q^p;$$

$$(6.2) \quad J_p^r J_{qrs} = J_q^r J_{prs} + J_s^r J_{pqr};$$

$$(6.3) \quad J_p^r J_s^q = J_s^r J_p^q + J_{sp}^{qr};$$

$$(6.4) \quad J_p^r J_{rs}^{pq} = J_p^q J_r^p J_s^r + J_{prs} J^{pqr};$$

$$(6.5) \quad J_r^p J_{sp}^{qr} = J_r^q J_s^p J_p^r + J_{prs} J^{pqr}.$$

It is important to note that identities (6.1)–(6.5) hold irrespective of the choice of the signature σ . For some of those choices, these identities are illustrated in Figure 15.

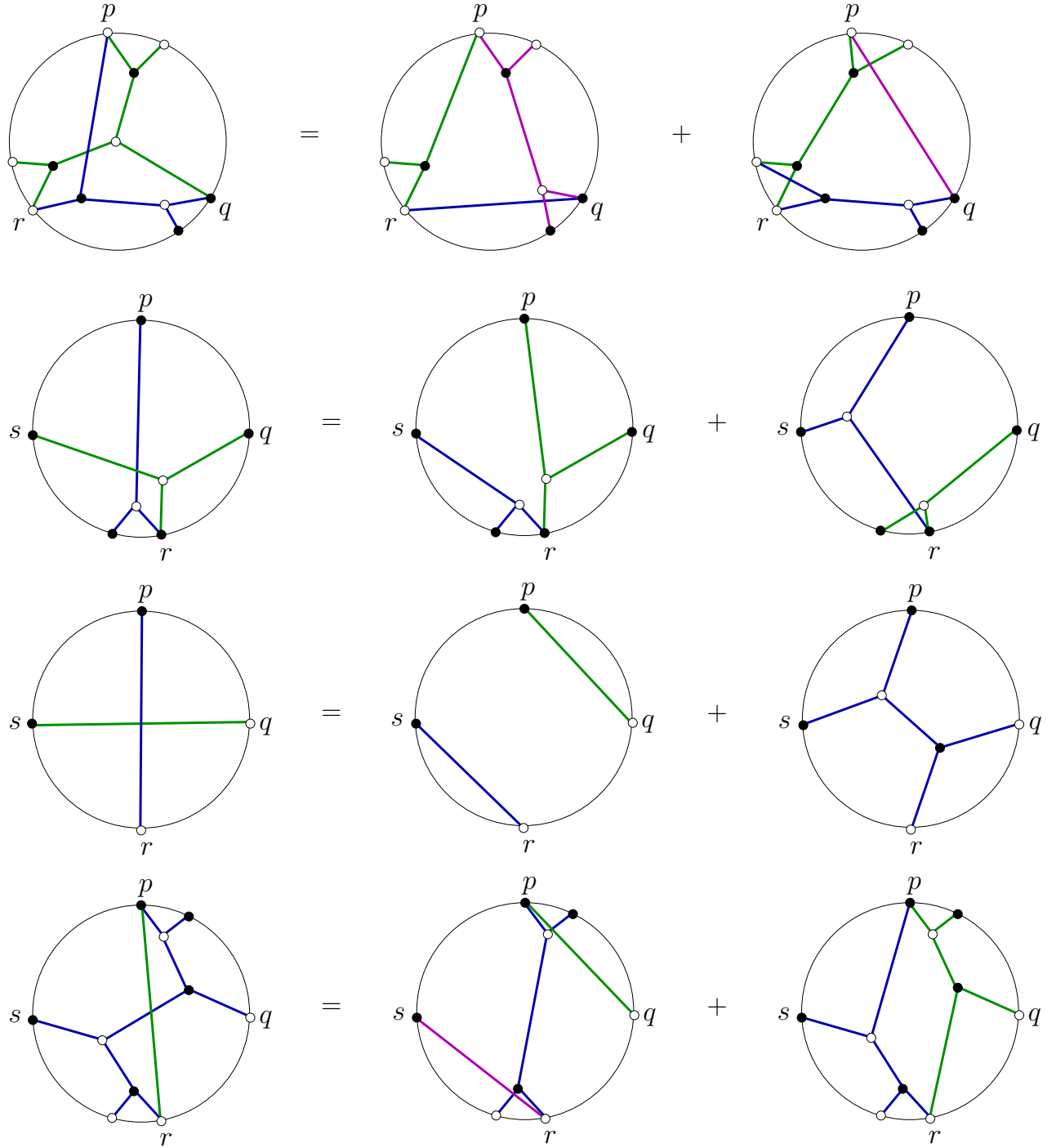


Figure 15: 3-term skein relations (6.1)–(6.4).

Remark 6.10. In each of identities (6.1)–(6.5), some special invariants might be equal to 0, while others might factor further. After everything is expressed in terms of irreducible special invariants, we either get a tautological formula $A = A$, or else a genuine 3-term relation. We call the latter relation the *distilled form* of the original one. While the distilled relation is always a skein relation of some sort, it does not have to be an instance of (6.1)–(6.5); an example is given in (6.6).

Example 6.11. Let $\sigma = [\circ \circ \circ \bullet \circ \circ \circ \bullet]$ as before. One instance of equation (6.1) is $J_{127} J^{127} = J_7^1 J_2^7 J_1^2 + J_7^2 J_1^7 J_2^1$. This does not yield a nontrivial identity: after substituting $J_1^2 = 0$, $J_{127} = J_8^2 J_2^1 J_1^7$, $J^{127} = J_1^7$, and $J_7^2 = J_8^2 J_1^7$, everything cancels out.

A more interesting example is $J_7^2 J_{258} = J_8^2 J_{257} + J_5^2 J_{278}$ (cf. (6.2)). Substituting the factorizations $J_7^2 = J_8^2 J_1^7$ and $J_{278} = J_8^7 J_8^2 J_2^1$ and simplifying, we get

$$(6.6) \quad J_1^7 J_{258} = J_8^7 J_5^2 J_2^1 + J_{257}.$$

7. SEEDS ASSOCIATED TO TRIANGULATIONS

In this section, we construct a family of distinguished seeds in (the quotient field of) the ring $R_\sigma(V) \cong R_{a,b}(V)$. These seeds will be used in Section 8 to define a cluster algebra structure in $R_\sigma(V)$.

Definition 7.1. Let T be a triangulation of our $(a + b)$ -gon by its diagonals. Let $K(T)$ be the collection of special invariants built as follows:

- for each diagonal or side pq in T , include J_p^q and J_q^p ;
- for each triangle pqr in T (here p, q, r are ordered clockwise), include J_{pqr} .

The *extended cluster* $\mathbf{z}(T)$ consists of all irreducible special invariants which appear in factorizations of nonzero elements of $K(T)$ into irreducibles. The *cluster* $\mathbf{x}(T) = \mathbf{z}(T) \setminus \mathbf{c}_\sigma$ consists of all non-coefficient invariants in $\mathbf{z}(T)$.

Theorem 7.2. *For any triangulation T as above, the following holds:*

- *the extended cluster $\mathbf{z}(T)$ contains the entire set \mathbf{c}_σ of coefficient invariants;*
- *$\mathbf{z}(T)$ consists of $3(a + b) - 8$ invariants;*
- *all special invariants in $\mathbf{z}(T)$ are pairwise compatible.*

Example 7.3. Let $\sigma = [\circ \circ \circ \bullet \circ \circ \circ \bullet]$. Then

$$\mathbf{c}_\sigma = \{J_2^1, J_3^2, J_4^3, J_4^5, J_6^5, J_7^6, J_8^7, J_8^1\}$$

(see Figure 14). For the triangulation T shown in Figure 16 on the left, we have

$$K(T) = \mathbf{c}_\sigma \cup \{J_7^1, J_1^7, J_2^7, J_7^2, J_2^5, J_5^2, J_7^5, J_5^7, J_5^3, J_3^5, J_{127}, J_{178}, J_{257}, J_{235}, J_{567}\}.$$

Now, $J_{178} = J_{345} = 0$ and $J_5^7 = J_6^5$, while several other elements of $K(T)$ factor:

$$J_7^1 = J_8^1 J_1^7, \quad J_7^2 = J_8^2 J_1^7, \quad J_3^5 = J_4^5 J_5^3, \quad J_{127} = J_8^2 J_2^1 J_1^7, \quad J_{235} = J_5^3 J_3^2, \quad J_{567} = J_6^5 J_7^6.$$

We conclude that $\mathbf{z}(T) = \mathbf{c}_\sigma \cup \mathbf{x}(T)$ where

$$(7.1) \quad \mathbf{x}(T) = \{J_8^2, J_2^7, J_1^7, J_2^5, J_5^2, J_7^5, J_5^3, J_{257}\}.$$

Figure 17 shows the webs corresponding to the elements of $\mathbf{x}(T)$.

Surprisingly, different triangulations may define the same cluster.

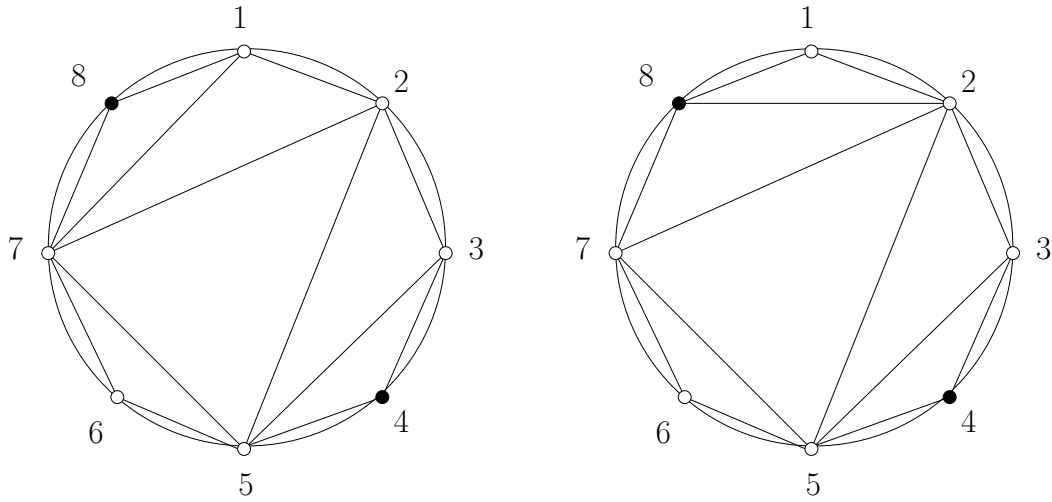


Figure 16: Triangulations T and T' of an octagon, $\sigma = [\circ \circ \circ \bullet \circ \circ \circ \bullet]$.

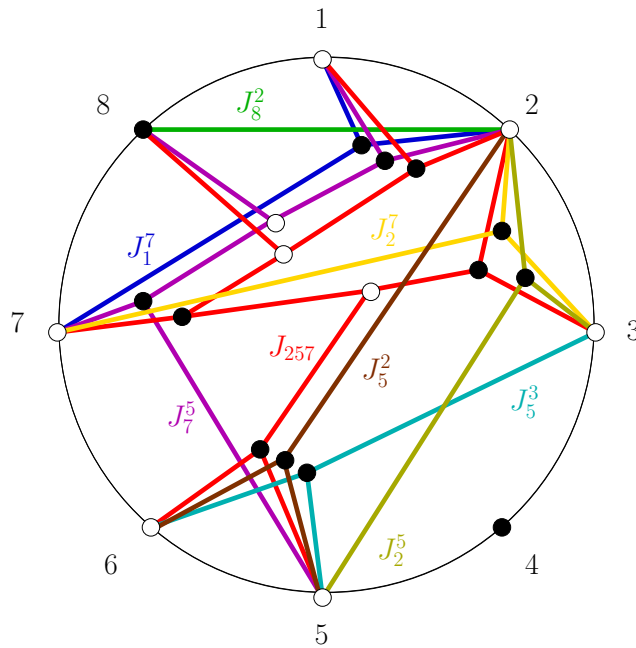


Figure 17: Cluster associated with the triangulations shown in Figure 16.

Proposition 7.4. *Let T and T' be triangulations which contain the diagonal $q(q+3)$ and coincide outside the quadrilateral $q(q+1)(q+2)(q+3)$. If the colors of the vertices $(q, q+1, q+2)$ alternate, then $\mathbf{x}(T) = \mathbf{x}(T')$.*

Example 7.5. The two triangulations in Figure 16 yield the same cluster. (Apply Proposition 7.4 with $q=7$.) To check this directly, refer to Example 7.3, write

$$K(T') = \{J_8^2, J_2^8, J_{128}, J_{278}\} \cup K(T) \setminus \{J_7^1, J_1^7, J_{127}, J_{178}\},$$

and use the factorizations $J_2^8 = J_8^2 J_2^1$, $J_{128} = J_8^2 J_2^1$, and $J_{278} = J_8^7 J_8^2 J_2^1$.

To complete our construction, we need to describe the quivers $Q(T)$ which, together with the extended clusters $\mathbf{z}(T)$, will form the seeds defining a cluster algebra structure in the ring R_σ . To put it differently, we need to write the corresponding exchange relations (3.1). These are obtained from the 3-term skein relations (6.1)–(6.5) using a couple of additional observations.

Let T be a triangulation as in Definition 7.1. If pqr and prs are triangles in T , then by construction the first factor on the left-hand side of each relation (6.1)–(6.5) is an element of $K(T)$. In order for such a relation (or rather its distilled form, see Remark 6.10) to be a good candidate for an exchange relation out of the extended cluster $\mathbf{z}(T)$, we would like the terms on the right-hand side to factor into the elements of $\mathbf{z}(T)$. For (6.1)–(6.2), this is true by design; for (6.3)–(6.5), the terms J_{sp}^{qr} and J^{pqr} will only have the requisite property in some special cases.

We say that a side pq of a triangle pqr is *exposed* if it lies on the boundary of the $(a + b)$ -gon; in other words, pq is exposed if $q = p + 1$.

Proposition 7.6. *Suppose a triangle pqr has an exposed side. Then*

$$J^{pqr} \in \{J_p^r, J_q^p, J_r^q, J_p^q J_r^q, J_q^r J_p^p, J_r^p J_p^q\}$$

(which element of this set J^{pqr} is equal to depends on the signature).

Proposition 7.7. *Let $(p, p + 1, p + 2, s)$ be distinct vertices of the $(a + b)$ -gon.*

$$(7.2) \quad \text{If } p \text{ is white and } p + 1 \text{ is black, then } J_{p+2}^p J_{p+1}^s = J_{p+1}^p J_{p+2}^s + J_p^s.$$

$$(7.3) \quad \text{If } p \text{ is black and } p + 1 \text{ is white, then } J_p^{p+2} J_s^{p+1} = J_p^{p+1} J_s^{p+2} + J_s^p.$$

Definition 7.8 (*Exchange relations for a cluster associated with a triangulation*).

Continuing in the setting of Definition 7.1, write the following identities:

- for each triangle pqr of the triangulation T , write formula (6.1);
- for each diagonal pr in T separating triangles pqr and prs :
 - write formula (6.2);
 - if one of the sides of pqr is exposed, write (6.4)–(6.5);
 - if two sides of pqr are exposed, write the appropriate instance of (7.2) or (7.3), if applicable.

It is easy to check, with the help of Proposition 7.6, that each of the two monomials on the right-hand side of each of resulting relations will either vanish (in which case the relation is of no use to us) or else factor into nontrivial irreducibles. In the latter case, we distill the relation (see Remark 6.10) to obtain a 3-term relation in irreducible special invariants all of which, with the exception of the second factor on the left, will belong to $\mathbf{z}(T)$.

To obtain the final list of exchange relations, we should also inspect all instances where we can apply Proposition 7.4 to get another triangulation T' with the same cluster $\mathbf{x}(T') = \mathbf{x}(T)$, then check whether applying the above recipe to T' yields any additional 3-term relations.

A few simple observations help reduce the amount of work required to write the 3-term relations of Definition 7.8 for a particular choice of T and σ . For example, if a triangle pqr has an exposed side, then one of the terms on the right-hand side of (6.1)

vanishes, by virtue of Proposition 6.2. Thus, we only need to write relations (6.1) for the triangles whose all sides are diagonals.

Proposition 7.9. *For any triangulation T of the $(a+b)$ -gon, the procedure described in Definition 7.8 yields as many relations as there are elements in the cluster $\mathbf{x}(T)$. More precisely, it yields one relation of the form*

$$xx' = M_1 + M_2$$

for each $x \in \mathbf{x}(T)$; here M_1, M_2 are monomials in the elements of $\mathbf{z}(T)$.

We are now ready to define the quiver associated with a given triangulation of the $(a+b)$ -gon.

Definition 7.10. The quiver $Q(T)$ associated with a triangulation T is constructed so that the exchange relations (3.1) match the 3-term relations obtained via the process described in Definition 7.8. This requirement defines $Q(T)$ up to simultaneous reversal of direction of all edges incident to any subset of connected components of the mutable part of the quiver. Typically, there will be a single connected component, so that $Q(T)$ is defined up to a global change of orientation. It is not hard to see that the choice of a particular incarnation of $Q(T)$ is inconsequential, as the resulting cluster structure will not depend on this choice. To simplify presentation, we henceforth use the notation $Q(T)$ without mentioning its ambiguity.

Example 7.11. We continue with the triangulation T discussed in Example 7.3; cf. Figure 16 on the left. The only relevant instance of formula (6.1) is

$$J_{257} J^{257} = J_7^2 J_5^7 J_2^5 + J_7^5 J_2^7 J_5^2 \quad (\text{for } p = 2, q = 5, r = 7).$$

After factoring J_7^2 into irreducibles and substituting $J_5^7 = J_6^5$ (so as to use consistent notation for the coefficient invariants), we obtain

$$(7.4) \quad J_{257} J^{257} = J_8^2 J_1^7 J_6^5 J_2^5 + J_7^5 J_2^7 J_5^2.$$

Among 10 instances of (6.2), the nontrivial identities are (in distilled form):

$$(7.5) \quad J_2^7 J_5^8 = J_6^5 J_8^2 J_2^1 + J_{257} \quad (\text{for } p = 2, q = 5, r = 7, s = 1),$$

$$(7.6) \quad J_2^5 J_7^4 = J_{257} J_4^5 + J_3^2 J_7^5 \quad (\text{for } p = 2, q = 3, r = 5, s = 7),$$

$$(7.7) \quad J_5^2 J_7^3 = J_8^2 J_1^7 J_5^3 + J_{257} \quad (\text{for } p = 5, q = 7, r = 2, s = 3),$$

$$(7.8) \quad J_7^5 J_2^6 = J_2^5 J_7^6 + J_{257} \quad (\text{for } p = 7, q = 2, r = 5, s = 6).$$

For each of (6.4) and (6.5), there are 7 instances to check. Equation (6.4) produces one nontrivial relation:

$$(7.9) \quad J_8^2 J_{25}^7 = J_8^1 J_2^7 J_5^2 + J_{257} \quad (\text{for } p = 7, q = 1, r = 2, s = 5),$$

Equation (6.5) yields three relations—but all of them replicate those obtained earlier:

- for $p = 7, q = 1, r = 2, s = 5$, we get (7.5);
- for $p = 2, q = 3, r = 5, s = 7$, we get (7.7);
- for $p = 5, q = 6, r = 7, s = 2$, we get (7.8).

The rule (7.2) supplies two equations one of which results in a new nontrivial identity:

$$(7.10) \quad J_5^3 J_4^2 = J_4^3 J_5^2 + J_3^2 \quad (\text{for } p = 3, s = 2);$$

and there are no instances of (7.3).

We have obtained 7 exchange relations (7.4)–(7.10), one for each element of $\mathbf{x}(T)$ (cf. (7.1)) except for J_1^7 . To get the missing relation, we need to replace T by the triangulation T' shown in Figure 16 on the right. (Cf. Example 7.5). The only new relation is obtained by applying (6.2) with $p = 7, q = 8, r = 2, s = 5$. As explained in Example 6.11, this results in the equation (6.6):

$$(7.11) \quad J_1^7 J_{258} = J_8^7 J_5^2 J_2^1 + J_{257}.$$

The corresponding quiver $Q(T)$ has 16 vertices: 8 frozen, labeled by the coefficient invariants (see Figure 14), and 8 mutable, labeled by the elements of the cluster $\mathbf{x}(T)$ (see (7.1)). One by one, we draw the edges incident to each mutable vertex using the corresponding exchange relation (7.4)–(7.11), so as to match the formula (3.1). This occasionally requires swapping the two terms on the right-hand side.

The resulting quiver $Q(T)$ is shown in Figure 18. It has cluster type E_8 .

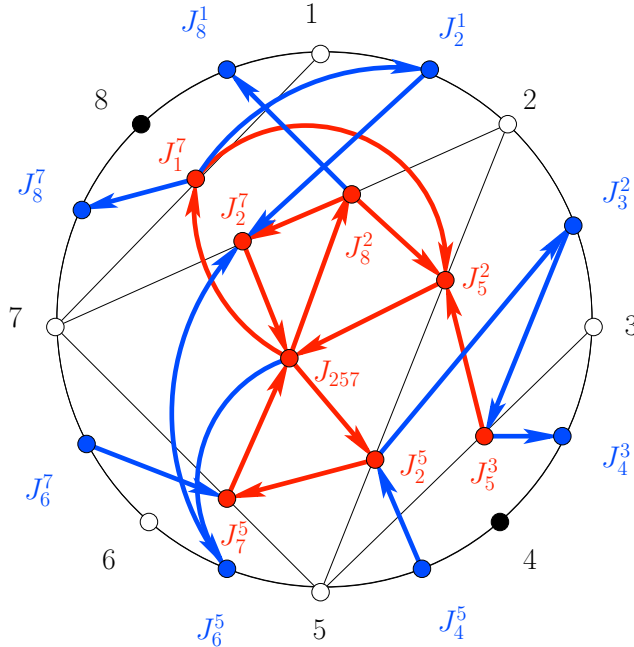


Figure 18: The quiver associated with the triangulations shown in Figure 16.

A general recipe for building the quiver $Q(T)$ associated with an arbitrary triangulation T of the polygon P_σ is described in Section 14.

Additional examples of seeds $(Q(T), \mathbf{z}(T))$ associated with particular triangulations T and signatures σ can be found in Sections 17 and 18.

Results and conjectures

8. MAIN RESULTS

After all the preparation of the preceding sections, the statement of our main theorem comes as no surprise: for any choice of a non-alternating cyclic signature, the construction described in Section 7 makes the ring of invariants $R_\sigma(V)$ into a cluster algebra. Here is a precise statement:

Theorem 8.1. *Let σ be a non-alternating cyclic signature of type (a, b) , let P_σ be a convex $(a + b)$ -gon with vertices colored according to σ , and let T be a triangulation of P_σ by its diagonals. Then the extended cluster $\mathbf{z}(T)$ and the quiver $Q(T)$ described in Definitions 7.1 and 7.10 form a seed in the quotient field of the ring of invariants $R_\sigma(V)$. The associated cluster algebra is $R_\sigma(V)$:*

$$R_\sigma(V) = \mathcal{A}(Q(T), \mathbf{z}(T)).$$

This cluster structure on $R_\sigma(V)$ does not depend on the choice of triangulation T .

Corollary 8.2. *Any element of $R_\sigma(V)$, and in particular any web invariant, can be expressed as a Laurent polynomial in the elements of any extended cluster $\mathbf{z}(T)$.*

For the record, we state below some basic properties of the cluster algebra $R_\sigma(V)$ that are immediate from its construction (as justified by Theorem 8.1).

Proposition 8.3. *The cluster algebra $R_\sigma(V)$ has the following properties:*

- (1) *The set of coefficient variables and cluster variables includes all irreducible special invariants, and in particular all Weyl generators.*
- (2) *The coefficient variables are the coefficient invariants (cf. Proposition 6.7).*
- (3) *Each extended cluster consists of $3(a + b) - 8$ elements;*
- (4) *The rank (the cardinality of each cluster) is $2(a + b) - 8$, except for the cases $\sigma = [\bullet \circ \bullet \circ \bullet]$ and $\sigma = [\circ \bullet \circ \bullet \circ]$ when it is equal to 1 (cf. Remark 6.8).*

Example 8.4. Let $a = 2$, $b = 3$, $\sigma = [\bullet \bullet \bullet \circ \circ]$. In this case, the cluster algebra $R_\sigma(V)$ has type A_2 . It has 5 coefficient variables, namely: J_{123} , J_{23}^{45} , J_3^4 , J_{12}^{45} , J_1^5 . (Some of these have alternative presentations, for example $J_{23}^{45} = J_{234} = J^{245} = J_2^3$.) The 5 cluster variables in $R_\sigma(V)$ are J_1^4 , J_2^4 , J_2^5 , J_3^5 , $J_{13}^{45} = J_{134} = J_1^3$. They form 5 clusters:

$$\{J_1^4, J_2^4\}, \{J_2^4, J_2^5\}, \{J_2^5, J_3^5\}, \{J_3^5, J_{13}^{45}\}, \{J_{13}^{45}, J_1^4\}.$$

The exchange relations are:

$$\begin{aligned} J_1^4 J_3^5 &= J_1^5 J_3^4 + J_{13}^{45}, \\ J_2^4 J_{13}^{45} &= J_{12}^{45} J_3^4 + J_{23}^{45} J_1^4, \\ J_2^5 J_1^4 &= J_{12}^{45} + J_1^5 J_2^4, \\ J_3^5 J_2^4 &= J_{23}^{45} + J_3^4 J_2^5, \\ J_{13}^{45} J_2^5 &= J_{23}^{45} J_1^5 + J_{12}^{45} J_3^5. \end{aligned}$$

Notice that the coefficient variable J_{123} does not appear in these relations. Accordingly, the frozen vertex corresponding to J_{123} is isolated in every quiver of $R_\sigma(V)$. One example of such a quiver is shown in Figure 19.

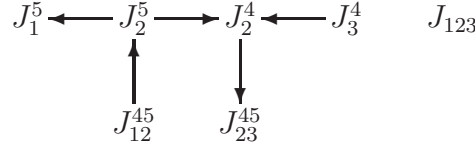


Figure 19: The quiver associated with the cluster $\{J_2^4, J_2^5\}$ in the cluster algebra $R_\sigma(V)$ with $\sigma = [\bullet \bullet \bullet \circ \circ]$.

While the cluster structure on $R_\sigma(V) \cong R_{a,b}(V)$ defined in Theorem 8.1 is independent of the choice of triangulation, it does critically depend on the signature σ . In fact, fixing the parameters a and b does not determine the cluster type of $R_\sigma(V)$, nor whether $R_\sigma(V)$ is of finite or infinite type. See Figure 20.

For each signature σ , there are choices of a triangulation T for which the construction of the quiver $Q(T)$ simplifies considerably. One such choice is presented in Section 17, providing an explicit rule for determining the (extended) cluster type of $R_\sigma(V)$ for any signature σ .

We next discuss the important special case $a = 0$ (ring of invariants of b vectors in 3-space), or equivalently the case of monochromatic signature

$$\sigma = [\bullet \bullet \bullet \cdots \bullet \bullet \bullet]$$

of type $(0, b)$. As mentioned in Section 3, cluster structures in the rings $R_{0,b}(V)$, and indeed in homogeneous coordinate rings of arbitrary Grassmannians $\text{Gr}_{k,b}$, were described by J. Scott [52] and extensively studied thereafter (cf., e.g., [25]).

Theorem 8.5. *The cluster algebra structure in the ring of invariants $R_{0,b}(V)$ (or equivalently in the homogeneous coordinate ring of the Grassmannian $\text{Gr}_{3,b}$) described in Theorem 8.1 coincides with the one given by J. Scott [52].*

In the Grassmannian case $a = 0$, our construction of seeds $(Q(T), \mathbf{z}(T))$ simplifies considerably, see Figure 21. This construction generalizes the one given by Scott [52] for a particular kind of triangulation T .

Example 8.6. For $b \leq 8$, the cluster algebras $R_{0,b}(V) \cong \mathbb{C}[\text{Gr}_{3,b}]$ are of finite type, so we can list all their generators explicitly. Unsurprisingly, we end up reproducing Scott’s original description of these generators [52] in the language of webs. In fact, Scott gave a geometric interpretation of these generators (for $b \leq 8$) which can be seen to match our construction.

The cluster types of the rings $\mathbb{C}[\text{Gr}_{3,b}]$, $b \leq 8$, are well known to be as follows: A_2 for $b = 5$, D_4 for $b = 6$, E_6 for $b = 7$, and E_8 for $b = 8$ (see, e.g., [16]; cf. Figure 20). The set of generators of each cluster algebra $R_{0,b}(V)$ includes the $\binom{b}{3}$ Plücker invariants $P_{pqr} = J_{pqr}$ given by tripod webs. Among them there are b coefficient variables of the form $P_{p,p+1,p+2}$.

For $b \geq 6$, there are also non-Plücker cluster variables. The simplest among them are the “hexapod” invariants given by webs of the kind shown in Figure 22 on the left. There are $2\binom{b}{6}$ of these hexapods in $R_{0,b}(V)$. For $b = 6$ and $b = 7$, the tripods and hexapods comprise the entire list of generators. For $b = 8$, there are 24 additional cluster variables, namely 8 (resp., 16) web invariants of the kind shown in the second (resp., third) picture in Figure 22.

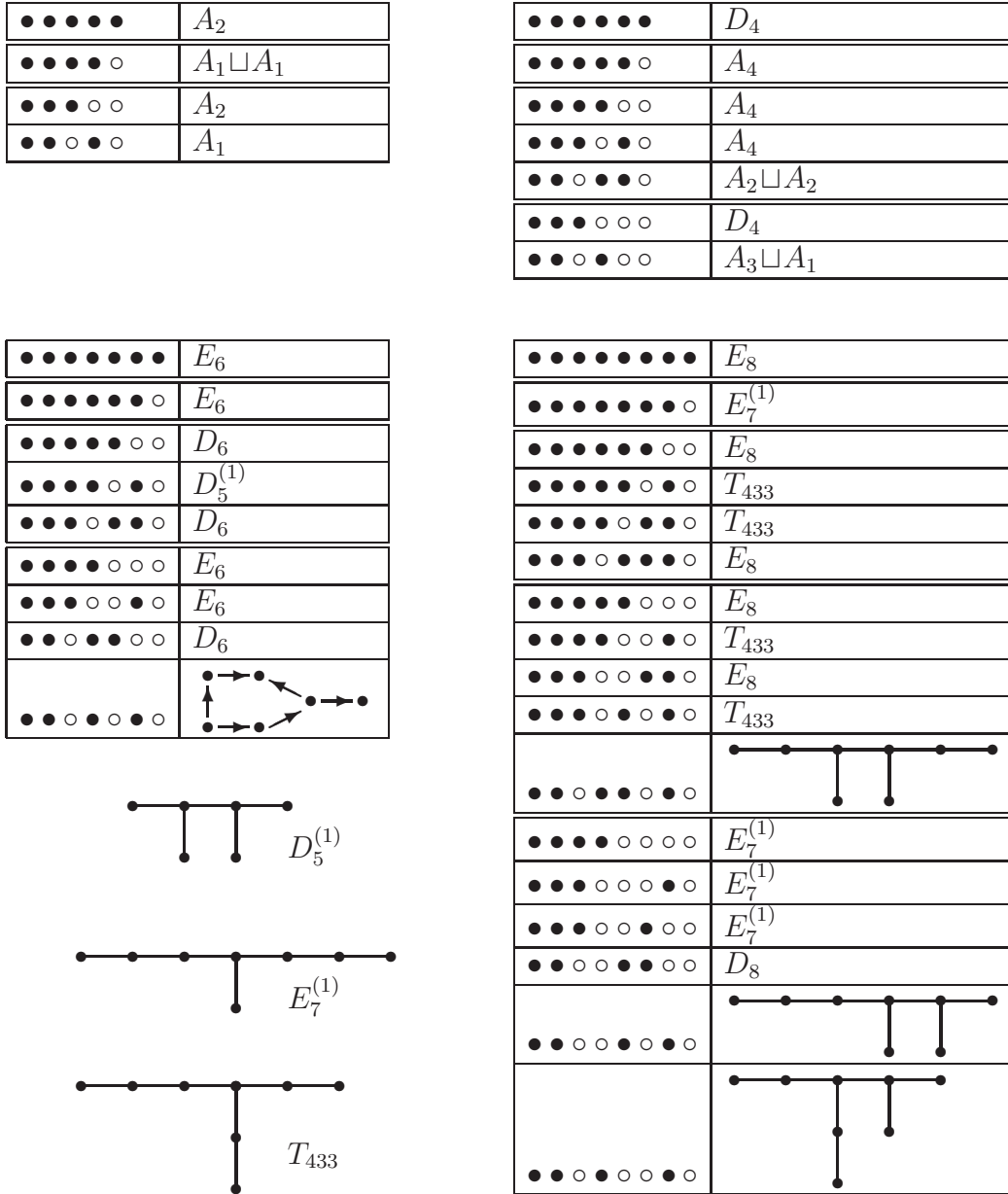


Figure 20: Cluster types of $R_\sigma(V)$ for non-alternating signatures σ of type (a, b) with $a+b \in \{5, 6, 7, 8\}$. These cluster types are invariant under dihedral symmetries and/or global change of coloring; we include one representative from each equivalence class. Take an arbitrary orientation of each tree to get the corresponding quiver.

Cluster algebra structures in rings of invariants $R_\sigma(V)$ behave nicely under two types of embeddings of such rings into one another. To state these results, we will need the following natural definition.

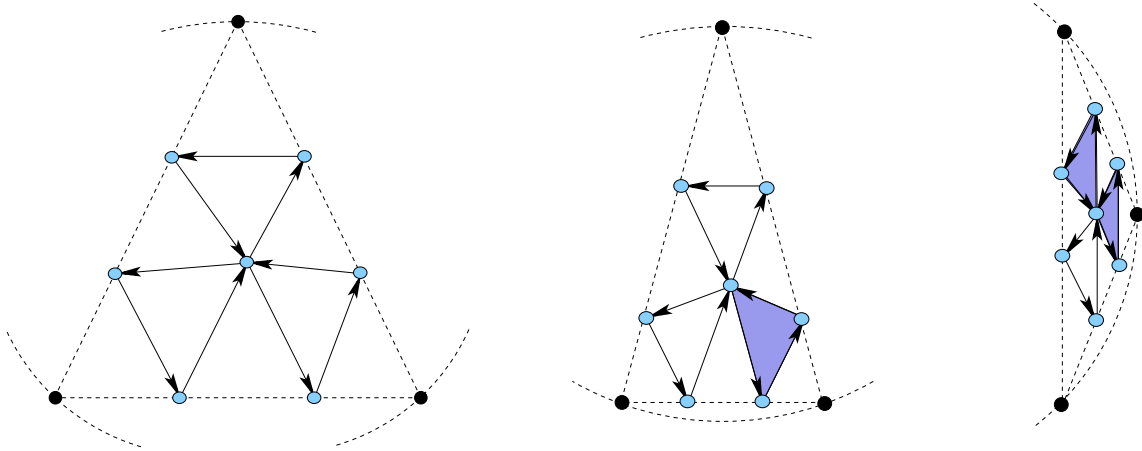


Figure 21: Given a triangulation T of a convex b -gon, the seed $(Q(T), \mathbf{z}(T))$ in the ring of invariants $R_{0,b}(V)$ is constructed as follows. Place one vertex of $Q(T)$ inside each triangle pqr of T ; it corresponds to the Plücker invariant P_{pqr} . Place two vertices of $Q(T)$ on each diagonal pq of T and on each side pq of the polygon; the vertex closer to p (resp., to q) corresponds to $P_{p,p+1,q}$ (resp., to $P_{p,q,q+1}$). For every triangle in T with no exposed sides, connect the seven associated vertices as shown on the left. If one or two sides are exposed (second and third pictures), identify the vertices of each solid triangular region, and remove the arrows bounding it. Finally, freeze the variables $P_{p,p+1,p+2}$.

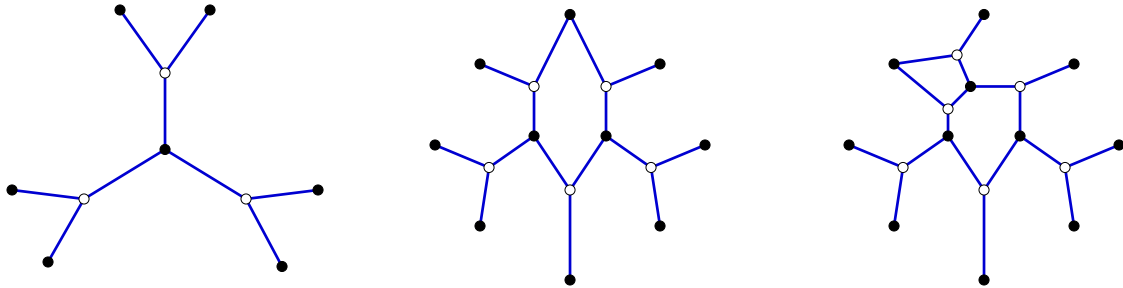


Figure 22: Non-Plücker cluster variables in $R_{0,b}(V)$, for $b \in \{6, 7, 8\}$. To get all of them, include rotations and, in the case of the rightmost web, the mirror images.

Definition 8.7. Let \mathcal{A} be a cluster algebra. Take a seed (Q, \mathbf{z}) of \mathcal{A} . Freeze some subset of cluster variables in \mathbf{z} (thus, some subset of mutable vertices in Q). If the resulting quiver has vertices that are not connected by an edge to a mutable vertex, remove some of them (and remove the corresponding elements from \mathbf{z}) to get a new seed (Q', \mathbf{z}') . The cluster algebra $\mathcal{A}' = \mathcal{A}(Q', \mathbf{z}')$ obtained in this way is called a *cluster subalgebra* of \mathcal{A} .

Theorem 8.8. Let σ and σ' be two non-alternating signatures such that σ' is obtained from σ by removing a single symbol. Then the image of $R_{\sigma'}(V)$ under the obvious tautological embedding $R_{\sigma'}(V) \rightarrow R_{\sigma}(V)$ is a cluster subalgebra of $R_{\sigma}(V)$.

Theorem 8.8 seems to be new even in the case of Grassmannians (cf. Theorem 8.5). For example, it implies that any web invariant of the form shown in Figure 22 is a cluster variable in $R_{0,b}(V)$ for any $b \geq 8$, or indeed in any cluster algebra $R_{a,b}(V)$ with $b \geq 6$, respectively $b \geq 8$.

Recall that V is a three-dimensional vector space endowed with a volume form. The *cross product* of two vectors $u, v \in V$ is the covector $u \times v$ given by $(u \times v)(w) = \text{vol}(u, v, w)$, for $w \in V$. One similarly defines a cross product of two covectors in V^* , which is a vector.

Theorem 8.9. *Let σ and σ' be two non-alternating signatures such that σ' is obtained from σ by replacing two consecutive entries of the same color by a single entry of the opposite color. Interpreting this operation algebraically as a cross product, consider the corresponding embedding $R_{\sigma'}(V) \rightarrow R_{\sigma}(V)$. Then the image of $R_{\sigma'}(V)$ under this embedding is a cluster subalgebra of $R_{\sigma}(V)$.*

Theorems 8.8 and 8.9 can be restated as saying that if σ' is obtained from σ by removing an entry, or by replacing $\bullet\bullet \rightarrow \circ$ or $\circ\circ \rightarrow \bullet$, or more generally by a sequence of such steps, then $R_{\sigma'}(V)$ can be viewed as a cluster subalgebra of $R_{\sigma}(V)$. In particular, in each of those cases the cluster type of $R_{\sigma'}(V)$ can be obtained by taking an induced subgraph inside some quiver for $R_{\sigma}(V)$.

One consequence of this hierarchy is that each cluster algebra $R_{\sigma}(V)$ can be interpreted as a cluster subalgebra of some Grassmann cluster algebra $R_{0,b}(V)$.

At the level of tensor diagrams, the embeddings in Theorems 8.8–8.9 correspond to simple transformations near the boundary of our disk. In the case of Theorem 8.8, passing from σ' to σ corresponds to adding an isolated vertex. For the cross product embedding of Theorem 8.9, we replace one boundary vertex by a pair of vertices of the opposite color, simultaneously adding *forks* to all edges of a tensor diagram which use this vertex, see Figure 23.

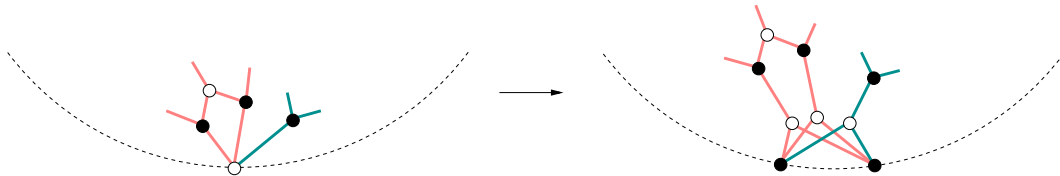


Figure 23: Adding a fork.

Theorems 8.8 and 8.9 can be used to obtain the following corollary.

Corollary 8.10. *If a tensor diagram D is a planar tree, then the corresponding web invariant $[D]$ is a cluster or coefficient variable in $R_{\sigma}(V)$.*

An observant reader may have noticed that our definition of the cluster structure in the ring $R_{\sigma}(V)$ does not treat the black and white colors in exactly the same way. The only place where the symmetry is broken is Definition 7.1: the set $K(T)$ used to define the extended cluster $\mathbf{z}(T)$ includes the invariants J_{pqr} —but not J^{pqr} .

Theorem 8.11. *Interchanging the two colors in the definition of the extended clusters $\mathbf{z}(T)$ does not change the resulting cluster structure in the ring $R_{\sigma}(V)$.*

Besides swapping the colors, one can also consider the “mirror image” of our main construction. We expect this version to yield the same result.

Conjecture 8.12. *Reversal of direction (more specifically, replacing the clockwise direction in the definition of special invariants by the counterclockwise one) does not affect the cluster structure in $R_\sigma(V)$.*

We do not know of a natural construction of a cluster algebra structure in the ring $R_\sigma(V)$ for the *alternating* signature $\sigma = [\bullet \circ \bullet \circ \dots]$; this case seems to be genuinely exceptional. If σ is alternating, then the structure one gets by applying the approach of Sections 6–7 is one of a “generalized cluster algebra” in which some of the exchange relations have more than two terms on the right-hand side.

9. MAIN CONJECTURES

In this section, we discuss conjectural links between

- the cluster structure in a ring of invariants $R_\sigma(V)$ (cf. Section 8) and
- Kuperberg’s basis of this ring formed by the web invariants (cf. Section 5).

The conjectures in this section are intentionally formulated in general terms, so as to suggest their possible extensions to other contexts, including other classical rings of invariants and cluster algebras associated with marked surfaces.

We call a web invariant z *indecomposable* if it cannot be expressed as a product of two web invariants. (This is likely equivalent to irreducibility of z .) For example, any coefficient variable is an indecomposable web invariant.

Conjecture 9.1. *All cluster variables are indecomposable web invariants.*

Two cluster variables are called *compatible* if they belong to the same cluster. Coefficient variables are compatible with each other, and with all cluster variables.

Conjecture 9.2. *Two cluster (or coefficient) variables are compatible if and only if their product is a web invariant.*

Note that by Proposition 6.7, the product of a coefficient variable and any web invariant (in particular, by Conjecture 9.1, any cluster variable) is a web invariant.

The simplest illustration of Conjecture 9.2 can be found in Figure 5: the invariants J_2^4 and J_{123} shown there are compatible with each other, and their product is a web invariant shown in Figure 4. To see more interesting examples, take any two (compatible) webs in Figure 17 and verify that their superposition can be converted into a single web by iterated skein transformations.

We conjecture that much more is true. Define a *cluster monomial* (cf. [16]) as a monomial in the elements of any given extended cluster. For cluster algebras defined by quivers, cluster monomials are known to be linearly independent [5].

Conjecture 9.3. *All cluster monomials are web invariants.*

Conjecture 9.3 suggests the following property of the web basis.

Conjecture 9.4. *Given a finite collection of distinct web invariants, if the product of any two of them is a web invariant, then so is the product of all of them.*

In Conjecture 9.4, we cannot replace “the product of all of them” by “any monomial in them:” it is possible to construct a web invariant (see Section 11.3) whose square is not a web invariant. This invariant is *not* a cluster monomial, or else its square would provide a counterexample to Conjecture 9.3.

We note that it is enough to prove Conjecture 9.4 for collections of three invariants. The general case would then follow by induction.

Conjecture 9.4 is inspired by the “flag property” of cluster complexes (conjectural, but proved in many instances, see [14, Conjecture 5.5, Theorem 5.6]), and by the analogous property of the dual canonical basis (cf. [27], [40, Corollary 1.4]).

We anticipate that all of the above conjectures generalize broadly. Our most optimistic hopes are expressed in Conjecture 9.5 whose statements (1)–(4) are patterned after Conjectures 9.2–9.4 and Proposition 6.7.

Conjecture 9.5. *In any cluster algebra \mathcal{A} of geometric type, there exists an additive basis \mathcal{B} with the following properties:*

- (1) *All cluster monomials in \mathcal{A} lie in \mathcal{B} .*
- (2) *Two cluster variables are compatible if and only if their product lies in \mathcal{B} .*
- (3) *The product of a coefficient variable and an element of \mathcal{B} lies in \mathcal{B} .*
- (4) *If B is a finite subset of \mathcal{B} such that the product of any two distinct elements of B lies in \mathcal{B} , then the product of all elements of B lies in \mathcal{B} .*

It is already nontrivial to show the existence of a basis \mathcal{B} satisfying a small subset of the conditions in Conjecture 9.5. For example, the existence of a basis \mathcal{B} satisfying (1) is equivalent to linear independence of cluster monomials, cf. [5].

Perhaps even more important is the problem of determining a cluster structure in a given ring which is in some sense “compatible” with a particular distinguished basis \mathcal{B} . In the case of the web basis, we used the properties (1)–(4) in Conjecture 9.5 as the guiding principles in designing the cluster structure in the rings of invariants $R_\sigma(V)$. One cannot help but wonder whether this kind of “reverse engineering” process can be made algorithmic, or at least axiomatic. A couple of approaches to this problem are outlined below.

At the heart of the matter lies this question: What distinguishes cluster variables among other indecomposable elements of the basis?¹ One conjectural answer involves an extension of the notion of compatibility of cluster variables. Let us call a set of distinct indecomposable web invariants a *clique* if their product (variant: the product of any two of them, cf. Conjecture 9.4) is again a web invariant. By Conjecture 9.3, any extended cluster is a clique.

Conjecture 9.6. *Among all cliques, extended clusters are precisely the ones of the largest cardinality. Thus, an indecomposable web invariant z is a cluster variable if and only if the largest clique containing z has the cardinality of an extended cluster.*

¹Unfortunately, in the case of the web basis, one cannot use B. Leclerc’s “reality check” criterion [28,37] according to which the cluster monomials are identified as the *real* basis elements, i.e., those whose square lies in the basis. There exist web invariants which are not cluster monomials, yet their squares are web invariants; see Section 11.2.

While Conjecture 9.6 may be aesthetically pleasing, it is rather impractical as a tool for determining whether a particular basis element is a cluster variable. It also is of little help in finding the exchange relations, or equivalently the quivers accompanying extended clusters. For that, we need to move beyond purely multiplicative properties of web invariants (to put it differently, beyond 2-term relations they satisfy) into the realm of *3-term relations*.

Conjecture 9.7. *Suppose that indecomposable web invariants z and z' satisfy the 3-term relation*

$$(9.1) \quad zz' = M_1 + M_2$$

such that $M_1, M_2, zM_1, zM_2, z'M_1, z'M_2,$ and M_1M_2 are web invariants. Then z and z' are cluster variables, and (9.1) is an exchange relation.

Note that by Conjectures 9.1–9.3, we expect each exchange relation in our cluster algebra to satisfy the conditions in Conjecture 9.7.

There is also a test that can (conjecturally) disqualify a web invariant from being a cluster variable.

Conjecture 9.8. *Suppose that an indecomposable web invariant z and a cluster variable z' satisfy a 3-term relation (9.1) such that $M_1, M_2, z'M_1,$ and $z'M_2$ are web invariants whereas zM_1 and zM_2 are not. Then z is not a cluster variable.*

In Conjecture 9.8, the requirement that $z'M_1,$ and $z'M_2$ be web invariants cannot be dropped—see Section 11.4 for a relevant counterexample.

Remark 9.9. We conjecture that *any* cluster structure can be uniquely recovered from a suitably chosen additive basis \mathcal{B} using appropriate versions of the criteria in Conjectures 9.6–9.8.

From its very inception, cluster theory was motivated by the desire to better understand the (dual) “canonical” bases in the corresponding rings. Recall that for most of the rings $R_\sigma(V)$ the dual canonical basis is *different* from the web basis—although the two bases share many important features, see Remark 5.6. The canonical basis is expected to have strong positivity properties, such as those spelled out in the conjecture below, which has long been part of the cluster algebras folklore.

Conjecture 9.10 (Strong Positivity Conjecture). *In any cluster algebra \mathcal{A} of geometric type, there is an additive basis \mathcal{C} which includes the cluster monomials and has nonnegative structure constants.*

That is, any product of elements of the basis \mathcal{C} should have nonnegative coefficients when expanded in the same basis. This condition suggests the existence of a monoidal categorification, wherein structure constants become tensor product multiplicities. See [28, 32, 46].

The web basis does not always satisfy the conditions of Conjecture 9.10:

Proposition 9.11. *For some choices of signature, some structure constants of the web basis are negative.*

An example justifying Proposition 9.11 is given in Section 11.5.

The *Laurent positivity conjecture* [15] predicts that the Laurent polynomial expressing any cluster variable in terms of any given seed has positive coefficients. This conjecture has been proved in many special cases, see in particular [4, 45, 46].

It is well known, and easy to see, that Conjecture 9.10 is *stronger* than Laurent positivity. To deduce the latter from the former, multiply a cluster variable by the denominator of its Laurent expansion. The result is a linear combination of cluster monomials. By Conjecture 9.10, they all belong to the basis \mathcal{C} ; moreover the coefficients in this linear combination must be positive, and we are done.

10. ARBORIZATION

By definition, a web invariant can be represented by a single planar tensor diagram (a web). We conjecture that the cluster variables in $R_\sigma(V)$ are distinguished from other web invariants by the property of possessing a particular kind of alternative presentation; informally speaking, they can be defined by tensor diagrams which are *trees*. Let us explain.

The *unclasp*ing of a tensor diagram D is the graph obtained from D by replacing each boundary vertex p , say of degree k , by k distinct vertices serving as endpoints of the edges formerly incident to p . By a harmless abuse of terminology, we shall call a tensor diagram D whose unclasp has no cycles a *forest diagram*; if moreover the unclasp is connected, we call D a *tree diagram*. We emphasize that such a diagram D does *not* have to be planar.

Conjecture 10.1. *A web invariant z is a cluster or coefficient variable if and only if z is indecomposable and $z = [D]$ for some tree diagram D .*

To illustrate, consider the webs for non-Plücker cluster variables in $R_{0,8}(V)$ shown in Figure 22. The first one is a tree. The second one has a 6-cycle but it goes through a boundary vertex. The third web does have an internal cycle—but the alternative presentation of this invariant shown in Figure 24 unclasps to a (non-planar) tree.

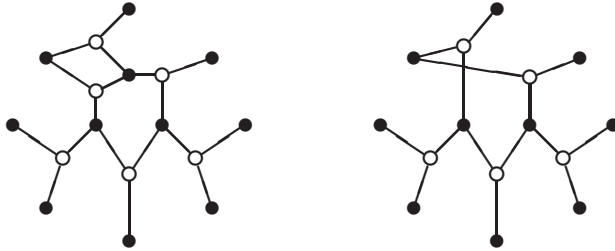


Figure 24: Two representations of a non-Plücker cluster variable in $R_{0,8}(V)$.

A much more complicated example is shown in Figure 25.

We note that Corollary 8.10 establishes a very special case of Conjecture 10.1, namely the case when the same tensor diagram is both a web and a tree.

An example given in Figure 26 shows that the condition of indecomposability in Conjecture 10.1 cannot be dropped: a decomposable web invariant representable by a tree diagram does not have to be a cluster monomial, let alone a cluster variable.

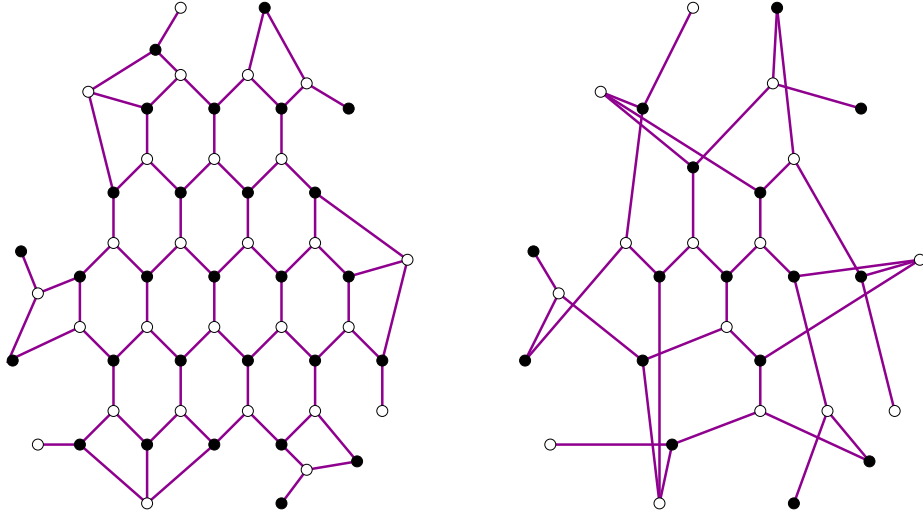


Figure 25: A cluster variable represented by a web and by a tree diagram.

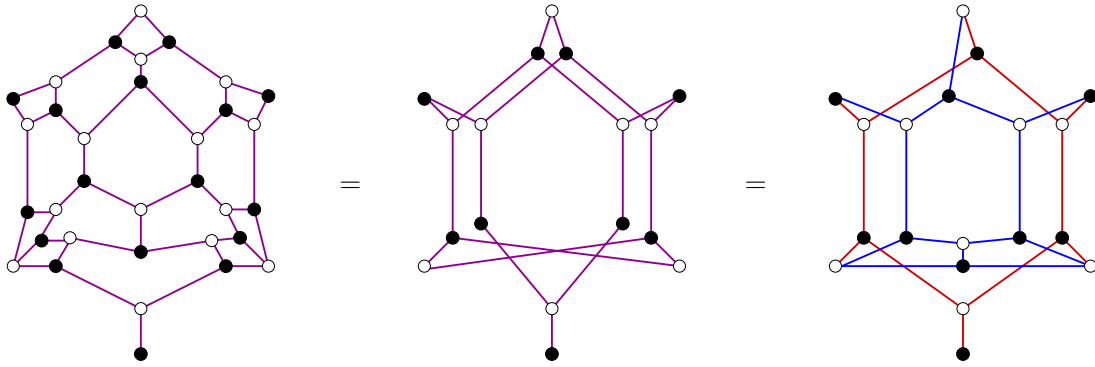


Figure 26: Three representations of the same invariant: (1) as a web invariant; (2) by a tree diagram; (3) as a product of two web invariants. It can be shown that this invariant is not a cluster monomial.

We next describe an algorithm that takes a web invariant z as input and conjecturally constructs a forest diagram defining z , or else concludes that none exists. This will require some preparation.

Definition 10.2. Let D be a tensor diagram, s_1 and s_2 two of its internal vertices, and e_1 and e_2 two edges incident to s_1 and s_2 , respectively. We call vertices s_1 and s_2 *siblings* of each other (more precisely, “siblings away from e_1 and e_2 ”) if the following happens. For $i \in \{1, 2\}$, let B_i denote the subgraph of D whose edge set consists of those edges which can be reached from s_i without going along e_i or connecting through a boundary vertex. (In particular, the edge e_i is not in B_i .) We then want B_1 and B_2 to be isomorphic binary trees having the same multisets of leaves on the boundary of the disk. Thus, s_1 and s_2 are siblings if they are obtained from the same multiset of boundary vertices by the same sequence of taking pairwise joins.

Definition 10.3. Suppose a tensor diagram D contains a fragment which is:

- a quadrilateral with one vertex on the boundary, or
- a four-edge path whose endpoints are siblings of each other, looking away from the edges of the path.

An *arborizing step* is the transformation of such a diagram D shown in Figure 27.

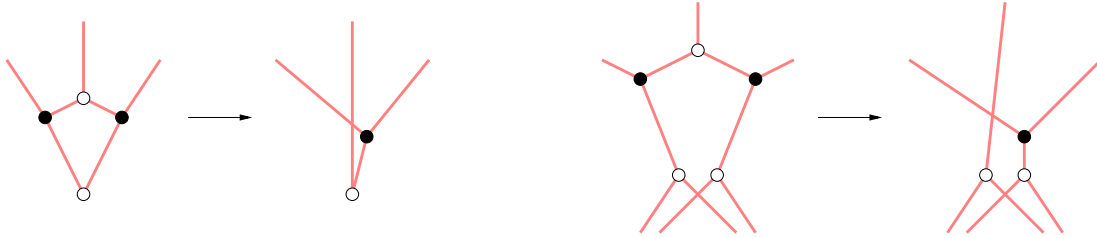


Figure 27: Arborizing steps. At left, the bottom vertex is on the boundary. At right, the boundary is further down (not shown).

Lemma 10.4. *An arborizing step does not change the value of the invariant defined by a tensor diagram.*

The *arborization algorithm* takes a tensor diagram (not necessarily planar) as input, and applies arborizing steps until unable to do so. See Figure 28.

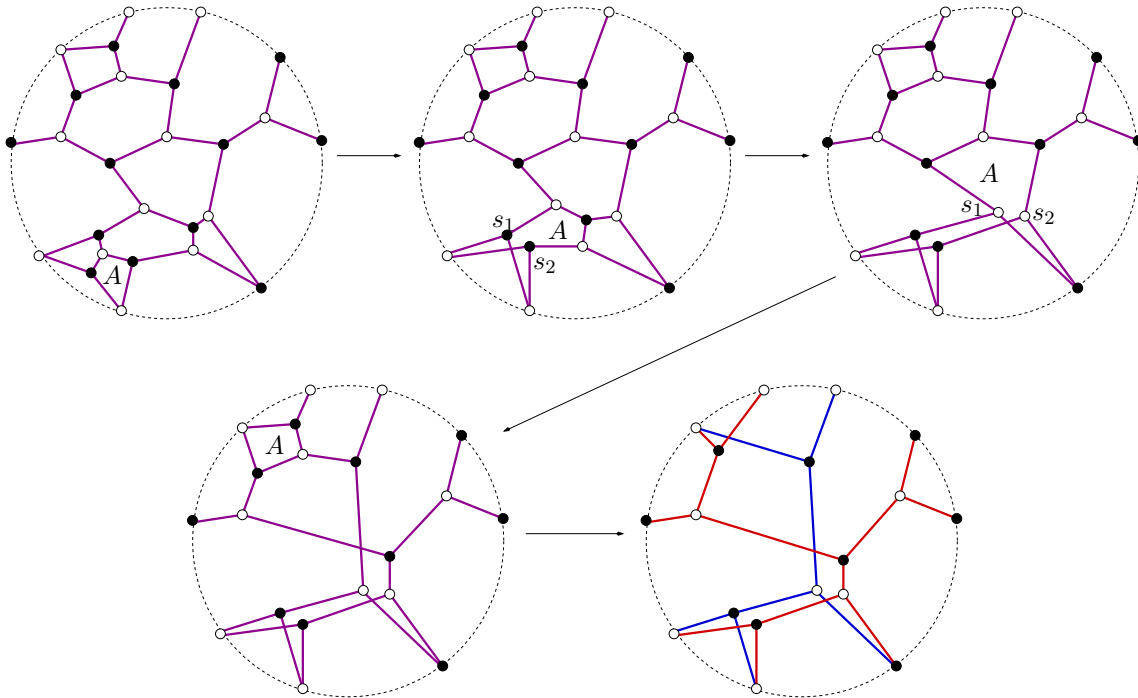


Figure 28: Arborization algorithm. The output is a forest diagram defining a cluster monomial, a product of two compatible special invariants. We indicate the location of each arborizing step and the two sibling vertices, if applicable.

Theorem 10.5. *The arborization algorithm is confluent. That is, its output does not depend on the choice of an arborizing step made at each stage.*

We are tempted to suggest the following enhancement of Conjecture 10.1.

Conjecture 10.6. *An indecomposable web invariant z is a cluster or coefficient variable if and only if the arborization algorithm applied to the web defining z outputs a tree diagram.*

If a web invariant arborizes to a tree diagram, then we expect it to be a cluster variable (cf. Conjecture 10.6), so its powers—which are cluster monomials—should be web invariants as well (cf. Conjecture 9.3). Theorem 10.7 below confirms this expectation, thereby providing indirect support for the aforementioned conjectures.

Theorem 10.7. *Let z be a web invariant defined by a web which arborizes to a tree diagram via the arborization algorithm. Then any power of z is a web invariant.*

We actually do a bit more: under the assumptions of Theorem 10.7, we explicitly describe the web that defines the power z^k of an arborizable web invariant z .

Definition 10.8 (*Thickening of a web*). Let k be a positive integer, and W a web. The k -*thickening* of W is obtained as follows:

- replace each internal vertex of W by a “honeycomb” fragment H_k of the kind shown in Figure 29 (boundary vertices stay put);
- replace each edge of W by a k -tuple of edges connecting the corresponding honeycombs and/or boundary vertices.

An example is shown in Figure 30.

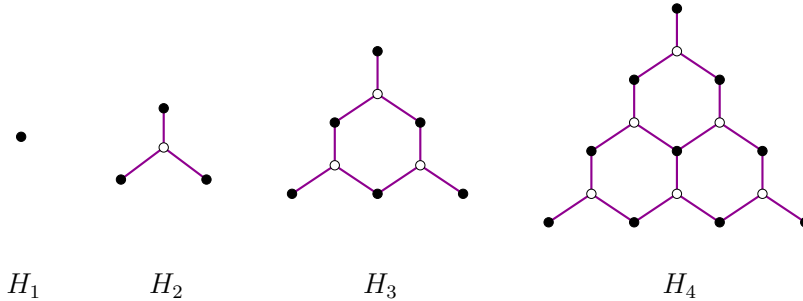


Figure 29: Honeycomb web fragments H_k used to replace a black vertex. When replacing a white vertex, reverse the colors.

Theorem 10.9. *Let z be a web invariant defined by a web W that arborizes to a tree diagram via the arborization algorithm. Then each power z^k is a web invariant defined by the k -thickening of W .*

11. WEB GALLERY

In this section, we present examples of web invariants possessing various notable properties.

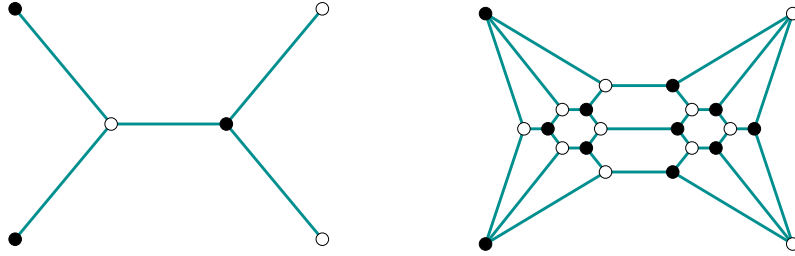


Figure 30: A quadripod web and its 3-thickening.

11.1. Non-arborizable indecomposable webs. By Conjecture 9.1, the set of indecomposable web invariants includes all cluster variables. Which other web invariants does it include? Conjecture 10.6 suggests an approach to constructing such invariants: if a web does not arborize to a tree diagram, then the corresponding invariant is not a cluster variable. A couple of examples are shown in Figure 31.

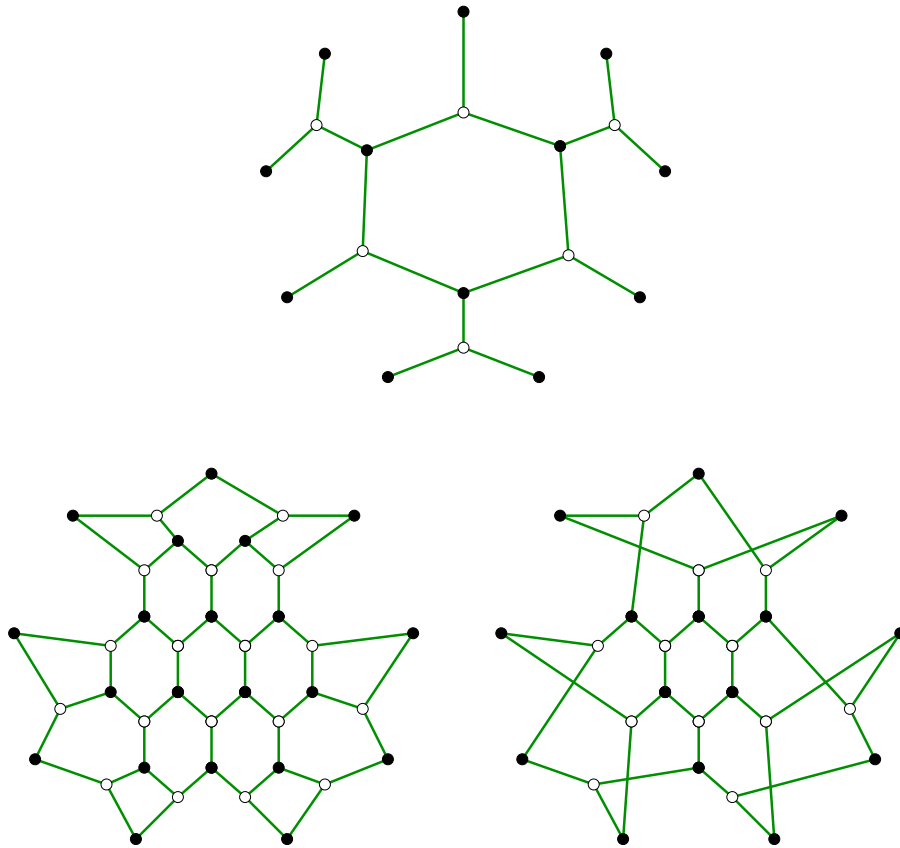


Figure 31: Indecomposable web invariants in $R_{0,9}(V)$ which do not arborize to trees. (We conjecture that there are infinitely many such invariants in $R_{0,9}(V)$.) The web at the top is its own arborization. At the bottom, we show a web together with its arborized form.

11.2. Non-arborizable web whose powers are obtained by thickening. The converse to Theorem 10.9 (or Theorem 10.7) is false: there are lots of web invariants which cannot be represented by a tree diagram, yet all their powers are web invariants themselves; moreover they can be obtained by the thickening procedure. The simplest example is shown in Figure 32.

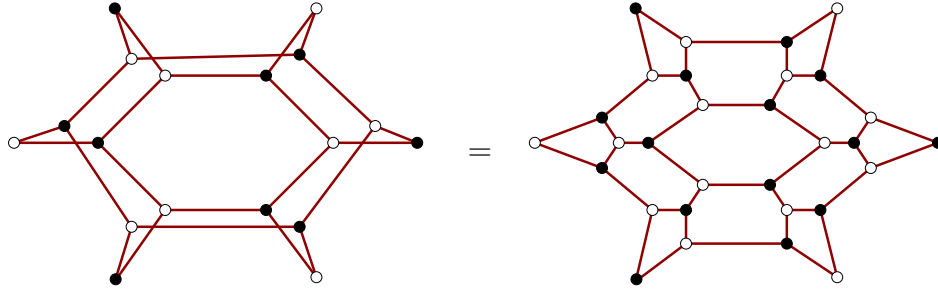


Figure 32: Any power of a single-cycle web is equal to its thickening. Add a dummy boundary vertex to make the signature non-alternating.

The unclasping of the second web in Figure 32 yields the minimal counterexample of M. Khovanov and G. Kuperberg [31, Theorem 4].

11.3. Imaginary elements. The square of the web invariant does not have to be a web invariant, see Figure 33. This phenomenon parallels the existence of “imaginary” elements in dual canonical bases, first discovered by B. Leclerc [37].

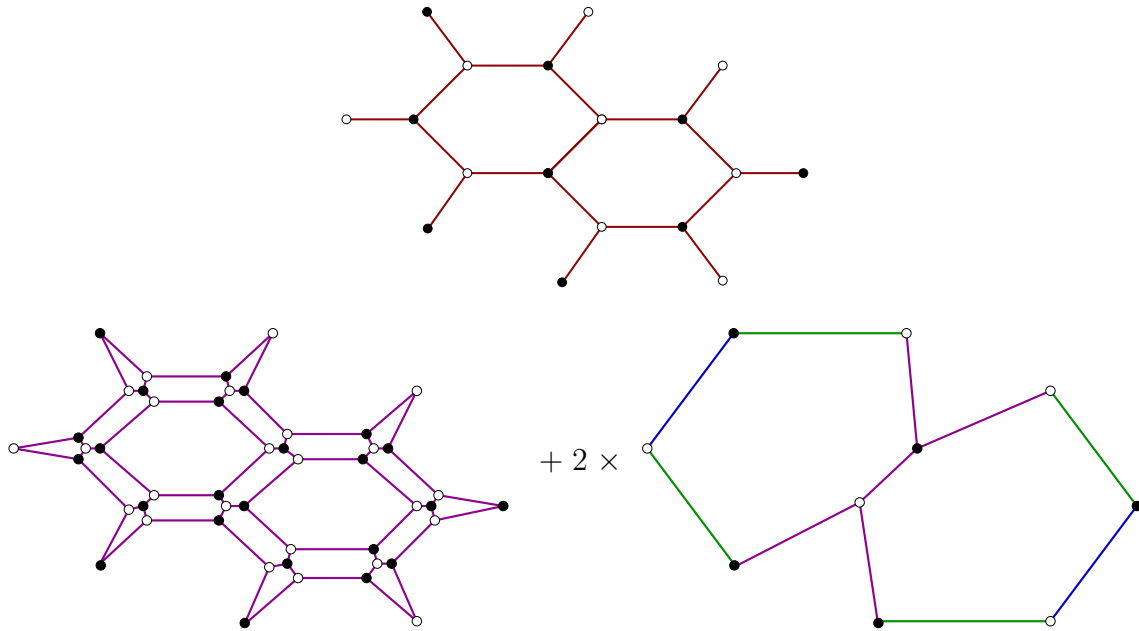


Figure 33: The square of the web invariant shown above is a linear combination of web invariants shown below.

11.4. Fake exchange relations. The identity presented in Figure 34 shows that in Conjecture 9.8, one cannot drop the requirement for $z'M_1$, and $z'M_2$ to be web invariants.

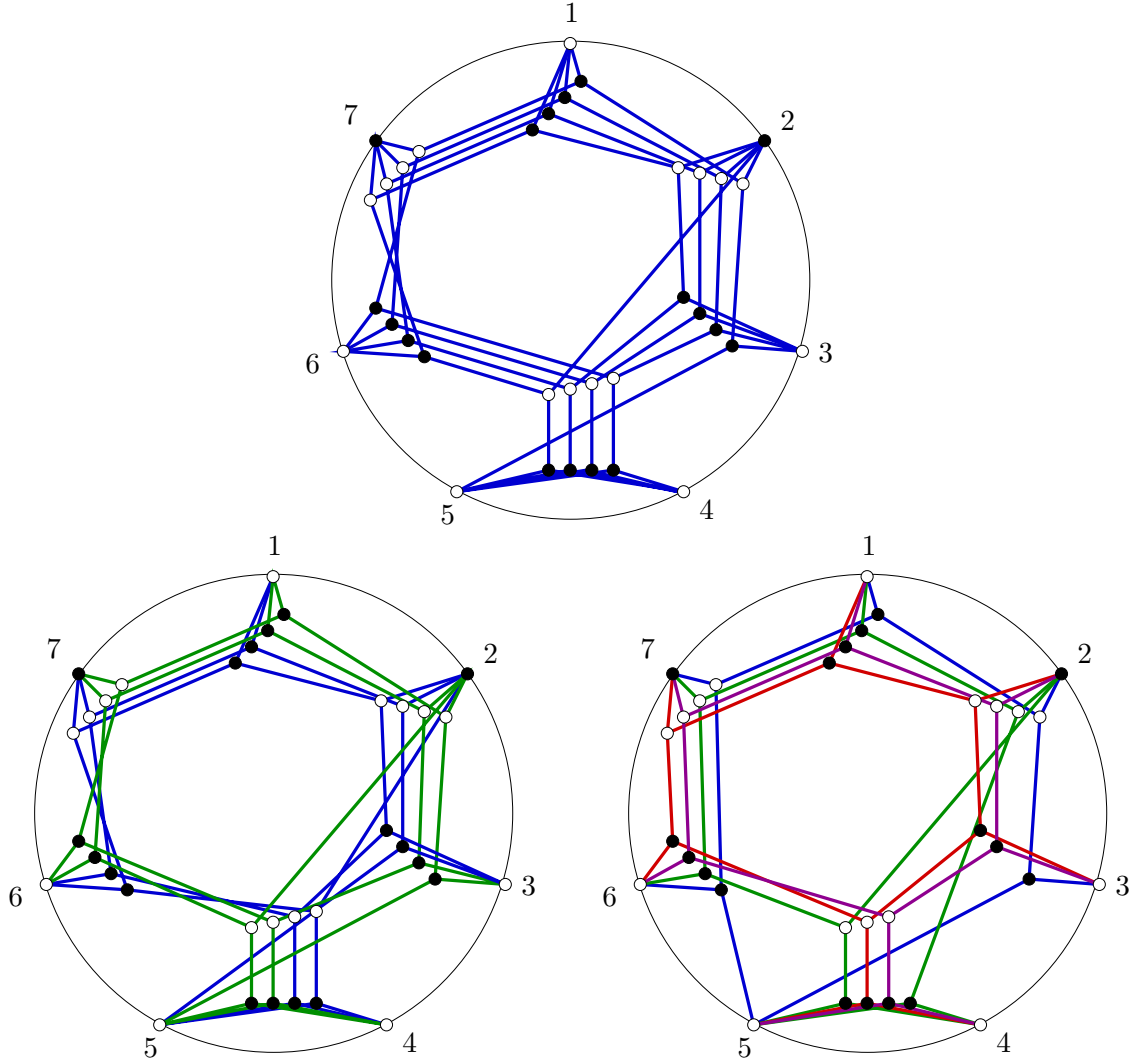


Figure 34: Let z be the cluster variable shown at the top. Let $z' = J_2^5$. These cluster variables satisfy the 3-term relation $zz' = M_1 + M_2$ where M_1 and M_2 are the web invariants shown at the bottom (in arborized form). None of zM_1 , zM_2 , $z'M_1$, $z'M_2$ are web invariants.

11.5. Negative structure constants. Figure 35 presents an instance where a particular structure constant for the web basis is negative. This example shows that even the product of two *cluster variables* may expand in the web basis with coefficients some of which are negative.

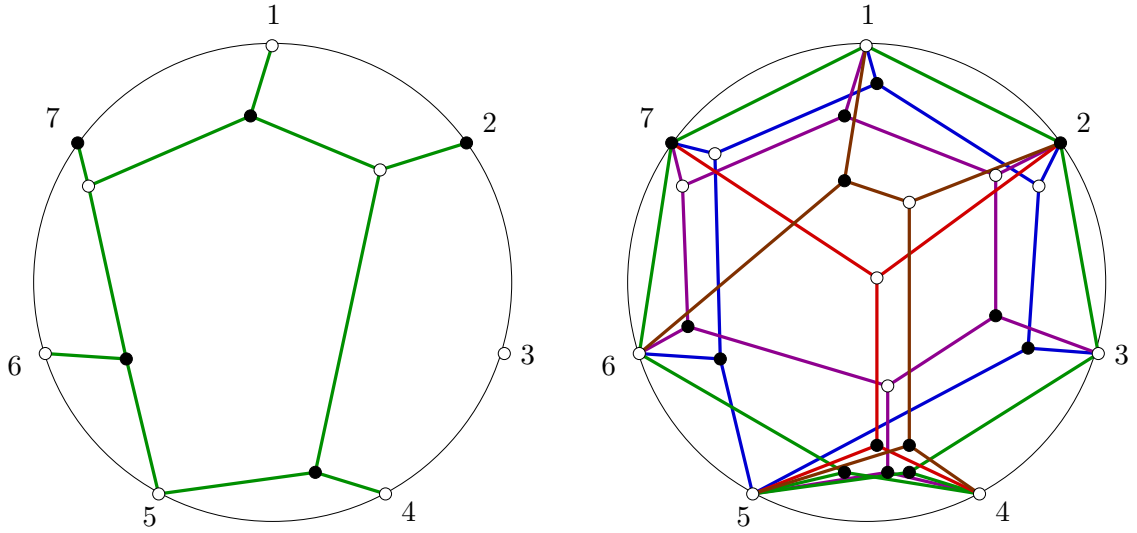


Figure 35: Let z be the cluster variable from Figure 34, and let u be the cluster variable shown on the left. The expansion of zu in the web basis contains the web invariant shown on the right with coefficient -1 .

Proofs

12. PROPERTIES OF SPECIAL INVARIANTS

Proof of Proposition 6.3. It is routine to examine the cases and check that any tensor diagram representing a special invariant “planarizes” (via repeated application of skein relations) into a single non-elliptic web. The key relation used in these verifications is shown in Figure 36. An example is given in Figure 37. \square

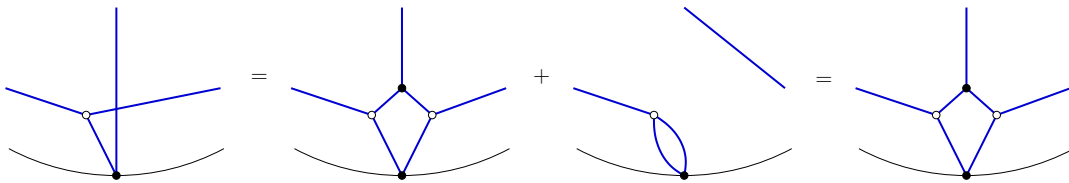


Figure 36: Basic planarizing step. Cf. Figure 27 on the left.

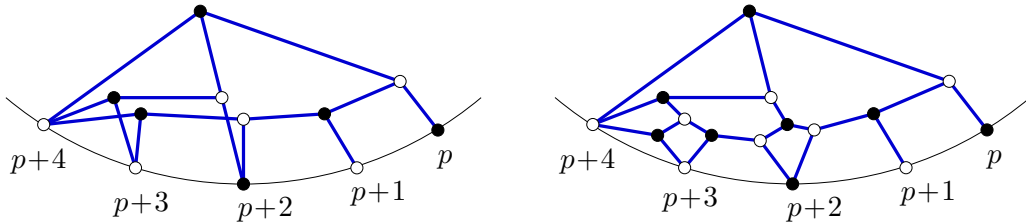


Figure 37: The special invariant $J^{p,p+2,p+4}$ is a web invariant.

The proof of Proposition 6.5 will require some preparations.

Lemma 12.1. *Assume that an invariant $X \in R_\sigma(V)$ is antisymmetric and linear with respect to its arguments v_p and v_{p+1} which have the same variance (i.e., are both contravariant or both covariant). Then X can be expressed as a linear combination of web invariants defined by webs which have a fork between vertices p and $p + 1$.*

Proof. We can write X as a linear combination of web invariants $X = \sum_i c_i Y_i$ where the web representing each Y_i has a single edge incident to p (resp., to $p + 1$). Let us attach a crossing to this web at vertices p and $p + 1$ to get an invariant \overline{Y}_i . (In other words, we redirect the edge incident to p so that it connects to $p + 1$, and vice versa.) Since $\overline{X} = \sum_i c_i \overline{Y}_i$ is obtained from X by interchanging v_p and v_{p+1} , and since X is antisymmetric in these arguments, it follows that $\overline{X} = -X$. On the other hand, applying the skein relation at the crossing gives $\overline{Y}_i = Y_i + Z_i$, where Z_i has a fork between p and $p + 1$. Taking linear combinations, we get $-X = X + \sum_i c_i Z_i$, implying $X = -\frac{1}{2} \sum_i c_i Z_i$, an expansion of the desired kind. \square

Lemma 12.2. *A web invariant defined by a planar tree is irreducible.*

Note that by Corollary 8.10, such an invariant is a cluster or coefficient variable in $R_\sigma(V)$. By [21, Theorem 1.3], every cluster variable in *any* cluster algebra is irreducible. At this point, we cannot of course rely on these statements, as we are still in the process of proving that $R_\sigma(V)$ is a cluster algebra.

Proof. We proceed by induction on the size of the tree. In the base cases of Weyl generators, irreducibility is well known (and easy to prove).

Suppose a web invariant X defined by a planar tree T has a nontrivial factorization $X = X_1 X_2$. It is easy to see that T must have a fork, say between vertices p and q (of the same color) associated with (co)vectors v_p and v_q , respectively. Without loss of generality, we may assume that $q = (p + 1) \bmod (a + b)$.

As X is multi-homogeneous, so must be X_1 and X_2 . Moreover X is multilinear, implying the dichotomy: either one of the factors X_i depends (linearly) on both v_p and v_q while the other depends on neither, or else one of the factors depends on v_p but not v_q while another depends on v_q but not v_p .

The latter option is ruled out by the fact that X is antisymmetric in v_p and v_q (because of the fork), so it must vanish if we substitute $v_p = v_q$. On the other hand, neither factor X_i vanishes under this substitution, and R_σ is a domain.

So v_p and v_q appear in the same factor, say X_1 . Then X_2 does not depend on v_p and v_q . Hence X_1 is antisymmetric in v_p and v_q . Applying Lemma 12.1, we express X_1 as a linear combination of web invariants whose webs have a fork between p and $q = p + 1$. Thus, v_p and v_q enter the identity $X = X_1 X_2$ exclusively through their cross product $v_p \times v_q$. This yields a nontrivial factorization of an invariant defined by a smaller planar tree, contradicting the induction assumption. \square

Proof of Proposition 6.5. Let X be a nonzero special invariant that does not have one of the forms listed in Proposition 6.4. We need to show that X is irreducible. We describe the general idea of the proof, omitting some details. The proof is by induction on the number of internal vertices in the tree diagram defining X .

Let $A \subset \{1, \dots, a + b\}$ denote the set of lower and upper indices appearing in the original notation for X (cf. Definition 6.1). Thus the cardinality of A is 2, 3, or 4.

If X is a planar tree, the statement reduces to Lemma 12.2. Otherwise the “tail” involved in building the proxy for some of the vertices in A (cf. Figure 10) is long enough to involve another such vertex. It is not hard to see that we can find two consecutive vertices $p, q \in A$ (going clockwise) such that the boundary segment between them is covered by only one such tail. Furthermore, for X to be indecomposable, this segment has to be sufficiently long, by definition. Assume without loss of generality that vertex p is white; then $p + 1$ is black, $p + 2$ is white, etc. We then define invariants X' and X'' as follows. (Consult Figure 38.) For X' , attach an outside fork to $p + 1$ and identify one of its endpoints with p . (This changes the color of the entry $p + 1$ of the signature.) For X'' , attach an outside fork to p and identify one of its endpoints with $p + 1$. (This changes the color of the p 'th entry.) Thus the invariants $X' = X'(\dots, v_p^*, v_{p+1}^*, v_{p+2}^*, \dots)$ and $X'' = X''(\dots, v_p, v_{p+1}, v_{p+2}^*, \dots)$ are obtained from $X(\dots, v_p^*, v_{p+1}^*, v_{p+2}^*, \dots)$ via the substitutions

$$(12.1) \quad X'(\dots, v_p^*, v_{p+1}^*, \dots) = X(\dots, v_p^*, v_p^* \times v_{p+1}^*, \dots),$$

$$(12.2) \quad X''(\dots, v_p, v_{p+1}, \dots) = X(\dots, v_p \times v_{p+1}, v_{p+1}, \dots).$$

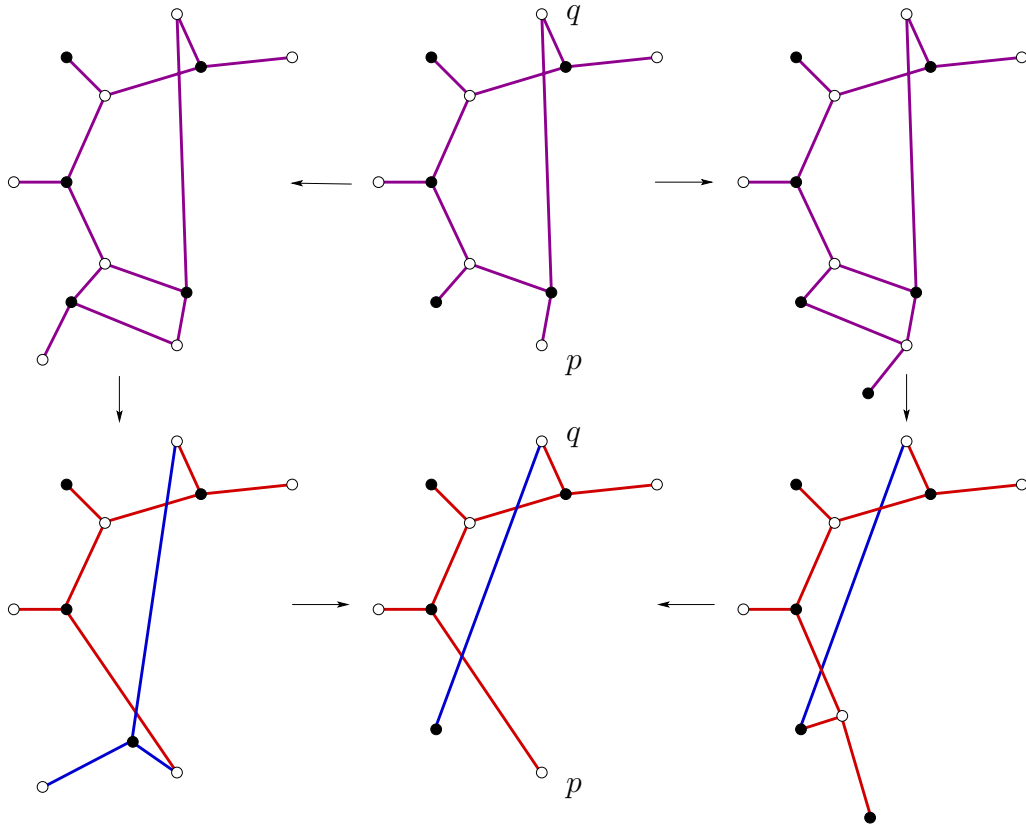


Figure 38: Top row: invariants X' , X , X'' .

Suppose X has a nontrivial factorization $X = YZ$; it then specializes into factorizations $X' = Y'Z'$ and $X'' = Y''Z''$. On the other hand, X' and X'' factor as shown in Figure 38 (bottom row), one of the factors (shown in red) being given by a planar tree and another (blue) factor being a special invariant of the same kind as X . The red factor is irreducible by Lemma 12.2 while the blue one is irreducible by the induction assumption: it is a special invariant of a kind not listed in Proposition 6.4, and it has fewer internal vertices. Since our rings of invariants are unique factorization domains, we conclude that factorizations $X' = Y'Z'$ and $X'' = Y''Z''$ must coincide with the ones shown in Figure 38.

Since X is linear in v_{p+1} , either Y or Z (say Y) does not depend on v_{p+1} . Thus Y is unaffected by the substitution (12.1), and $Y' = Y$ does not depend on v_{p+1}^* . Consequently, Y must be the invariant shown in red in the lower-left corner of Figure 38. Similarly, one of the factors Y and Z does not depend on v_p , is unaffected by the substitution (12.2), and appears in the factorization of X'' shown in Figure 38 in the lower-right corner; this must be the invariant shown in blue (and it must be Z). In conclusion, the factors Y and Z must match the ones shown in the center of the bottom row. But the product of these two special invariants yields a sum of two nonzero terms, one of them being X . Thus $YZ \neq X$, a contradiction. \square

Proof of Proposition 6.6. In view of Proposition 6.5, a nonzero special invariant can be factored into irreducible ones by repeated application of the rules (1)–(8) in Proposition 6.4. An easy check shows that this process terminates. Uniqueness of factorization follows from the fact that our ring is a UFD. See Figure 39 for an example. \square

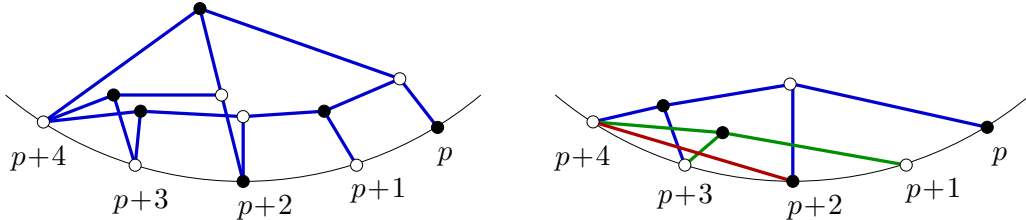


Figure 39: Factorization of $J^{p(p+2)(p+4)}$. The rules (1)–(8) can be applied in two different ways: $J^{p(p+2)(p+4)} = J_{p+2}^{p+4} J_{p+3}^p = J_{p+2}^{p+4} J_{p+3}^{p+1} J_p^{p+2}$ or $J^{p(p+2)(p+4)} = J_p^{p+2} J_{p+1}^{p+4} = J_p^{p+2} J_{p+3}^{p+1} J_{p+2}^{p+4}$, yielding identical results.

Proof of Proposition 6.7. First, we need to prove that a nonzero special invariant not on our list is not compatible with some other special invariant. This is checked on a case by case basis. For an invariant of the form J_p^q , one finds an incompatible special invariant J_r^s such that the diagonals pq and rs cross each other. Similarly, if our invariant is J_{pqr} or J^{pqr} , one can find an incompatible special invariant J_s^t such that the diagonal st crosses the triangle pqr . (These are special cases of failure of *weak separation*, cf. [41].) Special invariants J_{pq}^{rs} are handled analogously.

Another claim to check is that a nonzero invariant of the form $J_p^{p\pm 1}$ is compatible with any web invariant. Coefficient invariants come in two flavors: short and long,

see Figure 40. The short ones are obviously compatible with any web invariant. The relevant calculation for a long invariant is shown in Figure 41. Applying it around every vertex establishes the claim. \square

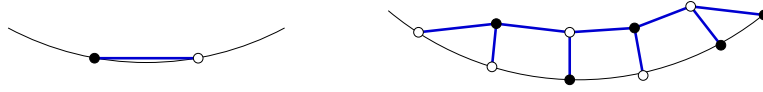


Figure 40: Two kinds of coefficient invariants: short and long.

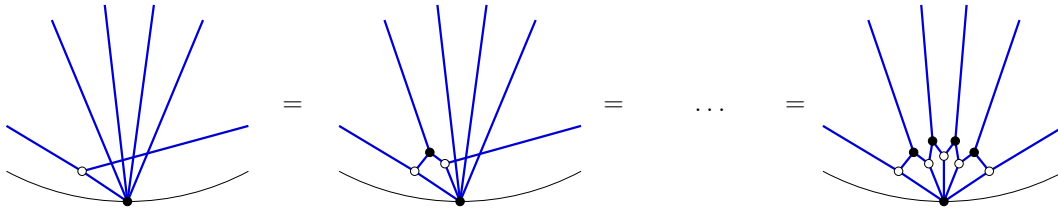


Figure 41: Compatibility of coefficient invariants with web invariants is verified by iterating the basic relation shown in Figure 36.

Proof of Proposition 6.9 . Each identity can be obtained by repeated application of skein relations. A key role is played by the relation shown in Figure 36. An example of a computation verifying the first relation is given in Figure 42. \square

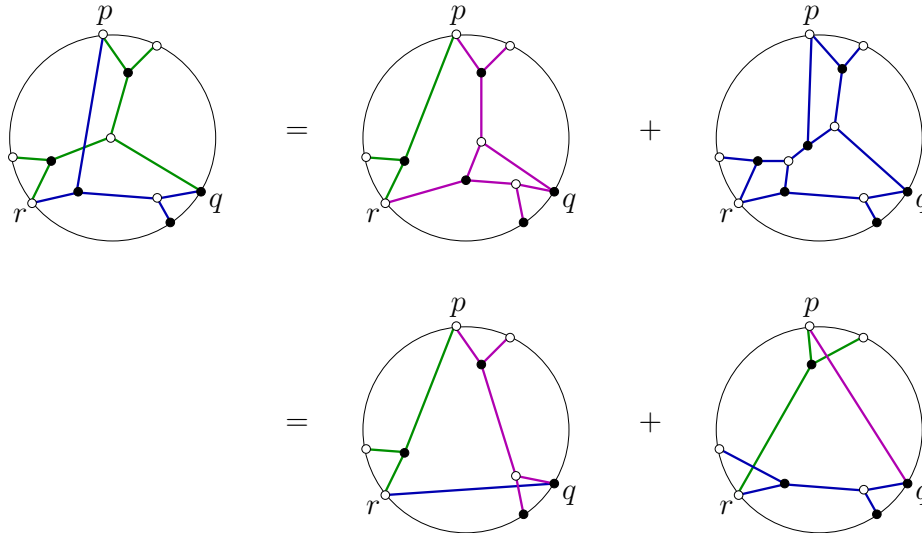


Figure 42: The verification of the relation $J_{pqr} J^{pqr} = J_r^p J_q^r J_p^q + J_r^q J_p^r J_q^p$.

Proof of Proposition 7.6. Without loss of generality, we can assume that side qr is exposed, so that $r = (q + 1) \bmod (a + b)$. One then checks that $J^{p q, q+1} = J_q^p$ if q is white, and $J^{p q, q+1} = J_{q+1}^p J_q^{q+1}$ if q is black. \square

Proof of Proposition 7.7. If p is white and $p + 1$ is black, then $J_{p+1,p+2}^{sp} = J_p^s$. Relation (6.3) then gives

$$J_{p+2}^p J_{p+1}^s = J_{p+1}^p J_{p+2}^s + J_{p+1,p+2}^{sp} = J_{p+1}^p J_{p+2}^s + J_p^s.$$

If p is black and $p + 1$ is white, then $J_{sp}^{p+1,p+2} = J_s^p$, and (6.3) gives

$$J_p^{p+2} J_s^{p+1} = J_s^{p+2} J_p^{p+1} + J_{sp}^{p+1,p+2} = J_s^{p+2} J_p^{p+1} + J_s^p. \quad \square$$

13. PROPERTIES OF SPECIAL SEEDS

Proof of Theorem 7.2. Denote $N = a + b$. Since the theorem can be verified by direct calculation for $N \leq 6$, we assume that $N \geq 7$ from now on.

By Proposition 6.7, each side of the N -gon P_σ produces one nonzero special invariant which by construction belongs to $\mathbf{z}(T)$; those are exactly the coefficient invariants.

Define the *length* of a diagonal pq in P_σ as the number $\min(|p - q|, |N - p - q|)$; this is the length of the shortest path from p to q along the perimeter of P_σ .

Lemma 13.1. *Assume that $N \geq 7$. Let P' denote the interior of P_σ with all diagonals of length 2 in T removed. The set P' uniquely decomposes into a disjoint union of “fundamental regions” of types A, B, C, D, E, F shown in Figure 43.*

An example is shown in Figure 44. We note that the lemma fails for $N = 6$ if T contains a diagonal of length 3. (The two regions of type E are not disjoint as they share this diagonal.)

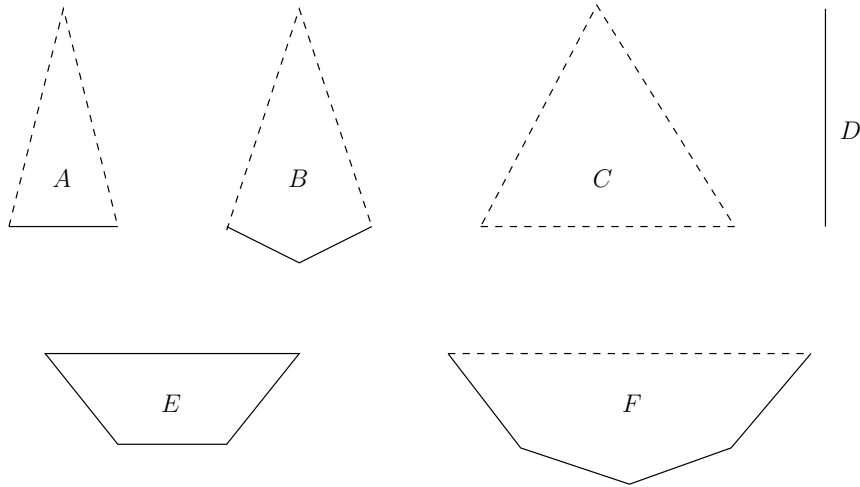


Figure 43: Fundamental regions. A dashed line means that the region does not include this diagonal. All dashed diagonals are of length at least 3. Type D includes diagonals of length at least 4. The short solid segments in A, B, E and F are sides of the polygon P_σ .

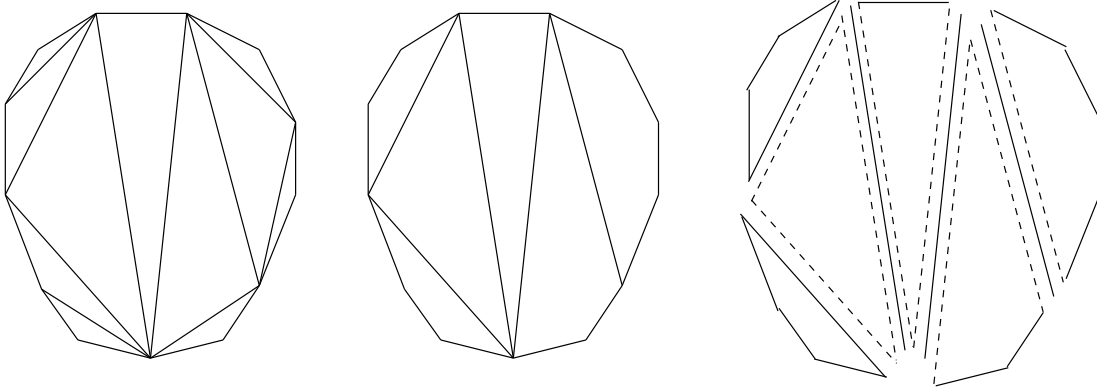


Figure 44: Decomposition of P_σ into fundamental regions.

Lemma 13.2. *Special invariants associated to each fundamental region contribute the following number of non-coefficient irreducible factors to the cluster $\mathbf{x}(T)$:*

type of a region	A	B	C	D	E	F
contribution to $\mathbf{z}(T)$	0	2	1	2	3	3

The contributions of different fundamental regions are disjoint. To clarify, if a region R does not include a (dashed) diagonal pq lying on its boundary, then the contributions of R exclude all irreducible factors appearing in J_p^q and J_q^p .

Proof. Case by case consideration depending on the signature. One typical example involving a region of type E (with two possible colorings) is shown in Figure 45. \square

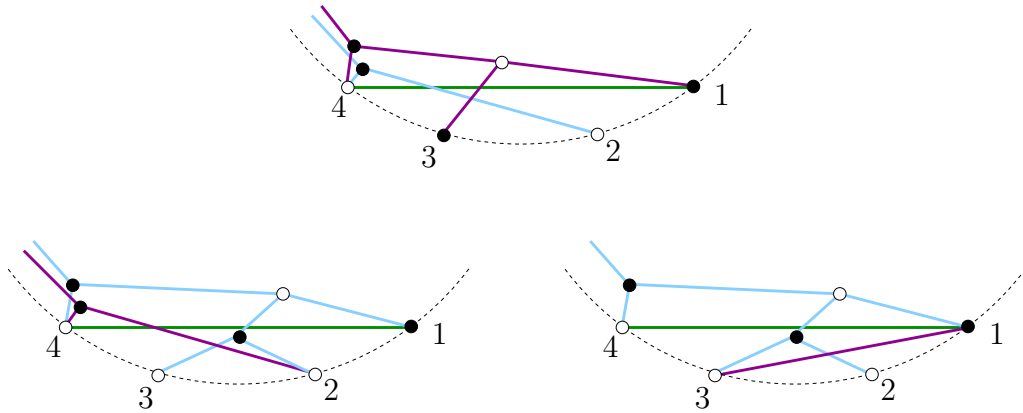


Figure 45: Two possible colorings for a region of type E . In the first case, regardless of which of the two short diagonals (13 or 24) is chosen, we obtain the same three variables J_1^4 , J_1^3 and J_4^2 . In the second case, depending on which short diagonal is used, we get either $\{J_1^4, J_4^1, J_4^2\}$ or $\{J_1^4, J_4^1, J_1^3\}$. Each case yields exactly three non-coefficient variables. The fact that they cannot come from other fundamental regions can be seen by performing a similar analysis for those regions.

We continue with the proof of Theorem 7.2. It is a simple counting exercise to check that the total contribution from all fundamental regions is exactly $2N - 8$ non-coefficient variables, as claimed. For example, in Figure 44 we get

$$3 + 3 + 1 + 0 + 2 + 3 + 2 + 2 + 2 = 18 = 2 \cdot 13 - 8.$$

It remains to check that the special invariants in $\mathbf{z}(T)$ are pairwise compatible. For invariants coming from the same fundamental region, this is done by direct case by case inspection. For invariants from different regions, the argument goes as follows. The “tails” of the special invariants (cf. Figure 10) do not create any obstructions to compatibility: just iterate the basic planarizing steps of Figure 36. The remaining pieces lie in different regions and thus do not intersect. \square

Proof of Proposition 7.4. The proof reduces to a direct verification comparing triangulations T and T' which differ by a flip that switches the diagonals $(q, q + 2)$ and $(q + 1, q + 3)$. A typical example is shown in Figure 50. \square

Proof of Proposition 7.9. The proof is a case by case verification, organized as follows. For each region R , the variables (i.e., irreducible factors) contributed by R are exchanged using only the variables defined within R and/or several adjacent regions. Specifically:

- regions of type A do not contribute any variables, so there is nothing to check;
- for regions of type B (resp., C , F), also consider two (resp., three, one) adjacent region(s) of types D or E ;
- for regions of type D (resp., E), also consider two (resp., one) adjacent region(s) of types A , B , C or F , as well as the regions of types D or E which are adjacent to those.

In each of these cases, the proof consists of a local verification (sometimes tedious but always straightforward) ranging over a finite list of possible patterns. \square

14. BUILDING A QUIVER

In this section, we provide a blueprint for building the quiver $Q(T)$ associated with an arbitrary triangulation T of the polygon P_σ . As mentioned earlier, a detailed description for a particular choice of T can be found in Section 17.

The simplest part of the recipe concerns the portions of $Q(T)$ coming from triangles pqr in T which have no exposed sides. We draw the vertex of $Q(T)$ representing the special invariant J_{pqr} inside the triangle pqr . The vertices representing cluster variables coming from J_p^q and J_q^p are placed on the diagonal pq (and similarly for qr and pr), with the former closer to q , and the latter closer to p . See Figure 46.

The above recipe may require adjustments if some of the sides of the triangle pqr are too short, so that the corresponding special invariants factor; cf., e.g., Figure 50.

For triangles with one or two sides on the boundary of P_σ , the basic principles remain the same, but the recipe changes somewhat. Figures 47 and 48 treat “generic” cases of one and two exposed sides, respectively.

In a few exceptional cases, additional adjustments have to be made to the construction of the quiver $Q(T)$ and/or to the rules of assigning special invariants to its

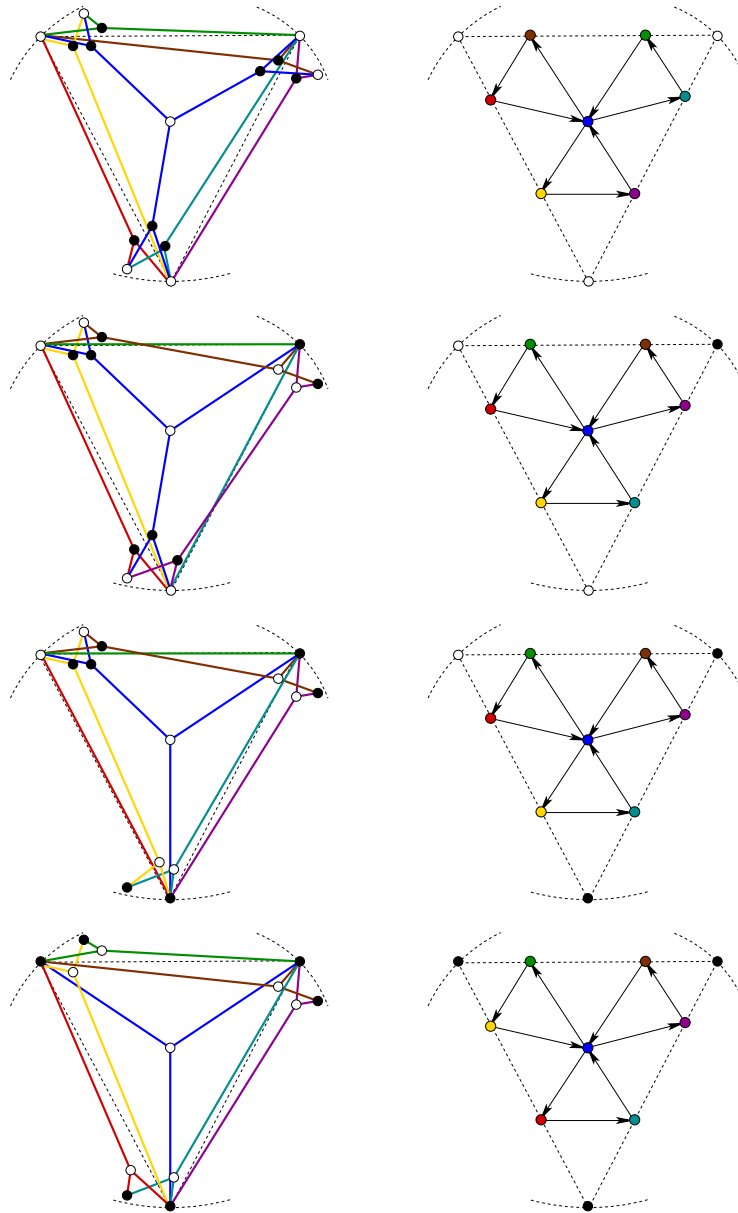


Figure 46: Special invariants around a triangle in a triangulation T , and the corresponding portion of the quiver $Q(T)$.

vertices. These adjustments are caused by nontrivial factoring of the special invariants involved. One such case is illustrated in Figure 49, which is in turn a special case of the pattern shown in Figure 48 on the upper right. Another example is shown in Figure 50. There are only a finite number of such exceptional situations, all of them arising when some sides of the relevant triangle(s) are short enough to make certain special invariants factor nontrivially. We refrain from exhaustively describing all these exceptional cases and the corresponding quiver-building instructions.

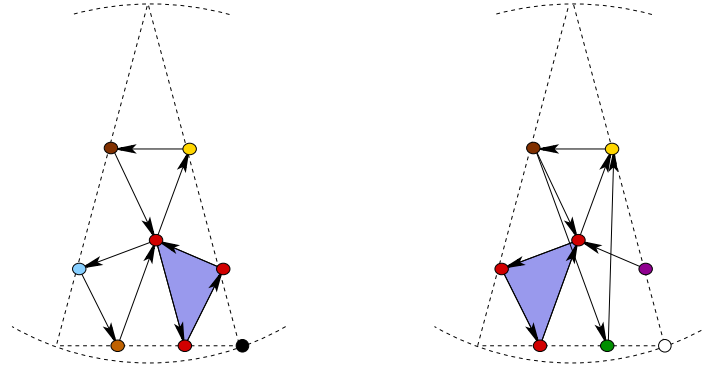


Figure 47: Portion of the quiver $Q(T)$ in a triangle $pq(q + 1)$ of T . There are two cases, depending on the color of q . In each case, three vertices collapse into a single vertex of $Q(T)$, represented by the solid triangle. All edges that used to go to/from those three vertices are still going to/from this new vertex.

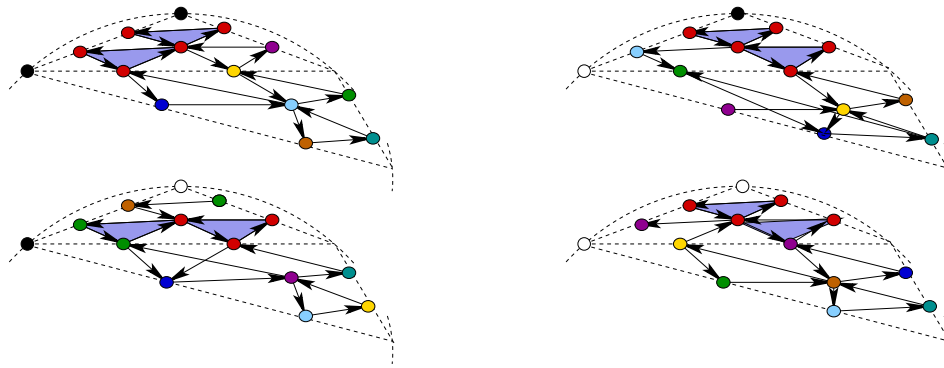


Figure 48: Portion of the quiver in a triangle with two exposed sides. The pattern only depends on the coloring of two of the vertices.

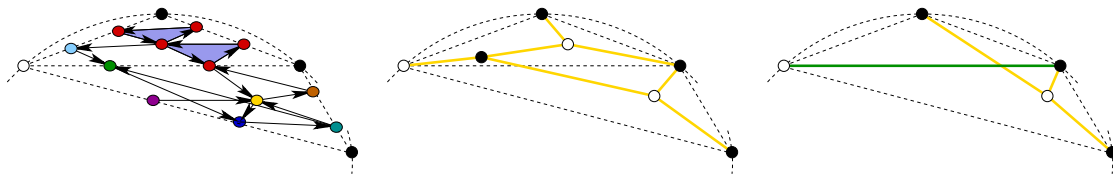


Figure 49: The special invariant corresponding to the yellow vertex Y of the quiver shown on the left is given by the yellow web in the middle; it factors into a product of two special invariants shown on the right. The green factor is already associated to the corresponding diagonal. We let the yellow factor be the cluster variable associated with Y .

15. PROOF OF THE MAIN THEOREM

Lemma 15.1. *The seeds $(Q(T), \mathbf{z}(T))$ are mutation equivalent.*

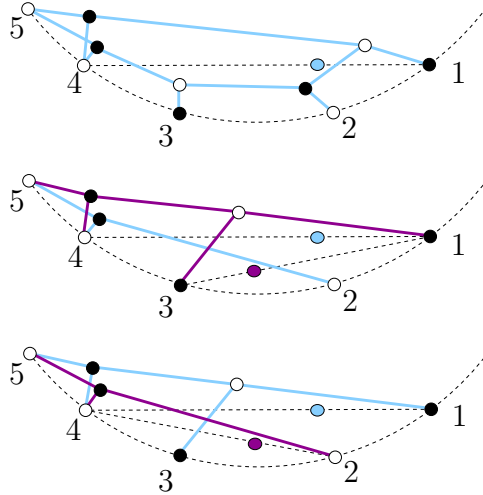


Figure 50: The special invariant J_4^1 factors: $J_4^1 = J_4^2 J_1^3$. Which of the two factors should be associated to the diagonal 14 depends on whether triangulation T contains diagonal 13 or diagonal 24. The clusters $\mathbf{x}(T)$ and $\mathbf{x}(T')$ associated to triangulations T and T' which differ by a flip replacing 13 by 24 are the same. Cf. Proposition 7.4.

Strictly speaking, we should not use the terms “seed” and “mutation” since we have not established yet that the elements of $\mathbf{z}(T)$ are algebraically independent. What we mean in Lemma 15.1 is that any two quivers $Q(T)$ and $Q(T')$ are related by a sequence of mutations, and applying the corresponding exchange transformations to the collection $\mathbf{z}(T)$ produces the collection $\mathbf{z}(T')$.

Proof. Since any two triangulations of the polygon P_σ can be connected by a sequence of *flips* (each flip replacing a single diagonal by another one), it suffices to show that for two triangulations that differ by a flip, the corresponding seeds are related by mutations. Typically, the required number of mutations is four, although in some cases it can be three, two, one, and even zero, see Proposition 7.4.

The verification of the claim is done on a case by case basis, depending on the color pattern of the vertices involved; as before, there are several exceptional cases where proximity of vertices to each other results in nontrivial factorization of the corresponding special invariant. Once again, we do not list all cases exhaustively, presenting instead a couple of “generic” cases which illustrate the checks one needs to perform; this is done in the next paragraph. But first, let us explain how one would exhaustively examine all possible “non-generic” cases. For each side of a quadrilateral, there are four options to consider: the side may be of length 1, 2, 3, or ≥ 4 . Once each of these four options has been selected for each side, one considers possible colorings of the vertices along the sides. For the sides of length ≥ 4 , the coloring of the intermediate vertices does not matter. In each case, it is possible to exhibit a sequence of ≤ 4 mutations which connects the two seeds under consideration. Details are omitted. We note that in the case of Grassmannians

(when all boundary vertices are of the same color), an exhaustive examination of all possibilities is given in Section 16.

The general rule (barring aforementioned exceptions) is as follows. Suppose that triangulations T and T' are related by a flip that replaces diagonal pr by diagonal qs ; thus T has triangles pqr and rsp while T' has triangles qrs and pqs . Then the seed $(Q(T'), \mathbf{z}(T'))$ is obtained from $(Q(T), \mathbf{z}(T))$ by a sequence of four mutations:

- replace J_r^p by J_{pqs} , and replace J_p^r by J_{qrs} (these two mutations commute);
- replace J_{prs} by J_q^s , and replace J_{pqr} by J_s^q (these two mutations commute).

The corresponding exchange relations are of the form (6.2). Figures 51 and 52 illustrate these sequences of mutations for two different color patterns. \square

In Section 16 (see the proof of Theorem 8.5), we examine exceptional instances of mutation sequences associated with diagonal flips in the special case of a monochromatic signature (equivalently, the case of a Grassmannian $\text{Gr}_{3,b}$).

Lemma 15.2. *The elements of each set $\mathbf{z}(T)$ (cf. Definition 7.1) are algebraically independent.*

Proof. Note that $\text{Spec}(R_{a,b}(V))$ has the same dimension as $\text{Spec}(R_{0,a+b}(V))$, the affine cone over the Grassmannian $\text{Gr}_{3,a+b}$; the latter dimension is equal to $3(a+b-3)+1=3a+3b-8$. To prove the equality of dimensions, assume without loss of generality that $a \geq 3$, and use the $\text{SL}(V)$ -equivariant birational isomorphism that sends an a -tuple of covectors $(u_1^*, u_2^*, \dots, u_a^*)$ to the a -tuple of vectors $(u_1^* \times u_2^*, u_2^* \times u_3^*, \dots, u_a^* \times u_1^*)$. In view of Lemma 15.1, the $(3a+3b-8)$ -tuples $\mathbf{z}(T)$ (cf. Theorem 7.2) are birationally related to each other, and collectively generate the field of fractions of R_σ (as they contain all Weyl generators). It follows that each of these tuples is algebraically independent. \square

Proof of Theorem 8.1. Lemma 15.2 means that $(Q(T), \mathbf{z}(T))$ is a seed. Lemma 15.1 means that the cluster algebra $\mathcal{A}(Q(T), \mathbf{z}(T))$ does not depend on T . Now we are going to use Corollary 3.7, which is applicable by Lemma 2.1. The elements of $\mathbf{z}(T)$ are irreducible. By construction in Proposition 7.9, all exchange relations from the special seeds $(Q(T), \mathbf{z}(T))$ involve exclusively special invariants. One can then verify using Lemma 6.5 that the cluster variables appearing in seeds adjacent to the special ones are irreducible as well. Then Corollary 3.7 yields the inclusion $R_\sigma(V) \supset \mathcal{A}(Q(T), \mathbf{z}(T))$.

The proof of the reverse inclusion is based on the second half of Corollary 3.7. Here we use Lemma 15.1, the First Fundamental Theorem of invariant theory, and the fact that all Weyl generators show up in extended clusters $\mathbf{z}(T)$. Hence $R_\sigma(V) = \mathcal{A}(Q(T), \mathbf{z}(T))$, and the theorem is proved. \square

16. OTHER PROOFS

Proof of Theorem 8.5. It is straightforward to verify that the construction described in [52] arises as a special case of our setup for the “zig-zag” triangulation that includes all diagonals of the form $(i, b-i)$ and $(i, B+1-i)$.

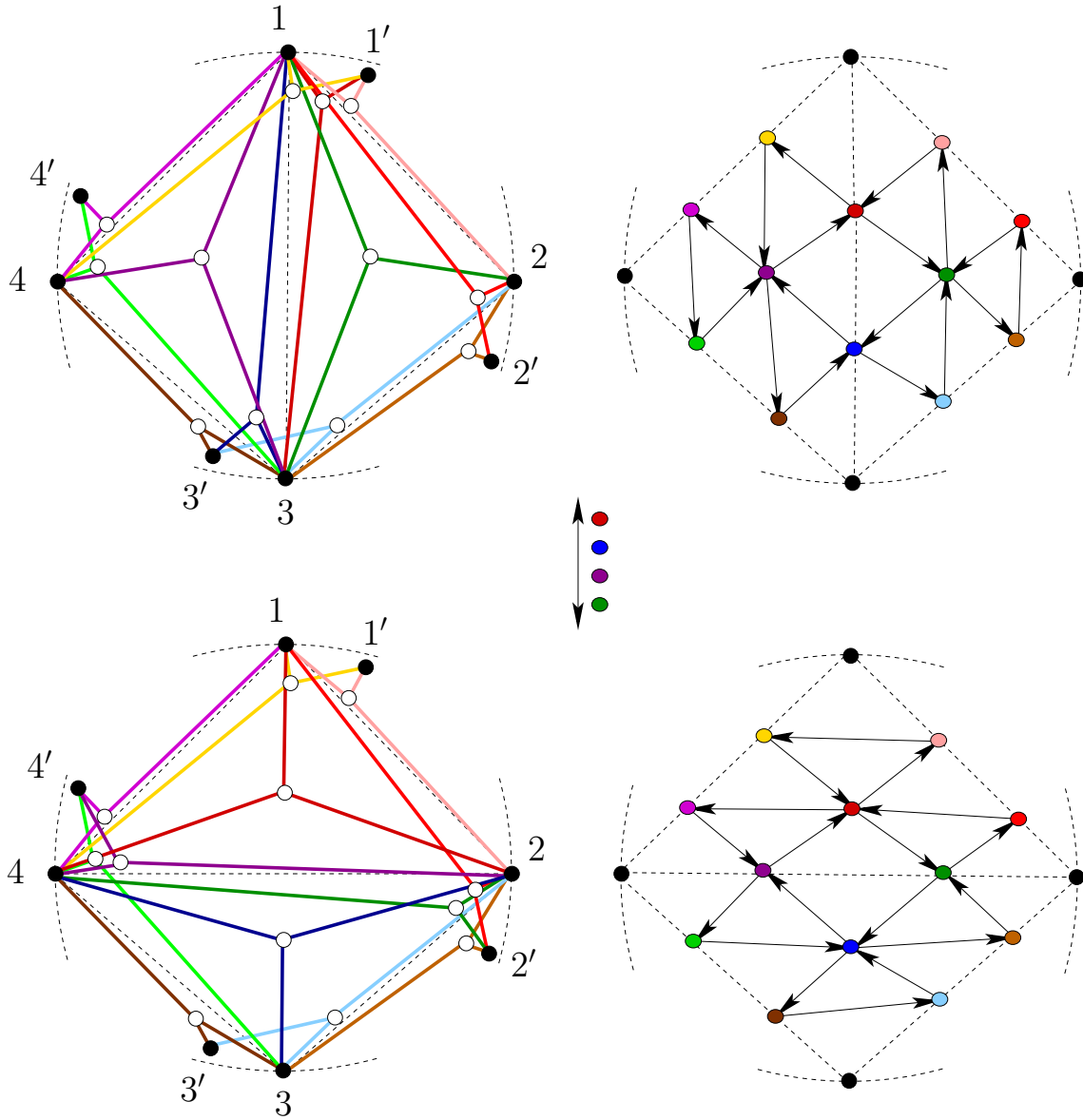


Figure 51: Diagonal flip in a quadrilateral with four black vertices. These seeds are related by a sequence of four mutations: $J_3^1 \rightarrow J_{124}$, $J_1^3 \rightarrow J_{234}$, $J_{134} \rightarrow J_2^4$, $J_{123} \rightarrow J_4^2$.

For the sake of completeness, we include a case-by-case verification that in the case of monochromatic signature, the seeds $Q(T), \mathbf{z}(T)$ related by a single flip are indeed obtained from each other by mutations. We stated this claim in Section 15 for an arbitrary signature, but did not conduct an exhaustive examination of all possible non-generic cases. Such an examination (for $a = 0$) is presented in Figures 53–56. \square

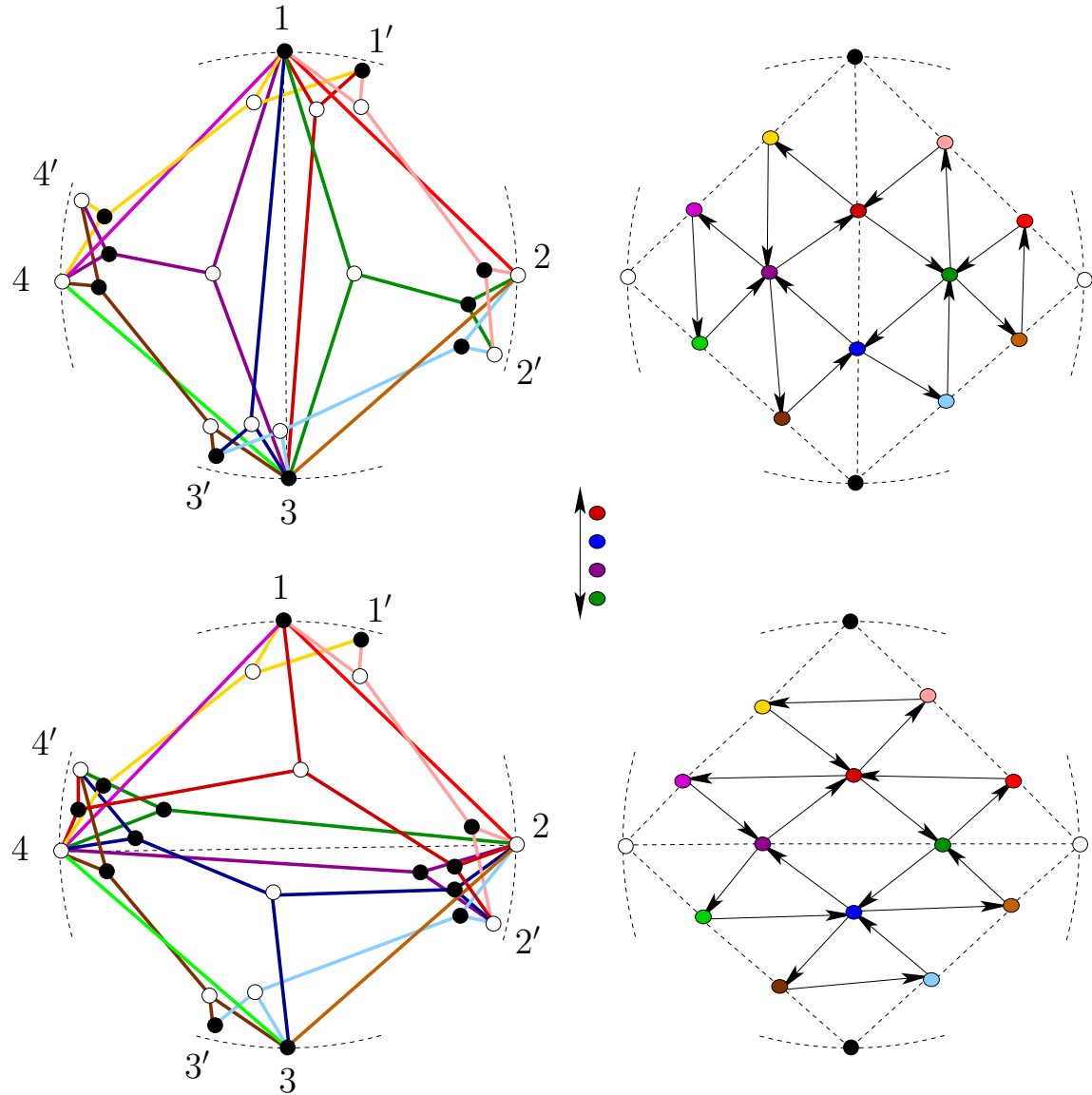


Figure 52: Diagonal flip in a quadrilateral with two black and two white vertices, with opposite vertices of the same color. Mutations to perform: $J_3^1 \rightarrow J_{124}$, $J_1^3 \rightarrow J_{234}$, $J_{134} \rightarrow J_2^4$, $J_{123} \rightarrow J_4^2$.

Proof of Theorem 8.8. Our goal is to identify the cluster structure after dropping a boundary vertex with a part of the original cluster structure. There are several cases to consider. Figure 57 explains how to handle the case where the color of the dropped vertex differs from both of its neighbors. Other cases are treated in a similar way. \square

Proof of Theorem 8.9. We follow the pattern of the proof of Theorem 8.8, examining one characteristic example (see Figure 58) instead of conducting a formal case by

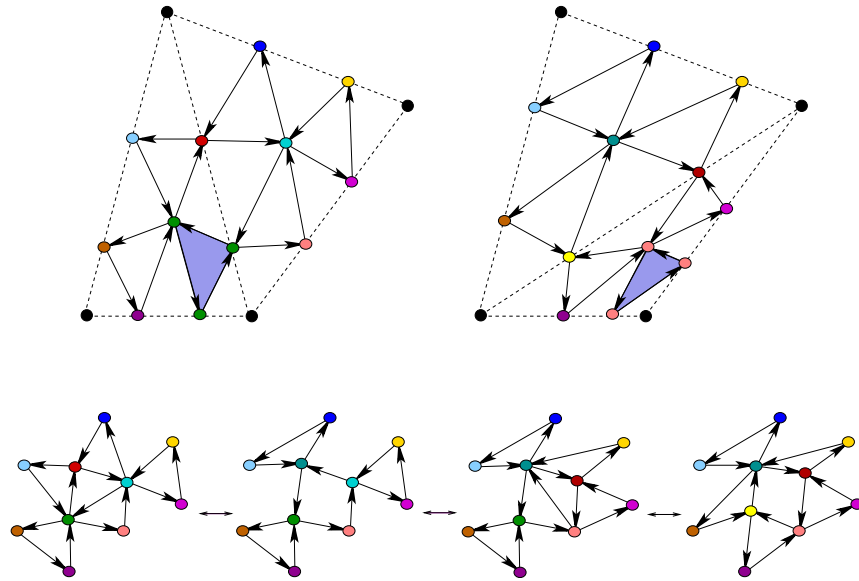


Figure 53: A flip in $R_{0,b}(V)$: one exposed side, three mutations.

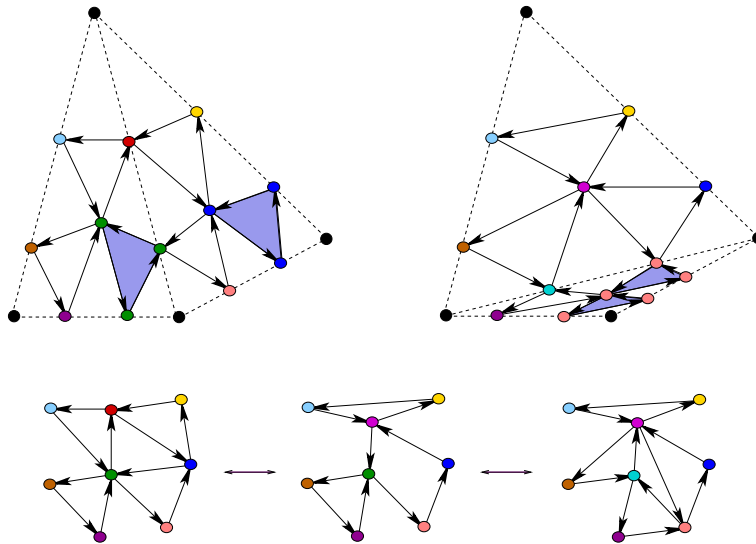


Figure 54: A flip in $R_{0,b}(V)$: two adjacent exposed sides, two mutations.

case analysis. The size of this example is large enough to demonstrate what happens in general. \square

Proof of Corollary 8.10. Any planar tree can be grown by repeated application of the operations of adding a fork and dropping a vertex. Make sure to never pass through an alternating signature; this can indeed be done. We omit the details. \square

Proof of Theorem 8.11. The construction of an extended cluster $\mathbf{z}(T)$ can be carried out verbatim with the black and white colors swapped. Let us denote the resulting

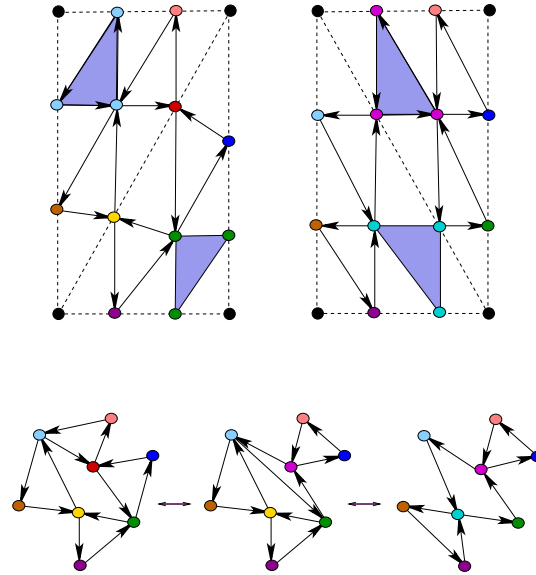


Figure 55: A flip in $R_{0,b}(V)$: two non-adjacent exposed sides, two mutations.

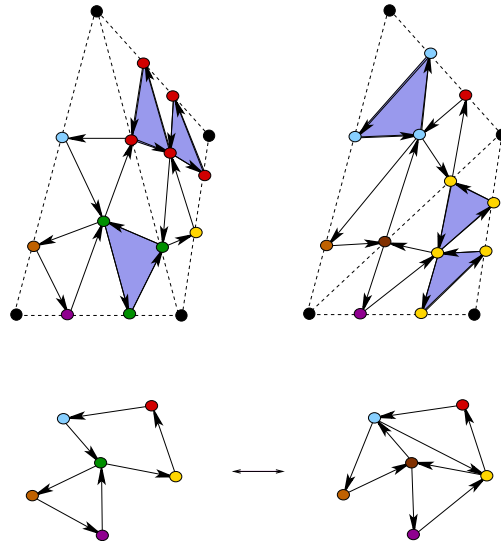


Figure 56: A flip in $R_{0,b}(V)$: three exposed sides, one mutation.

set by $\mathbf{z}'(T)$. Note that the definition of a proxy vertex remains the same. The only difference between the two constructions is that for each triangle pqr in T , we use (the factors of) the special invariant J_{pqr} to build $\mathbf{z}(T)$ whereas the construction of $\mathbf{z}'(T)$ involves J^{pqr} . In each instance where the latter choice yields an irreducible factor that does not come from any special invariant contributing to $\mathbf{z}(T)$, one can use the relation (6.1) to mutate between the two seeds. This can be verified on a case by case basis, treating each fundamental region separately. \square

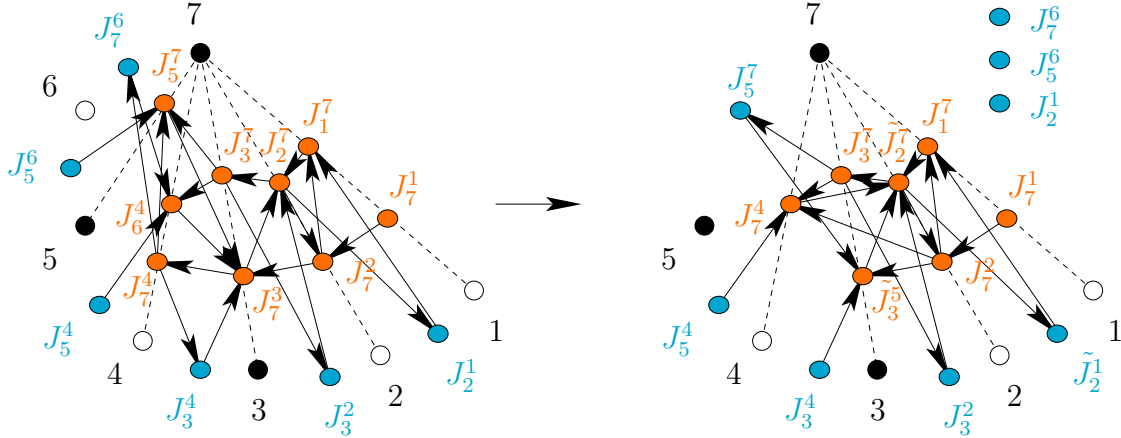


Figure 57: Vertex 6 is being dropped. Notation \tilde{J} refers to special invariants after the removal. The identification is achieved by exchanging J_6^4 for $J_{357} = \tilde{J}_3^5$, then J_7^3 for \tilde{J}_2^7 , and finally J_2^7 for \tilde{J}_2^1 ; then freezing J_5^7 and \tilde{J}_2^1 and subsequently throwing away J_2^1 , J_5^6 , and J_7^6 . The relevant exchange relations are: $J_6^4 J_{357} = J_3^7 + J_7^3 J_7^6 J_5^4$, $J_7^3 \tilde{J}_2^7 = J_2^7 J_{357} J_7^4 + J_7^6 J_5^7 J_5^4 J_3^4 J_7^2 J_3^7$, and $J_2^7 \tilde{J}_2^1 = \tilde{J}_2^7 J_2^1 + J_7^6 J_5^7 J_5^4 J_3^4 J_3^2 J_1^7$.

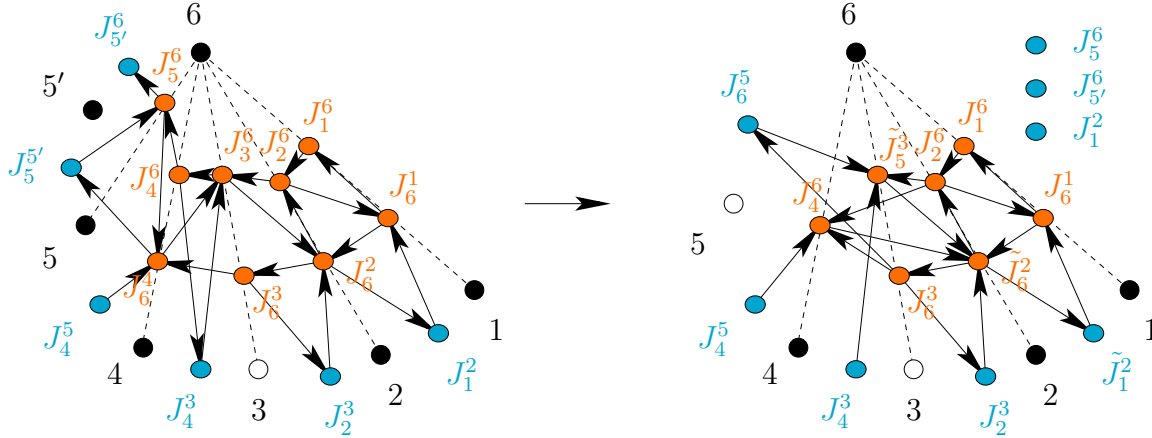


Figure 58: Replacing black vertices 5 and 5' by the white vertex 5. Notation \tilde{J} refers to special invariants after the replacement. We go counterclockwise along the boundary until the colors repeat (at vertices 1, 2). The identification is achieved by exchanging J_6^4 for \tilde{J}_5^3 , then J_3^6 for \tilde{J}_2^6 , and finally J_6^2 for \tilde{J}_1^2 ; then freezing J_5^6 and \tilde{J}_1^2 , and throwing out J_1^2 , $J_5'^6$, and J_5^6 . The exchange relations are: $J_6^4 \tilde{J}_5^3 = J_5'^6 J_3^6 + J_5^4 J_6^3$, $J_3^6 \tilde{J}_2^6 = J_4^6 \tilde{J}_5^3 J_6^2 + J_5^6 J_6^3 J_2^6 J_4^3 J_5^4$, and $J_6^2 \tilde{J}_1^2 = \tilde{J}_6^2 J_1^2 + J_5^6 J_6^1 J_4^5 J_4^3 J_2^3$.

Proof of Lemma 10.4. A skein relation yields the identity shown in Figure 59. It remains to note that the second term vanishes as it is both symmetric and antisymmetric with respect to the (co)vectors corresponding to the two sibling vertices. \square

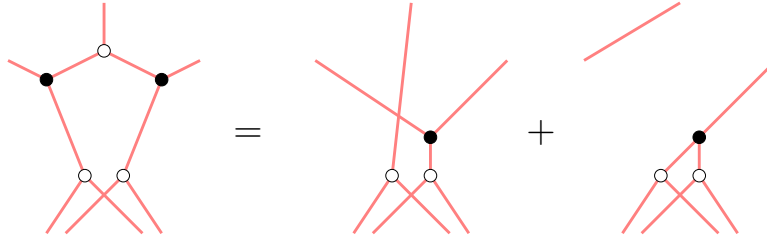


Figure 59: Skein relation justifying an arborizing step.

Proof of Theorem 10.5. The proof is a straightforward application of the Diamond Lemma (see, e.g., [6, Lemma 1.4.1]). The five possible nontrivial diamonds are shown in Figure 60. \square

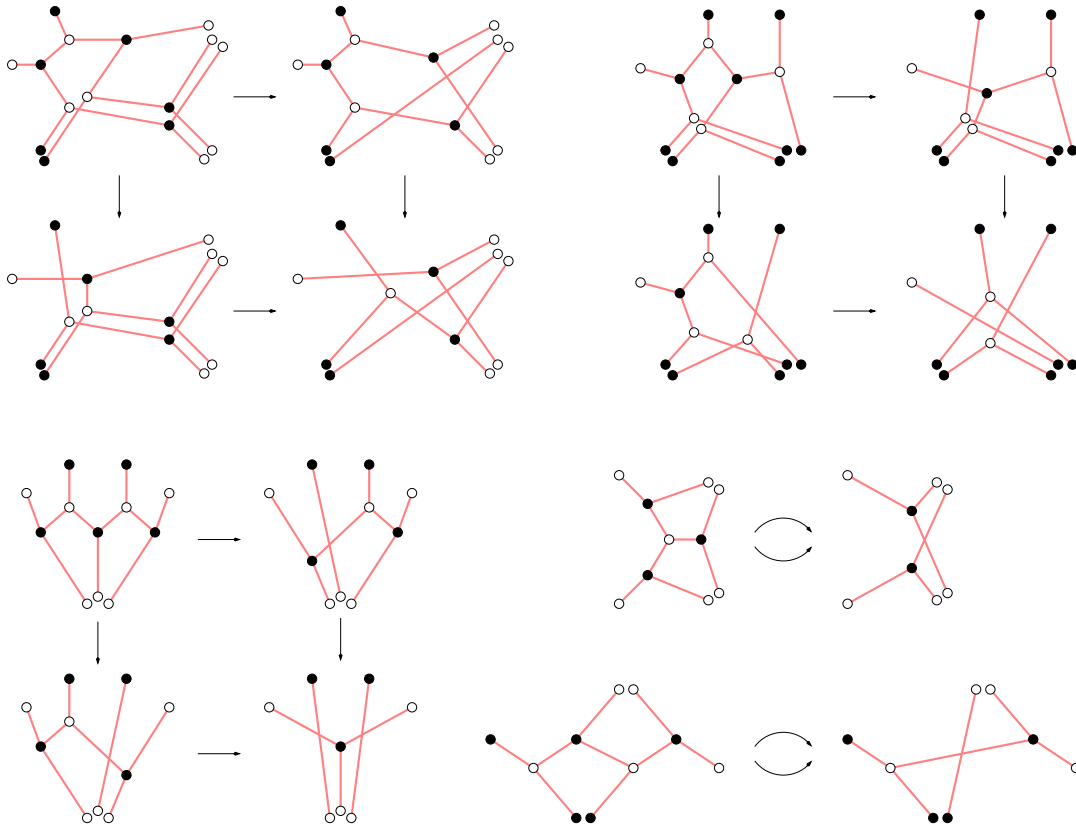


Figure 60: Proving the confluence of the arborization algorithm.

Proof of Theorem 10.9. The idea of the proof is as follows. Assume that W arborizes to a tree diagram D . Let us reverse the arborization process: starting with D , we step by step “planarize” it (cf. Figure 36), each time creating a four-edge fragment of one of the two kinds described in Definition 10.3. Now make a tensor diagram for z^k by bundling together k copies of D , and apply a planarization procedure following

the same steps, each time planarizing all k copies. At the end of this process, we are going to obtain the k -thickening of W , thereby proving the theorem.

We illustrate how this works using the example in Figure 61. The left picture shows an intermediate stage of the planarization process, with $k = 3$. The six white vertices correspond to two sibling vertices in D . Remember that we are transforming our tensor diagram from the inside out, i.e., moving towards the boundary. The portions attached underneath those six vertices all look identical: they are patterned after the same subtree of D . We proceed in two stages as shown in the figure. At the first stage, we planarize around the two triples of black vertices, using skein relations (including the square move). Each time, all terms but one vanish because they can be seen to be both symmetric and antisymmetric with respect to a pair of arguments. At the second stage, we planarize the intersection of k -thickenings of two edges of D using a similar calculation.

□

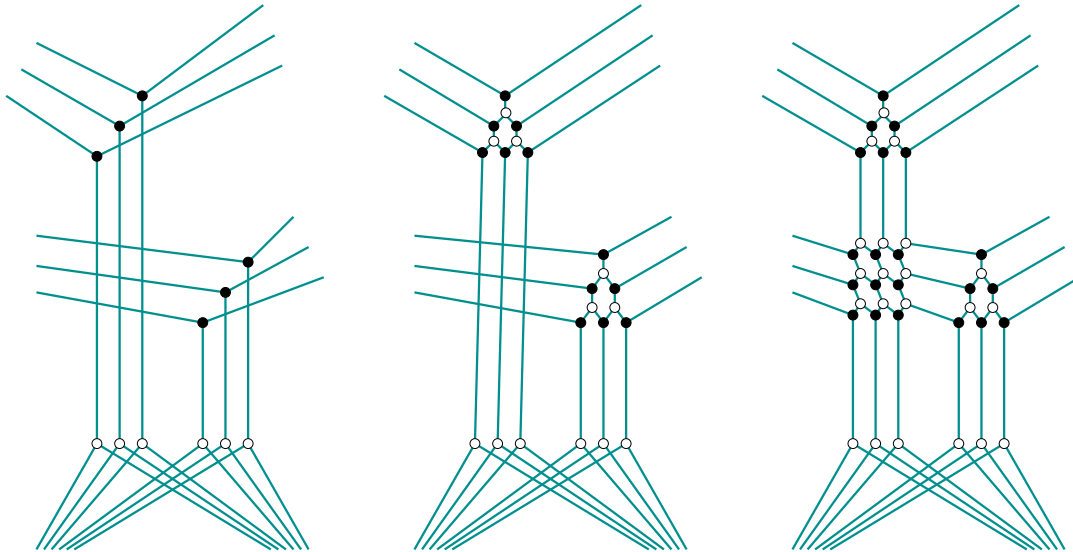


Figure 61: L'Ouvrier et la Kolkhoziennne

Appendices

17. SPECIAL CHOICE OF AN INITIAL SEED

The cluster structure in the ring of invariants $R_\sigma(V)$ is in principle determined by a single initial seed $(Q(T), \mathbf{z}(T))$. Consequently, one may be interested in identifying a particular choice of a triangulation T for which the seed $(Q(T), \mathbf{z}(T))$ has a simpler and more explicit description than the general case as presented in Sections 6–7. One such choice is discussed in this section.

Denote $N = a + b$. Since the signature σ is non-alternating, we can assume without loss of generality that the vertices 1 and 2 are black. (If we can only find two adjacent white vertices, then use the same recipe with the colors swapped, cf. Theorem 8.11.)

The case $a = 0$ has been covered in Figure 21. So let σ be non-monochromatic. Without loss of generality, we can assume that the vertex N is white.

Let T_1 be the triangulation of the N -gon P_σ obtained by drawing all diagonals with an endpoint at the vertex 1. The quiver $Q(T_1)$ is constructed as follows.

- (1) Place two (mutable) vertices of $Q(T_1)$ on each diagonal of T_1 . Place one frozen vertex on each side of P_σ .
- (2) Fill each triangle in T_1 with arrows as shown in Figure 62. The choice of a pattern is determined by the color of the right endpoint of the base side.
- (3) Assemble a quiver from these pieces, removing 2-cycles if necessary.
- (4) On the diagonal 13, freeze the vertex closer to 1, and identify it with the frozen vertex 12.
- (5) On the diagonal $1(N - 1)$, freeze one vertex, namely the one closer to 1 (resp., $N - 1$) if $N - 1$ is white (resp., black). Identify it with $(N - 1)N$ if $N - 1$ is white, and with $1N$ if it is black.
- (6) Add arrows connecting the mutable vertices on diagonals 13 and $1(N - 1)$ to the frozen vertices 12, 23, $(N - 1)N$, and $1N$ as shown in Figure 62 on the right. Remove 2-cycles if necessary; this will happen if vertex 3 is black.
- (7) If $N - 1$ is black, replace the portions of the resulting quiver inside the pentagon $1(N - 3)(N - 2)(N - 1)N$ as shown in Figure 63.

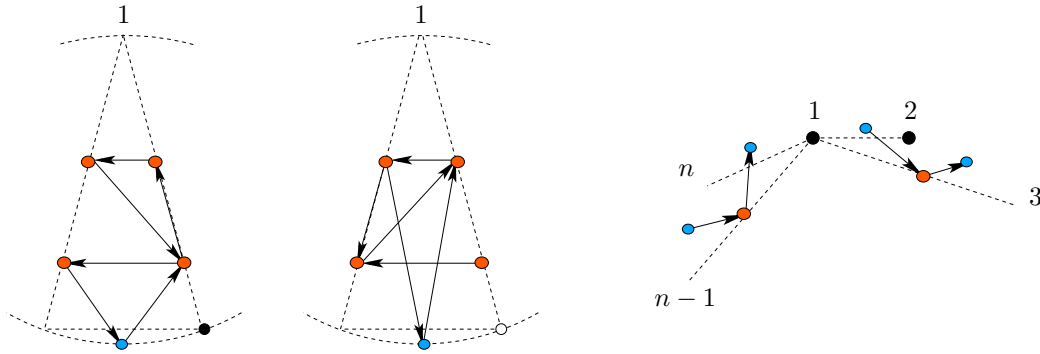


Figure 62: Constructing the quiver $Q(T_1)$: Building blocks

Figure 64 shows an example of applying this construction.

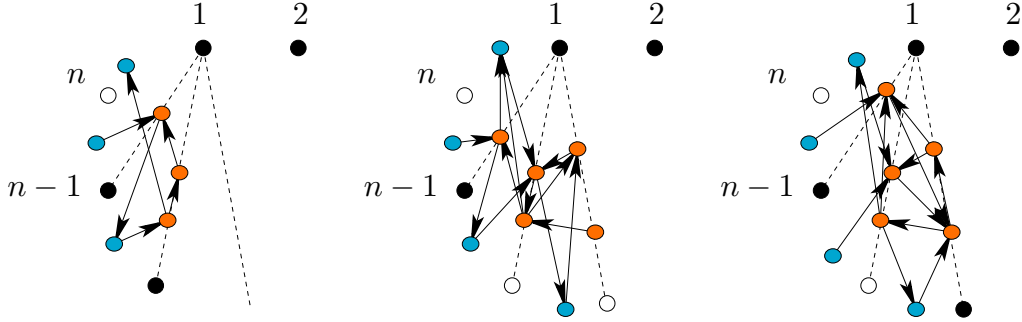


Figure 63: Constructing the quiver $Q(T_1)$: Exceptional cases

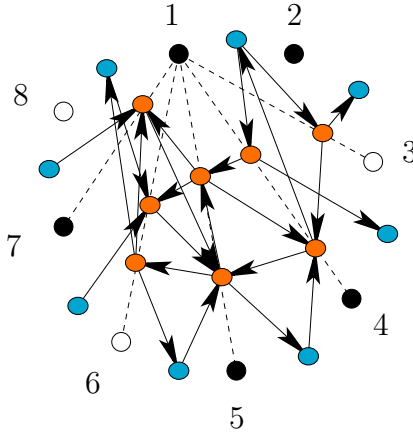


Figure 64: Constructing the quiver $Q(T_1)$. In this example, one of the exceptional cases in step (7) applies.

When the vertex $N - 1$ is white, the above construction of the quiver $Q(T_1)$ simplifies substantially as we do not have to make the adjustments described in step (7). If one is only interested in the cluster type of $R_\sigma(V)$, the description simplifies further:

Proposition 17.1. *Let $\sigma = [\sigma_1 \cdots \sigma_N]$, $N \geq 6$, be a signature such that $\sigma_1 = \sigma_2 = \bullet$ and $\sigma_{N-1} = \sigma_N = \circ$. Let T_1 be the triangulation of P_σ by the diagonals incident to the vertex 1. Then the mutable part of the quiver $Q(T_1)$ is obtained by taking the vertices s_3, s_4, \dots, s_{N-1} and t_4, t_5, \dots, t_{N-2} together with the following edges:*

- for $3 \leq i \leq N - 2$, draw an edge $s_i \rightarrow s_{i+1}$;
- for $4 \leq i \leq N - 3$, draw an edge $t_i \rightarrow t_{i+1}$;
- for $3 \leq i \leq N - 3$, if $\sigma_i = \bullet$, then draw an edge $t_{i+1} \rightarrow s_i$;
- for $3 \leq i \leq N - 3$, if $\sigma_i = \circ$, then draw an edge $t_{i+1} \rightarrow s_{i+1}$;
- for $4 \leq i \leq N - 2$, if $\sigma_i = \bullet$, then draw an edge $s_i \rightarrow t_i$;
- for $4 \leq i \leq N - 2$, if $\sigma_i = \circ$, then draw an edge $s_{i+1} \rightarrow t_i$.

18. ADDITIONAL EXAMPLES OF SEEDS

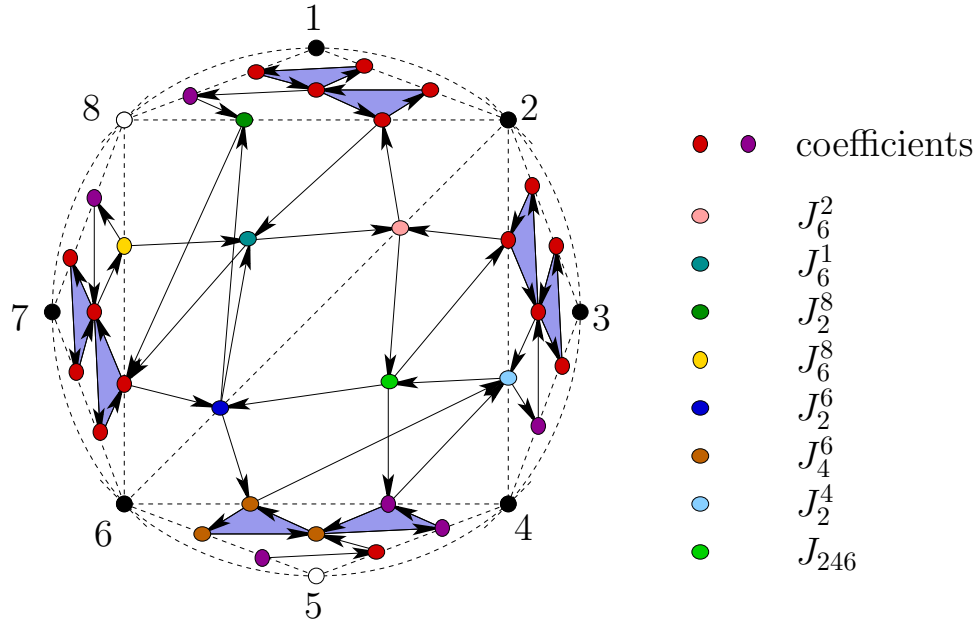


Figure 65: An example of a seed $(Q(T), \mathbf{z}(T))$ for $\sigma = [\bullet \bullet \bullet \bullet \circ \bullet \bullet \circ]$.

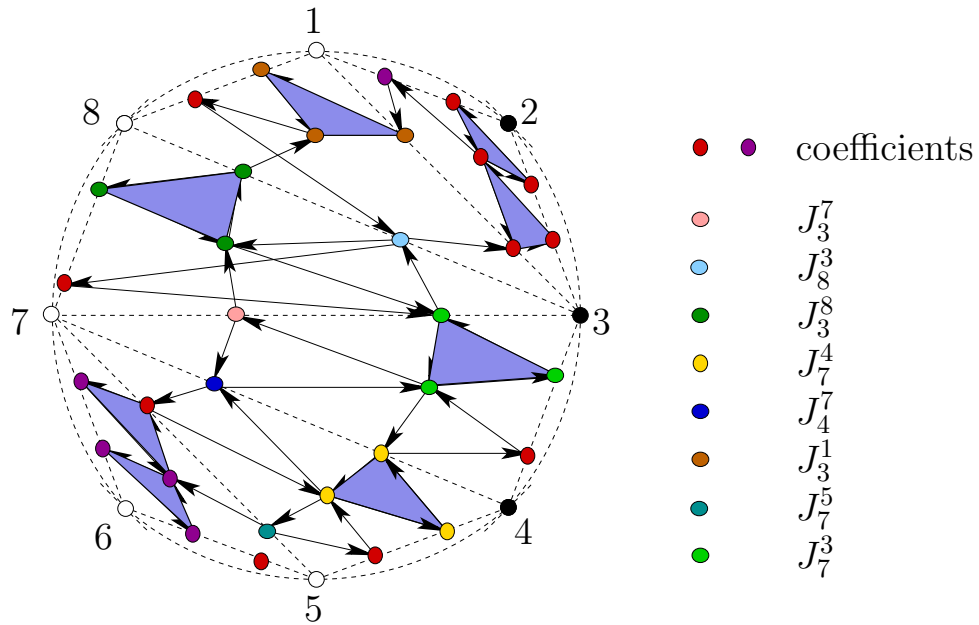


Figure 66: An example of a seed $(Q(T), \mathbf{z}(T))$ for $\sigma = [\circ \circ \circ \circ \circ \bullet \bullet \bullet]$.

REFERENCES

- [1] A. Abdesselam and J. Chipalkatti, Brill-Gordan loci, transvectants and an analogue of the Foulkes conjecture, *Adv. Math.* **208** (2007), no. 2, 491–520.
- [2] J. F. Blinn, *Using tensor diagrams to represent and solve geometric problems*, course notes for *SIGGRAPH 2002*, available at <http://research.microsoft.com/apps/pubs/default.aspx?id=79791>.
- [3] A. Berenstein, S. Fomin and A. Zelevinsky, Cluster algebras III: Upper bounds and double Bruhat cells, *Duke Math. J.* **126** (2005), 1–52.
- [4] P. Caldero and M. Reineke, On the quiver Grassmannian in the acyclic case, *Journ. Pure Appl. Alg.* **212** (2008), 2369–2380.
- [5] G. Cerulli Irelli, B. Keller, D. Labardini-Fragoso, and P.-G. Plamondon, Linear independence of cluster monomials for skew-symmetric cluster algebras, *Compos. Math.* **149** (2013), 1753–764.
- [6] P. M. Cohn, *Further algebra and applications*, Springer-Verlag London, 2003.
- [7] P. Cvitanović, *Group theory. Birdtracks, Lie's, and exceptional groups*, Princeton University Press, Princeton, NJ, 2008.
- [8] V. I. Danilov, Algebraic varieties and schemes. *Algebraic geometry I*, 167–297, Encyclopaedia Math. Sci. **23**, Springer, Berlin, 1994.
- [9] H. Derksen, J. Weyman, and A. Zelevinsky, Quivers with potentials and their representations II: applications to cluster algebras, *J. Amer. Math. Soc.* **23** (2010), 749–790.
- [10] I. Dolgachev, *Lectures on invariant theory*, Cambridge University Press, Cambridge, 2003.
- [11] V. V. Fock and A. B. Goncharov, Moduli spaces of local systems and higher Teichmüller theory, *Publ. Math. Inst. Hautes Études Sci.* **103** (2006), 1–211.
- [12] V. V. Fock and A. B. Goncharov, Moduli spaces of convex projective structures on surfaces, *Adv. Math.* **208** (2007), 249–273.
- [13] S. Fomin and P. Pylyavskyy, Tensor diagrams and cluster algebras, [arXiv:1210.1888v1](https://arxiv.org/abs/1210.1888v1), October 5, 2012.
- [14] S. Fomin, M. Shapiro, and D. Thurston, Cluster algebras and triangulated surfaces. Part I: Cluster complexes, *Acta Math.* **201** (2008), 83–146.
- [15] S. Fomin and A. Zelevinsky, Cluster algebras I: Foundations, *J. Amer. Math. Soc.* **15** (2002), 497–529.
- [16] S. Fomin and A. Zelevinsky, Cluster algebras: Notes for the CDM-03 conference, *Current Developments in Mathematics, 2003*, 1–34, Int. Press, 2004.
- [17] S. Fomin and A. Zelevinsky, Cluster algebras II: Finite type classification, *Invent. Math.* **154** (2003), 63–121.
- [18] S. Fomin and A. Zelevinsky, Cluster algebras IV: Coefficients, *Compos. Math.* **143** (2007), 112–164.
- [19] C. Geiss, B. Leclerc, and J. Schröer, Preprojective algebras and cluster algebras, *in: Trends in representation theory of algebras and related topics*, 253–283, *EMS Ser. Congr. Rep.*, Eur. Math. Soc., Zürich, 2008.
- [20] C. Geiss, B. Leclerc, and J. Schröer, Semicanonical bases and preprojective algebras, *Ann. Sci. École Norm. Sup.* **38** (2005), 193–253.

- [21] C. Geiss, B. Leclerc, and J. Schröer, Factorial cluster algebras, *Doc. Math.* **18** (2013), 249–274.
- [22] C. Geiss, B. Leclerc, and J. Schröer, Cluster algebras in algebraic Lie theory, *Transformation Groups* **18** (2013), Issue 1, 149–178.
- [23] C. Geiss, B. Leclerc, and J. Schröer, Generic bases for cluster algebras and the Chamber ansatz, *J. Amer. Math. Soc.* **25** (2012), 21–76.
- [24] M. Gekhtman, M. Shapiro and A. Vainshtein, Cluster algebras and Poisson geometry, *Moscow Math. J.* **3** (2003), No. 3, 899–934.
- [25] M. Gekhtman, M. Shapiro and A. Vainshtein, *Cluster algebras and Poisson geometry*, American Mathematical Society, Providence, RI, 2010.
- [26] J. E. Grabowski and S. Launois, Quantum cluster algebra structures on quantum Grassmannians and their quantum Schubert cells: the finite-type cases, *Int. Math. Res. Not.* **2011**, no. 10, 2230–2262.
- [27] D. Hernandez, Simple tensor products, *Invent. Math.* **181** (2010), 649–675.
- [28] D. Hernandez and B. Leclerc, Cluster algebras and quantum affine algebras, *Duke Math. J.* **154** (2010), 265–341.
- [29] B. Keller, Algèbres amassées et applications, *Séminaire Bourbaki, 62e année, 2009–2010, exposé 1014, Astérisque* **339** (2011), Exp. No. 1014, vii, 63–90.
- [30] B. Keller, Cluster algebras, quiver representations and triangulated categories, *Triangulated categories*, 76–160, London Math. Soc. Lecture Note Ser., 375, Cambridge Univ. Press, Cambridge, 2010.
- [31] M. Khovanov and G. Kuperberg, Web bases for $\mathfrak{sl}(3)$ are not dual canonical, *Pacific J. Math.* **188** (1999), 129–153.
- [32] Y. Kimura and F. Qin, Graded quiver varieties, quantum cluster algebras and dual canonical basis, *Adv. Math.* **262** (2014), 261–312.
- [33] Y. Kodama and L. K. Williams, KP solitons, total positivity, and cluster algebras, *Proc. Natl. Acad. Sci. USA* **108** (2011), no. 22, 8984–8989.
- [34] H. Kraft and C. Procesi, Classical invariant theory, a primer, lecture notes, 1996, ii+125 pp. Available at <http://www.math.unibas.ch/~kraft/>.
- [35] G. Kuperberg, Spiders for rank 2 Lie algebras, *Comm. Math. Phys.* **180** (1996), 109–151.
- [36] P. Lampe, A quantum cluster algebra of Kronecker type and the dual canonical basis, *Int. Math. Res. Not. IMRN* **2011**, no. 13, 2970–3005.
- [37] B. Leclerc, Imaginary vectors in the dual canonical basis of $U_q(\mathfrak{n})$, in: *Transform. Groups* **8** (2003), 95–104.
- [38] B. Leclerc, Canonical and semicanonical bases, talk at the University of Reims, November 2008, <http://loic.foissy.free.fr/colloque/Leclerc.pdf>.
- [39] B. Leclerc, Cluster algebras and representation theory, *Proceedings of the International Congress of Mathematicians, vol. IV*, 2471–2488, Hyderabad, 2010.
- [40] D. Hernandez and B. Leclerc, Quantum Grothendieck rings and derived Hall algebras, *Crelle*, to appear.
- [41] B. Leclerc and A. Zelevinsky, Quasicommuting families of quantum Plücker coordinates, in: Kirillov’s Seminar on Representation Theory, in: *Amer. Math. Soc. Transl. (2)*, vol. 181, Amer. Math. Soc., Providence, RI, 1998, 85–108.

- [42] H. Li, *Invariant algebras and geometric reasoning*, World Scientific, 2008.
- [43] G. Lusztig, *Introduction to quantum groups*, Birkhäuser Boston, 1993.
- [44] G. Lusztig, Semicanonical bases arising from enveloping algebras, *Adv. Math.* **151** (2000), 129–139.
- [45] G. Musiker, R. Schiffler, and L. Williams, Positivity for cluster algebras from surfaces, *Adv. Math.* **227** (2011), 2241–2308.
- [46] H. Nakajima, Quiver varieties and cluster algebras, *Kyoto J. Math.* **51** (2011), 71–126.
- [47] P. Olver, *Classical invariant theory*, Cambridge University Press, Cambridge, 1999.
- [48] V. L. Popov and E. B. Vinberg, *Invariant theory*, in: *Algebraic geometry. IV, Encyclopaedia of Mathematical Sciences, vol. 55*, Springer-Verlag, Berlin, 1994, 123–284.
- [49] A. Postnikov, D. Speyer, and L. Williams, Matching polytopes, toric geometry, and the totally non-negative Grassmannian, *J. Algebraic Combin.* **30** (2009), 173–191.
- [50] C. Procesi, *Lie groups. An approach through invariants and representations*, Springer, New York, 2007.
- [51] J. Richter-Gebert and P. Leeb, Diagrams, tensors and geometric reasoning, *Discrete Comput. Geom.* **42** (2009), 305–334.
- [52] J. Scott, Grassmannians and cluster algebras, *Proc. London Math. Soc.* **92** (2006), 345–380.
- [53] J. Scott, Quasi-commuting families of quantum minors, *J. Algebra* **290** (2005), 204–220.
- [54] P. Sherman and A. Zelevinsky, Positivity and canonical bases in rank 2 cluster algebras of finite and affine types, *Mosc. Math. J.* **4** (2004), 947–974, 982.
- [55] G. Stedman, *Diagram techniques in group theory*, Cambridge University Press, Cambridge, 1990.
- [56] B. Sturmfels, *Algorithms in invariant theory*, Springer-Verlag, 1993.
- [57] H. Weyl, *The classical groups. Their invariants and representations*, Princeton University Press, Princeton, NJ, 1997. (Original edition: 1939.)

DEPARTMENT OF MATHEMATICS, UNIVERSITY OF MICHIGAN, ANN ARBOR, MI 48109, USA
E-mail address: fomin@umich.edu

DEPARTMENT OF MATHEMATICS, UNIVERSITY OF MINNESOTA, MINNEAPOLIS, MN 55414, USA
E-mail address: ppylyavs@umn.edu